MASTERARBEIT / MASTER'S THESIS

Titel der Masterarbeit / Title of the Master's Thesis

„Methods for the detection of autoantibodies in seronegative Myasthenia Gravis patients"

verfasst von / submitted by

Veronica Bruno

angestrebter akademischer Grad / in partial fulfilment of the requirements for the degree of

Master of Science (MSc)

Wien, 2021 / Vienna, 2021

Studienkennzahl lt. Studienblatt / degree programme code as it appears on the student record sheet:	UA 066 830
Studienrichtung lt. Studienblatt / degree programme as it appears on the student record sheet:	Master Study Program Molecular Microbiology, Microbial Ecology and Immunobiology
Betreut von / Supervisor:	Assoc. Prof. Priv.-Doz. Dr. Romana Höftberger

Declaration of authorship:

I hereby certify that the thesis I am submitting is entirely my own original work, except where otherwise indicated. I am aware of the University's regulations concerning plagiarism, including those regulations concerning disciplinary actions that may result from plagiarism. Any use of the works of any other author, in any form, is properly acknowledged at their point of use.

Furthermore, I assure that the (printed and electronic) copies I have submitted are identical.

Date: ..... Signature:

Abstract

Myasthenia gravis (MG) is an autoimmune disorder that affects the neuromuscular junction (NMJ) whose main symptom is represented by skeletal muscle weakness. Around 85% of MG patients have been diagnosed with autoantibodies against the acetylcholine receptor (AChR), and 30% of the remaining 15% displayed antibodies against muscle-specific kinase receptor (MuSK). The ones without antibodies against AChR or MuSK are considered seronegative MG (SNMG). SNMG patients are a heterogeneous group in which pathogenicity, age of onset, and affected muscle groups are highly variable.

The aim of the study was the detection of antibodies and unknown antigens involved in SNMG, using both primary muscle cell cultures and muscle tissues.

20 SNMG sera have been tested with cell-based assays (CBA) and tissue-based assays (TBA) to assess the presence of antibodies against the NMJ. Human myotubes in vitro did not display clustered AChR and a total of 39 different conditions have been tested to induce it. Finally, an immunoprecipitation assay was performed to isolate unknown molecules in SNMG patients.

The results of the experiments highlighted different conditions that allowed clustering of AChR in human myotubes, but none of the conditions showed a fully developed postsynaptic region. The immunoprecipitation did not allow the isolation of neither human IgG nor NMJ, indicating that the assay may need distinct cell models to detect antibodies and antigens.

In conclusion, it has been highlighted the need for different models to study the mechanisms of NMJ formation and maintenance. Moreover, the approach here presented may be used to screen SNMG sera for the presence of antibodies against components of the NMJ, to detect the unknown antigens.

Abstrakt

Myasthenia gravis (MG) ist eine Autoimmunerkrankung, die den neuromuskulären Übergang (NMJ) betrifft, dessen Hauptsymptom in einer Schwäche der Skelettmuskulatur besteht. Bei rund 85% der MG-Patienten wurden Autoantikörper gegen den Acetylcholinrezeptor (AChR) diagnostiziert, und 30% der verbleibenden 15% zeigten Antikörper gegen den muskelspezifischen Kinase-Rezeptor (MuSK). Diejenigen ohne Antikörper gegen AChR oder MuSK gelten als seronegative MG (SNMG). SNMG-Patienten sind eine heterogene Gruppe, in der Pathogenität, Erkrankungsalter und betroffene Muskelgruppen sehr unterschiedlich sind. Das Ziel der Studie war der Nachweis von Antikörpern und unbekannten Antigenen, die an SNMG beteiligt sind, sowohl unter Verwendung von primären Muskelzellkulturen als auch von Muskelgewebe.

20 SNMG-Seren wurden mit zellbasierten Assays (CBA) und gewebebasierten Assays (TBA) getestet, um das Vorhandensein von Antikörpern gegen das NMJ zu bewerten. In vitro zeigten humane Myotuben kein geclustertes AChR, und insgesamt 39 verschiedene Bedingungen wurden getestet, um es zu induzieren. Schließlich wurde ein Immunpräzipitationsassay durchgeführt, um unbekannte Moleküle bei SNMG-Patienten zu isolieren.

Die Ergebnisse der Experimente hoben verschiedene Bedingungen hervor, die eine Clusterbildung von AChR in menschlichen Myotubes ermöglichten, aber keine der Bedingungen zeigte eine vollständig entwickelte postsynaptische Region. Die Immunpräzipitation erlaubte weder die Isolierung von menschlichem IgG noch von NMJ, was darauf hinweist, dass der Assay möglicherweise unterschiedliche Zellmodelle zum Nachweis von Antikörpern und Antigenen benötigt.

Zusammenfassend wurde die Notwendigkeit verschiedener Modelle hervorgehoben, um die Mechanismen der Bildung und Aufrechterhaltung von NMJ zu untersuchen. Darüber hinaus kann der hier vorgestellte Ansatz verwendet werden, um SNMG-Seren auf das Vorhandensein von Antikörpern gegen Komponenten des NMJ zu screenen, um die unbekannten Antigene nachzuweisen.

Table of Contents

ABSTRACT 3

ABSTRAKT 4

TABLE OF CONTENTS 4

1 INTRODUCTION 8

1.1 AUTOIMMUNE DISEASES 8
1.2 PHYSIOLOGY OF THE NEUROMUSCULAR JUNCTION 8
1.2.1 Development and maintenance of the neuromuscular junction 10
1.2.2 AChR clustering 11
1.2.3 Model organisms for the NMJ 12
1.3 SATELLITE CELLS 13
1.4 MYASTHENIA GRAVIS 15
1.4.1 AChR-associated MG 16
1.4.2 MuSK-associated MG 17
1.4.3 Pathogenic mechanism of antibodies against AChR 17
1.4.4 Pathogenic mechanism of MuSK antibodies 19
1.4.5 Seronegative MG 20
1.5 AIM OF THE STUDY 21

2 MATERIALS AND METHODS 22

2.1 MATERIALS 22
2.2 ANTIBODIES 23
2.3 CELL CULTURE 24
2.3.1 Culture of HEK 293 and L6.C11 24
2.3.2 Culture of C2C12 cells 24
2.3.3 Isolation of Primary Muscle Cells from Muscle Biopsies 24
2.3.4 Culture of Primary Muscle Cells 25
2.3.5 Splitting 25
2.3.6 Freezing 26
2.3.7 Thawing of cells 26
2.3.8 Differentiation of muscle cells 26
2.4 CELL-BASED ASSAYS (CBA) 27
2.4.1 Transfection of HEK293 with AChR and MuSK plasmids 27
2.4.2 Incubation with human serum 27
2.5 TISSUE-BASED ASSAYS (TBA) 28
2.6 IMMUNOPRECIPITATION ASSAY (IP) 29
2.6.1 Cell lysate 29
2.6.2 SDS-PAGE 30
2.7 CHARACTERIZATION OF MYOGENIC CELLS 30
2.7.1 MyoD staining for muscle cells identification 30
2.7.2 Identification of cells' surface markers 31
2.8 ACHR CLUSTERING ASSAY 31
2.6.1 Permanox experiment 32
2.9 MAXIPREP 32
2.10 MSI 1436 TEST 33
2.10.1 MSI 1436 test with 24 well plate 33
2.10.2 MSI 1436 test with 35 mm dishes day counting test 33
2.10.3 MSI 1436 test with 35 mm dishes titration test 33

2.11 WESTERN BLOT 34
2.11.1 Protein concentration *34*
2.11.2 SDS-PAGE *34*
2.11.3 Western blot *35*
2.11.4 Immunodetection *35*

3 RESULTS **37**

3.1 IDENTIFICATION OF SERONEGATIVE MYASTHENIA GRAVIS PATIENTS 37
3.1.1 Exclusion of sera with antibodies against AChR or MuSK *37*
3.1.2 Screening for autoantibodies against NMJ with tissue-based assays *38*
3.2 DEVELOPMENT OF AN *IN VITRO* MODEL OF THE NEUROMUSCULAR JUNCTION 40
3.2.1 Establishment of primary muscle cells culture *40*
3.2.2 Early characterization of myogenic cells: MyoD staining *41*
3.2.3 Differentiation and myotubes staining *42*
3.3 ACHR CLUSTERS ON HUMAN MYOTUBES 43
3.3.1 Soluble stimulation *44*
3.3.2 Soluble agrin for stimulation *44*
3.3.3 Coating *45*
3.3.4 Soluble agrin and fibronectin coating *45*
3.3.5 Soluble agrin and laminin coating *45*
3.3.6 Soluble agrin in combination with agrin-laminin coating *47*
3.3.7 Soluble laminin on different coating *48*
3.3.8 Soluble agrin and laminin *49*
3.3.9 Permanox slides *51*
3.4 IMMUNOPRECIPITATION 52
3.5 CELL SURFACE MARKERS IDENTIFICATION 53
3.6 MSI-1436 55
3.6.1 Effect of different MSI concentrations *55*
3.6.2 MSI effects on the morphology of cells *58*
3.6.3 MSI effects on differentiation of human muscle cells *59*
3.7 CELL LINE CHARACTERIZATION 59

4 DISCUSSION **61**

4.1 IDENTIFICATION OF SNMG PATIENTS 61
4.2 DETECTION OF AUTOANTIBODIES AGAINST NMJ WITH TBA 62
4.3 CULTURE OF PRIMARY MUSCLE CELLS 62
4.4 ACHR CLUSTERS ON HUMAN MYOTUBES 63
4.5 IMMUNOPRECIPITATION 64
4.6 CELL SURFACE MARKERS IDENTIFICATION 65
4.7 MSI 1436 65
4.8 WESTERN BLOT 66
4.9 ANTIGEN DISCOVERY IN MYASTHENIA GRAVIS 67
4.10 FINAL CONSIDERATIONS 67
4.11 OUTLOOK 68

5 BIBLIOGRAPHY **69**

LIST OF FIGURES **80**

LIST OF TABLES **85**

APPENDIX **86**

LIST OF ABBREVIATIONS

AChR – Acetylcholine receptor

BSA- Bovine serum albumine

CBA – Cell-based assay

C2C12- a subclone of an immortalized mouse myoblast cell line

ColQ- collagen Q

DM – Differentiation Medium

DMEM - Dulbecco's modified eagle medium

DMSO - Dimethyl sulfoxide

Dok7 - Docking protein 7

ECM – Extracellular Matrix

EDTA - Ethylenediaminetetraacetic acid

EGF – Epidermal growth factor

FBS – Fetal bovine serum

FGF – Fibroblast growth factor

GM – Growth medium

HEK 293 - Human embryonic kidney 293

HGM- Human growth medium

IP- Immunoprecipitation test

L6.C11- A subclone of L6, a rat thigh muscle cell line

Lrp4 – Low-density lipoprotein receptor-related protein 4

MG – Myasthenia Gravis

MuSK – Muscle specific kinase

NDS – Normal Donkey Serum

NMJ – Neuromuscular Junction

PBS - Phosphate-buffered saline

Pen-Strep - Penicillin-Streptomycin

PIC- Protease inhibitor cocktail

PLL – Poly-L-Lysine

RT – Room temperature

SNMG – Seronegative Myasthenia Gravis

TBA – Tissue-based assay

1 Introduction

1.1 Autoimmune diseases

Between the 19th and the 20th century, Paul Ehrlich coined the term horror autotoxicus to describe a disease in which it is the immune system to self-harm[1]. Autoimmune diseases occur as a result of an immunological tolerance breakdown, in which the immune system recognizes self-molecules as pathogenic[4]. Immune cells are activated causing an immune response and a production of antibodies thus damages the tissue that expresses the antigen[2,3]. Several causes have been identified as the basis of the loss of this tolerance, including both genetic and/or environmental factors[3], even though they are not the only cause of autoimmune disorders. A study on concordance with identical twins highlighted a percentage of 12 to 67% of concordance concerning autoimmune disorders, confirming that genetic and environmental factors are not the only cause of autoimmunity[2]. Nowadays, despite autoimmune diseases have been considered rare, they have been demonstrated to affect 3–5% of the population[2]. Within the different diseases, autoimmune thyroid disease and type I diabetes represent the most diffuse conditions[2]. Ernst Witebsky described the characteristics of autoimmune diseases with his postulates, which are similar to the Koch's postulate on infectious diseases. To classify a disease as autoimmune firstly pathogenic antibodies or pathogenic T-cells must be recognized as the cause of the disease; secondly, it must be possible to induce the autoimmune disease in experimental animals; and finally, clinical circumstantial evidence is needed, meaning that the same individual/family should have an association with other immune conditions[5]. After the Witebsky's postulates, in the early 1960s the term 'hypersensitivity' was coined and was determined to describe these autoimmune reactions[6]. Gell and Coombs postulates described in this way the different types of hypersensitivity[8]. The Gell and Coombs's classification, which has been published more than 30 years ago, is still broadly used to describe autoimmune reactions[7]. The classification divides the autoimmunity into four different types, according to the causes and effects: immediate hypersensitivity (type I), antibody-mediated hypersensitivity (type II), immune complex-mediated hypersensitivity (type III), and delayed-type hypersensitivity (type IV)[6,7]. Amongst them, type II hypersensitivity refers to the autoimmune diseases caused by antibodies against self-molecules[8,9]. This type of disease is diagnosed by the presence of autoantibodies in serum, whereas antibodies arise from antibody-secreting cells and self-reactive B cells[9,10]. A well-known example of type II hypersensitivity disease is represented by myasthenia gravis. This disease affects the neuromuscular junction and the main symptom is a characteristic muscle weakness. Myasthenia has been formerly reported to fulfill the criteria of the Witebsky postulates because pathogenic antibodies have been identified. The disease has been induced in experimental animals and the patients have clinically improved following a plasma exchange[11]. In myasthenia gravis, antibodies of the IgG class have been identified and isolated at the neuromuscular junction (NMJ), causing the loss of NMJ function and resulting in muscle weakness[12].

1.2 Physiology of the Neuromuscular Junction

The neuromuscular junction (NMJ) is the synaptic connection between the motor nerve end terminal and the muscle, where there is the transmission of action potential from the nervous system to the muscle[12]. The terminal axon sprouts innervate the myotubes, and the space between the nerve end and the muscle membrane is referred to as the synaptic cleft[13,14]. This area, including the cleft and the postsynaptic membrane of the fiber, is named neuromuscular junction[14]. The role of the NMJ is to

transmit the contraction stimulus from the nerve to the muscle[15]. The transmission begins when an action potential stimulates the distal motor nerve, resulting in an opening of Ca2+ ion channels throughout the nerve membrane[13]. The Ca+ influx induces an increase of Ca2+ level throughout the nerve. This causes the synaptic vesicles, concentrated in specific sites of the plasma membrane called "active zones", to have a Ca^{2+}-triggered fusion with the nerve membrane[13]. The fusion allows the release of the vesicle content, acetylcholine (Ach), into the synaptic cleft. The signal is then received by acetylcholine receptors (AChR) located at the postsynaptic muscle membrane[14]. The binding of Ach with the receptors represents the signal to open Na+ ion channels, prompting an influx of ions. This influx results in the depolarization of the membrane, enabling muscle contraction (Figure 1)[18].

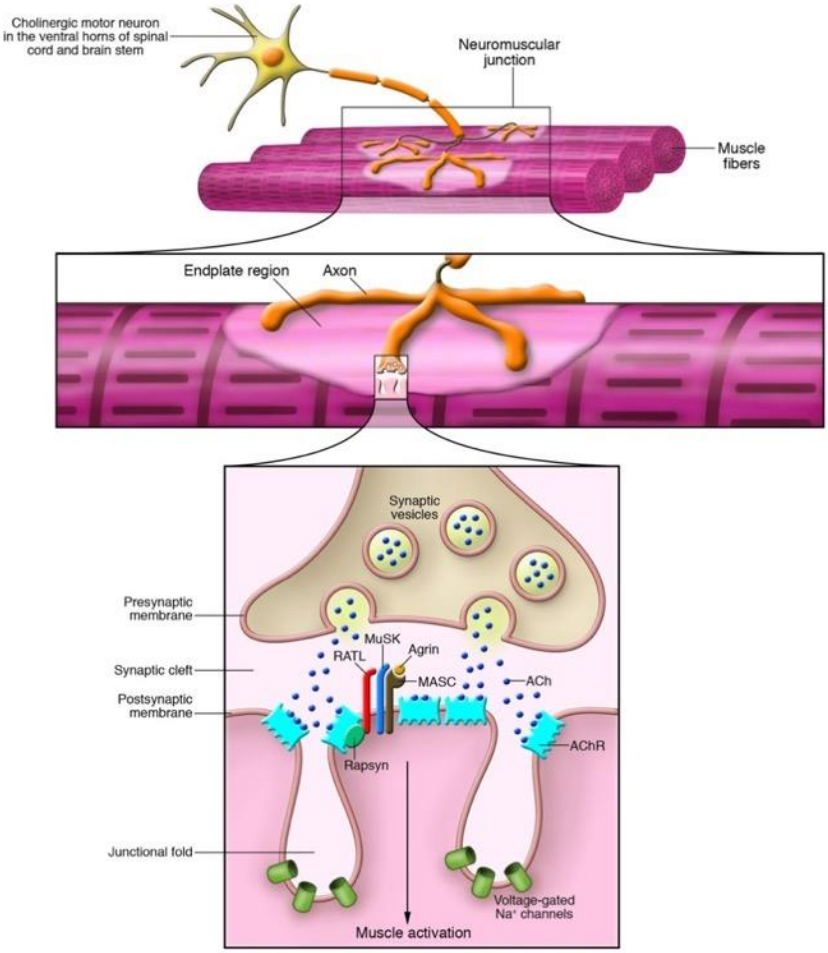

Figure 1: A schematic representation of the neuromuscular junction. Each branch of the motor neuron innervates more muscle fibers. At the NMJ, the end of the nerve has a button shape, in which Ach-loaded vesicles are accumulated. The nerve and the postsynaptic membrane are separated by the area referred as to the synaptic cleft. The NMJ postsynaptic membrane has several folds, containing many ion Na+ channels. On the top of the folds, AChR is densely clustered. When the nerve action potential arrives, the increase of Ca2+ causes the fusion of the vesicles with the membrane and the following release of Ach in the synaptic cleft. Ach binds to the clustered AChR on the muscle membrane, and this phenomenon triggers the opening of the ion Na+ channels. The following influx of Na+ ions allows the muscle to contract. The additional proteins in the picture are rapsyn, MuSK, and agrin[14,15]. These proteins are located in the closeness of AChR due to their role in clustering and maintenance of the postsynaptic area. MASC, myotube-associated specificity component, proposed to be a binding site for agrin[17]; RATL, rapsyn-associated transmembrane linker, proposed to be associate with the clustering machinery for AChR[18]. Extracted from [16].

1.2.1 Development and maintenance of the neuromuscular junction

The postsynaptic membrane is a specialized area that provides a rapid response to Ach. The formation and maintenance of this area are tightly regulated by various proteins from the basal lamina and the cytoskeleton of the muscle fiber[19]. During the development of the NMJ one of the first events is the release of agrin and of other neuroregulins [19]. The release of agrin from the nerve represents the early signal which induces AChR and the other proteins of the muscle synapse to accumulate, determining the area referred to as the motor endplate [20,21]. AChR subunit genes are expressed in myoblasts at a low level, increasing their expression during the differentiation. This process allows the formation of the contractile apparatus. The AChR subunits are translated and expressed in the plasma membrane, in a diffuse localization on the muscle fiber[25]. Strictly associated with the clustering of AchR and maintenance of the postsynaptic apparatus, there is the cytoskeletal machinery (Figure 2). An additional proposed role of the cytoskeleton is to decrease furthermore the amount of AChR expressed in the non-innervated regions of the myotube[20]. This complex has not fully been understood yet and comprises a large number of different proteins with structural and support roles for the myotube[25]. Within the different cytoskeletal proteins, a lot is known about rapsyn, utrophin, and α-dystrobrevin-1, which are colocalized with AChRs and are involved in the process of clustering[26,23]. Dystrophin and α-dystrobrevin are concentrated at the depths of folds[29] that anchors the sarcomere, through actin filaments, to the sarcolemma of the muscle[28]. In skeletal muscle dystrophin is additionally associated with many other sarcolemmal glycoproteins, resulting in a large oligomeric complex, the dystrophin-glycoprotein complex (DGC)[30,31]. Within the DGC, a specific complex has been identified as "the sarcoglycan complex", composed of α-, β-, γ- and δ-sarcoglycans[31]. The sarcoglycan complex has functions which are not fully understood yet, but this complex is believed to have both mechanical and signaling roles[33]. Dysferlin, a membrane- associated protein, notwithstanding its close location to the complex does not appear to have an interplay with the DGC. This protein is highly expressed in myotubes and appears to be involved in different processes of muscle repair[34]. Studies have shown that it might regulate vesicle fusion with the sarcolemma in the areas of muscle injury [35]. Beneath the sarcolemma, desmin protein, an intermediate filament, connects the whole myofibrillar apparatus to the sarcolemma[36]. Together, the cytoskeleton proteins and the motor endplate then serve as a scaffold for several molecules involved in binding to the extracellular matrix[22]. The major components of muscle extracellular matrix are represented by collagen IV, laminin, entactin, and heparan sulfate proteoglycans. These proteins are involved in the mechanical proprieties of the muscle, as well as a representation of a reservoir for growth factors and several bioactive molecules[37].

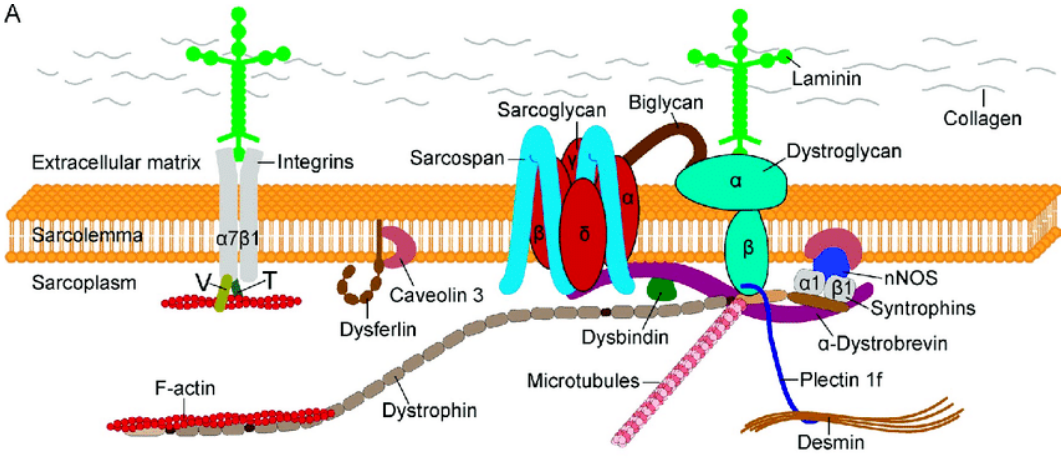

Figure 2: Schematic overview of the principal cytoskeletal and extracellular matrix proteins. The dystrophin-associated protein complex represents is a group of heterogeneous proteins. The main sarcoplasmic proteins are α-dystrobrevin, syntrophins, and nNOS; the transmembrane ones are represented by β-dystroglycan, sarcoglycans, caveolin-3, and sarcospan and some of them have an extracellular location, such as α-dystroglycan. These proteins are involved in the link of dystrophin to the extracellular matrix. Dystrophin complex is also liked to desmin, via α-dystrobrevin-syncoilin, providing a mechanical link to the fiber. Finally, dysferlin and caveolin are implied in injury repair of the muscle. Extracted from [38].

1.2.2 AChR clustering

The clustering of AChR outlines one of the fundamental mechanisms for the proper signal transmission at the NMJ. As previously mentioned, the clustering process is performed and maintained by several different proteins. Within the most known proteins required for the clustering process it is reasonable to mention rapsyn, agrin, MuSK, Lrp4, and Dok7 [39] (Figure 3). The clustering process starts when agrin, released from the nerve, binds to Lrp4. The binding enables the molecules to form a complex that dimerizes, forming an agrin-Lrp4 tetramer[41]. The tetramer stimulates MuSK, a co-receptor on the extracellular domain, leading to a conformational change and a consequent autophosphorylation[41]. MuSK activation, at the same time, allows the interaction of the protein with Dok7, a cytoplasmatic protein. Dok7 owns a phosphotyrosine-binding domain and a C-terminal region, in which tyrosine residues are present for phosphorylation[42,43]. Following MuSK activation there is an activation of the signaling pathway that causes the accumulation of AChR and the cluster stabilization. Together with those mechanisms, agrin stimulates also the AChR interaction with rapsyn, promoting the binding of AChR with the cytoskeleton and the subsequent remodeling of the clusters[44]. Previous studies have confirmed that rapsyn, which interacts directly with AChR, it is crucial for clustering and stabilization playing a structural role in those processes[45]. Despite not all the mechanisms behind the clustering of AChR have been fully understood yet, the above-mentioned proteins seem to have a structural role in this phenomenon. Different studies performed on animal models deficient in agrin, MuSK, Lrp4, or Dok7 confirmed that the loss of these proteins leads to a failure of postsynaptic NMJ development, and the animal died slightly after birth [46].

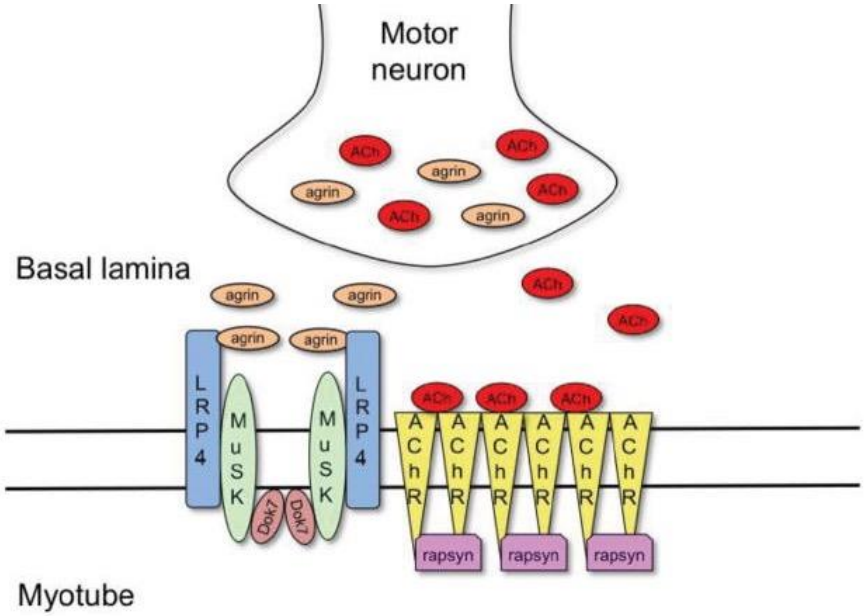

Figure 3:Schematic representation of the proteins involved in clustering of AChR. The clustering process promoted by the agrin-Lrp4-MuSK complex; AChR is linked to rapsyn, which connects the clusters to the cytoskeleton. Image extracted from [40].

1.2.3 Model organisms for the NMJ

For a long time, studies have attempted to reveal the different mechanisms underlying the development and maintenance of NMJ. Nevertheless, they have not fully been understood yet. Numerous diseases affecting the involved proteins resulted in muscle degeneration[,38,39], and for this reason several studies have been attempting to fully characterize this phenomenon. However, the high complexity and the large number of proteins involved in NMJ development and maintenance make *in vivo* studies particularly challenging to perform[46]. To overcome this problem, several *in vitro* models investigating the NMJ have been developed, representing an important tool to study the molecules and the events involved in the process[47,49]. Different methods have been described in literature, including the use of both primary muscle cells and immortalized cell lines [49,53]. Different studies, nevertheless, indicated the immortalized C2C12 mouse cell line and L6 rat cell line as the main tool for the NMJ developmental studies[51,52]. The C2C12 cells are derived from murine skeletal muscle, are a well-established line, and different culturing and differentiation protocols are well known [51,53]. Additionally, despite human primary cells, C2C12 myoblasts undergo also the remodeling process to form mature postsynaptic apparatus[52]. As discussed before, the secreted agrin from motor neurons activates the process of AChR clustering during NMJ development. In C2C12 it is possible to induce this phenomenon by adding neural agrin to the medium, without the need for co-cultures[55]. This permits also the study of the expression of muscle-specific genes, the detection of the associated proteins and the study of a fully remodeled postsynaptic membrane without the presence of the nerve[51,52]. L6 are another valuable tool to study *in vitro* muscle without the need for animal models[53]. As C2C12, they are shown to express most of the NMJ proteins, and with agrin it is possible to induce the clustering of AChR[49]. The different immortalized cell lines have represented until now one of the most worthy tool to study and characterize the roles of the different molecules in myotube growth and disease[51].

1.3 Satellite cells

Skeletal muscle is composed of striated myofibers, each one formed by elongated and multinucleated myotubes. After the birth, the number of differentiated fibers in the body does not increase in quantity but grows in volume[58,59]. Nevertheless, the muscle has still the ability to regenerate itself after injury[60]. Skeletal muscle has a high regeneration capacity, with the rapid repair of full strength even after severe damage[61,62]. As muscle myotubes cells are terminally differentiated, muscle repair and regeneration are performed by the stem cell population. Satellite cells, which are the postnatal adult muscle stem cells, differentiate in myogenic cell lineage and fuse in order to form a new myotube. Satellite cells represent mitotically quiescent cells, which are located between the basal lamina and the plasma membrane of the myofibril[61,62] (Figure 4). After muscle injury, different signaling molecules and epigenetic regulatory factors[63] activate satellite cells.

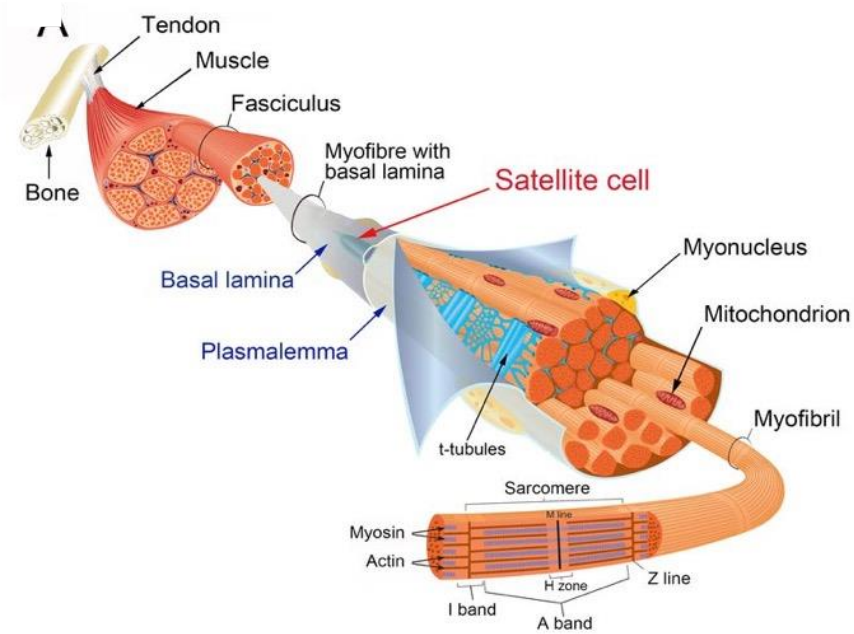

Figure 4: Schematic representation of the muscle fiber structure highlighting the satellite cell niche. Image from [62].

Committed myogenic cells, including the satellite cells after injury, are characterized by the expression of different regulatory factors which might be used as biomarkers for their identification (Figure 5)[57,61]. The process of myogenesis is tightly controlled by a set of regulatory factors named myogenic regulatory factors (MRF)[57]. The MRF family is composed of four main transcription factors: myogenic differentiation factor (MyoD), myogenin (MyoG), myogenic factor 5 (Myf5), and myogenic regulatory factor 4 (MRF4)[57]. The presence of one or more MRF factors has been shown to commit also different cell types to myogenesis. The expression profile of the different MRF changes before, during and after the differentiation of the cell (Figure 5). During development and in injury repair, Myf5, MyoD, and MRF4 are expressed, directing stem cells to the skeletal muscle cell lineage. After, during the differentiation, the expressed factors are MyoG, MyoD and MRF4[61]. MyoD, which is the only factor expressed at different steps of the differentiation, is a well-studied molecule with a helix–loop–helix structure. It is expressed both in proliferating myoblasts and differentiating ones[61]. Nevertheless, after the differentiation of the cells, MyoD is not detectable

anymore in the nuclei [64]. Differentiated cells require distinct biomarkers than MRF. Myogenin, a myogenic regulatory protein[67], has been extensively used as a biomarker for myotubes. An additional molecule that can be used as a biomarker for terminally differentiated cells is desmin[65]. The formerly mentioned intermediate filament is expressed in terminally differentiated skeletal muscle cells, thus indicating that they have exit the mitotic cycle[66].

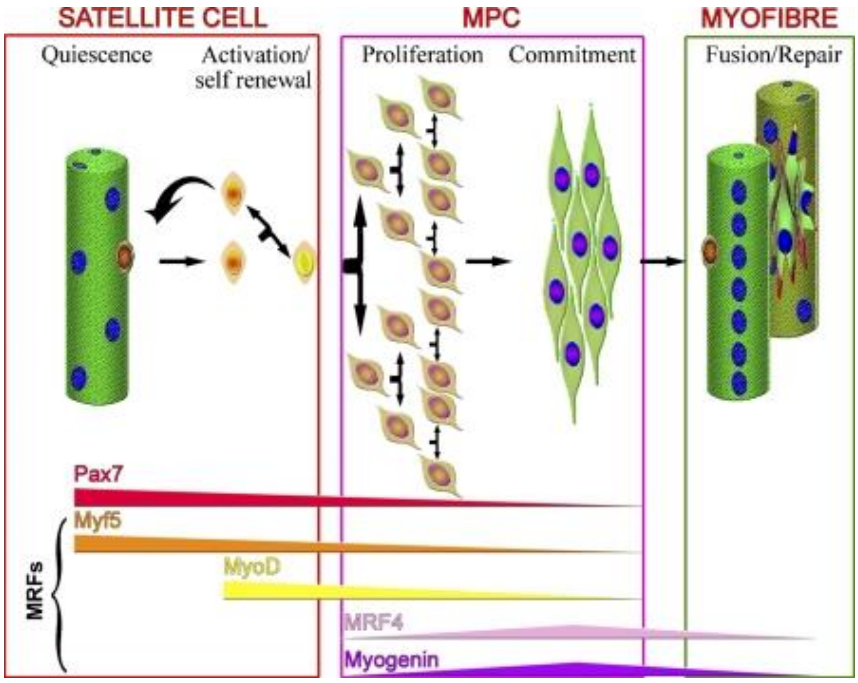

Figure 5: Schematic representation of the myogenic lineage progression. Satellite cells, when quiescent, are characterized from the expression of Pax7 and Myf5. Following activation, the cells express MyoD and Myf5, and proliferate. The pool of muscle precursor cells (MPC) represents the committed muscle cells. MPC start then to express MRF4 and myogenin, fusing and differentiating into myotubes. The pool of cells that do not divide, and come back to the satellite niche, downregulate MyoD and come back to the quiescent state. Figure from[68].

The use of primary satellite cells to induce myoblast cultures is a key tool for the study of muscular diseases, due to the absence of side effects typical of the immortalization process. Primary muscle cell cultures allow having a reliable representation of the physiological development and the expressed molecules in the muscle. Diverse methods have been described in literature to isolate skeletal satellite cells. Amongst them, the mainly practiced method have been the enzymatic digestion of the muscle biopsy, following the culture of the satellite cells on dish. The other reported method implied the isolation of the satellite cell from its niche in the myofiber. Within the two methods, the first one has a major risk of having fibroblasts contaminated cultures, although the second one is technically more challenging[58]. Notwithstanding the chosen method, myogenic progenitors can be isolated from skeletal muscle and differentiated, allowing the study of muscular development physiology. This method has been used for the identification of unknown antigens at NMJ. However, in contrast with mouse and rat models, in human myotubes it has not been possible until today to induce an AChR clustering and complete remodeling of the postsynaptic machinery (Figure 6). Several studies have compared the clustering and remodeling of postsynaptic machinery in C2C12 with the results achieved in humans[123]. Until now, no studies without electrical stimulation or co-

culture with the nerve showed significant results, confirming that the entire machinery is required for the clustering in humans and probably there are some proteins that satellite cells in culture are not able to express[54].

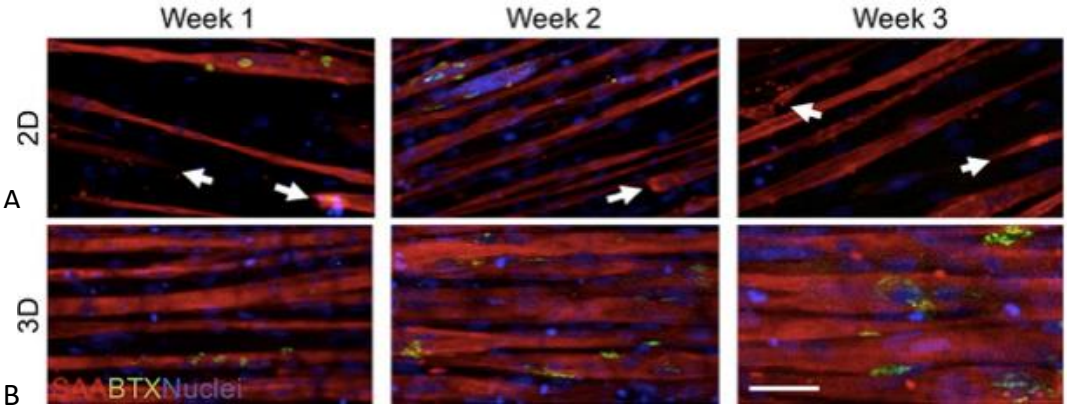

Figure 6:Human myoblast in culture, 2D classical technique and 3D technique. Nuclei in blue, AChR in green and membrane in red; a) human primary myotubes culture without external innervation; b) co-culture with nerve cells, fully developed postsynaptic membrane. Extracted from [54]. Arrows indicates broken muscle fibers in the 2D culture, indicating that the muscle without proper postsynaptic development is additionally more fragile compared to the innervated one.

1.4 Myasthenia Gravis

Myasthenia gravis (MG) is an autoimmune disease that affects neuromuscular transmission[69]. As above discussed, in MG pathogenic autoantibodies attack different proteins of the NMJ. This provokes a decrease of Ach binding to its receptors, a phenomenon that prevents endplate potential and sequent muscle contraction (Figure 7)[73]. As a consequence, the main symptom of MG is skeletal muscle weakness. The age of onset, as well as the severity of the symptoms, is highly variable within individuals[71]. The muscular weakness occurs within specific muscle groups[72]. If the ocular muscles are affected, it leads to drooping eyelid or double vision. If bulbar muscles are affected, the main symptoms are dysarthria and dysphagia. Finally, if also limb and the respiratory muscles are affected, the main symptoms are orthopnea, tachypnea, and respiratory failure[70]. The most common age of MG onset is between 20 and 40 years, with an incidence between 0.25 and 20 per million each year[71]. It is considered a rare disorder, and 30% of patients have other autoimmune diseases[71,72]. In 85% of MG patients the detectable antibodies are directed against the AChR. The percentage highlight that this represents the most common type of MG. Around 50% of the remaining MG patients displayed autoantibodies towards MuSK. Among the remaining patients, conventional assay could not detect the presence of autoantibodies against AChR and/or MuSK[73].

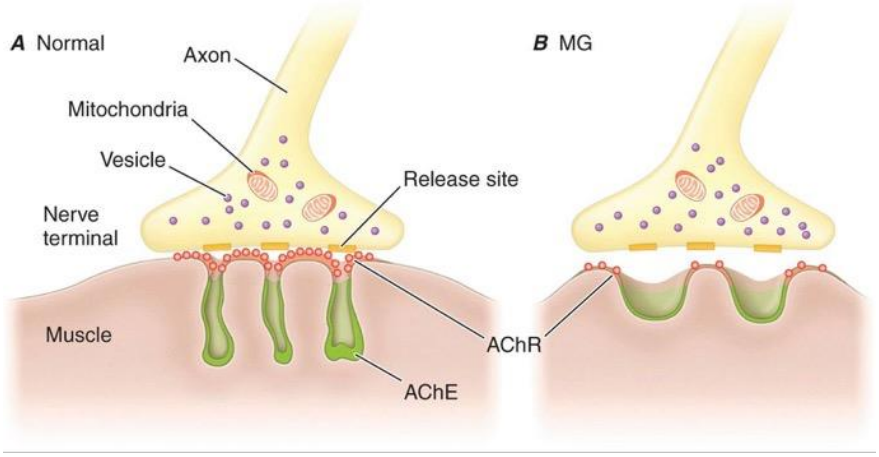

Figure 7: Schematic representation of normal and myasthenic neuromuscular junctions; a) the normal neuromuscular transmission, described in 1.2; b) reduced number of AChR, flattened folds. Image extracted from [74].

1.4.1 AChR-associated MG

As above discussed, AChR are transmembrane proteins that are responsible for the binding of acetylcholine, a neurotransmitter, at the postsynaptic region of NMJ[75]. In AChR MG, it is possible to identify three major subtypes of the disease (Table 1). The Early-onset MG (EOMG) is characterized by an onset of the disease prior the 40th year. In this group, it is possible to detect a male:female ratio of 1:3. Extraocular muscle weakness has been described as the most common symptom of this type of MG[75]. It is characterized, besides, by hyperplastic thymus glands and this group is generally treated with thymectomy and sequent immunosoppression[76]. The second group of AChR MG is represented by late-onset MG (LOMG). In this group the male:female ratio is 1.5:1, the disorder is characterized by an age of onset after 50 years and the thymic hyperplasia is rare. Furthermore, there might be present also antibodies directed against other proteins of the AChR clustering machinery[76,77]. The main symptoms detected in patients with late-onset MG do not differ much from those observed in patients with early-onset MG, although the disease is likely to be more severe in patients in whom MG develops after the age of 50 years[77]. The third main group of MG is the thymoma-associated MG (TAMG). This group represents about 10% of the anti-AChR MG, producing autoantibodies against several other neuromuscular antigens in addition to AChR[78].

MG subtype	Age at onset	Thymic histology	Muscle autoantibodies
Early onset	<40 years	hyperplasia	AChR
Late onset	>40 years	normal	AChR titin, ryanodine
Thymoma	any age; peak at 40–60 years	neoplasia	AChR titin, ryanodine
Generalized low-affinity AChR antibodies	variable	hyperplasia in some	antibodies against clustered AChR
Ocular	variable	unknown	AChR (50%)

Table 1. Overview of the different clinical subgroups of myasthenia gravis. Focus on age of onset, thymic histology and antibodies. Extracted from[75].

1.4.2 MuSK-associated MG

MuSK MG is a rare subtype of MG characterized by different pathogenesis and more severe symptoms[79], and different clinical features compared to the AChR-positive MG. This subtype of MG has an overall prevalence of 5–8% among MG patients and 37% among AChR antibody-negative MG patients[80]. This type of MG affects mostly females, and the age of onset is around the fourth decade for the majority of patients[81,82]. MuSK-associated MG symptoms evolve more rapidly compared to other types of MG and is characterized by bulbar muscles affected in the early stage[80].

1.4.3 Pathogenic mechanism of antibodies against AChR

The antibodies identified in MG pathogenesis appear to belong to the IgG class. The IgG antibodies have two structurally different regions, referred to as the Fc and the Fab region. The Fab region (fragment antigen binding) contains both the variable regions of the heavy and the light chain. This region is committed to antigen recognition and specific binding. The Fc region (fragment crystallized)[84] is composed of the constant region of the antibody, with the two heavy chains. The Fc region is involved in the determination of the antibody class, subclass, localization and effector mechanism[82] (figure 8). The IgG subclass represents the most abundant class in human serum. The four different antibodies classes differ in their constant region and in the response that they activate. The activated mechanisms can include complement system activation, opsonization, blocking receptors or the formation of immune complexes[84].

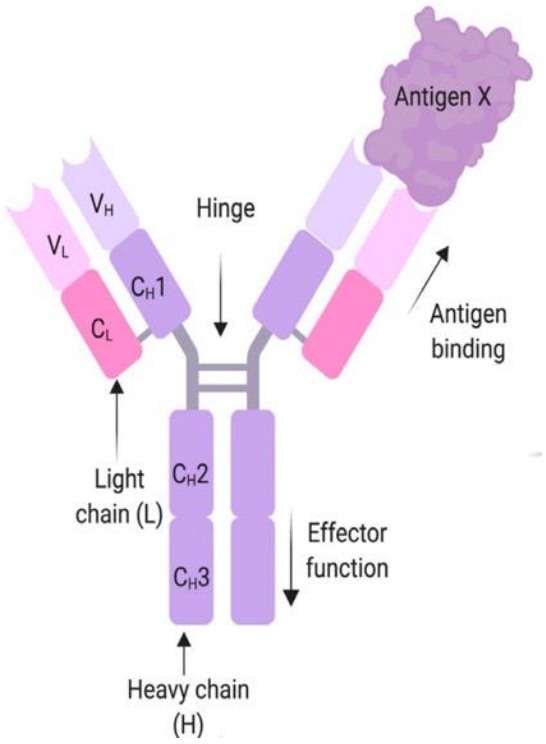

Figure 8: Schematic representation of the structure of IgG antibodies. Extracted from [82].

The autoantibodies of MG against AChR arise from the IgG1 and IgG3 subclasses. These types of antibodies can activate the complement cascade as an effector mechanism, leading to the destruction of the postsynaptic region[85]. The activation of the complement leads to a severe loss of AChR and destruction of the postsynaptic architecture[86,82]. A second pathogenic mechanism of anti-AChR antibodies is the binding and cross-linking of AChR[82]. This can cause the endocytosis of the receptor, reducing the density of AChR and the transmission. The third proposed mechanism of pathogenicity is through the direct inhibition of AChR by the antibodies[82,87]. All these mechanisms together lead finally to a deficient postsynaptic region, where the loss of AChR (figure 9) causes the loss of an efficient signal transmission[86,82].

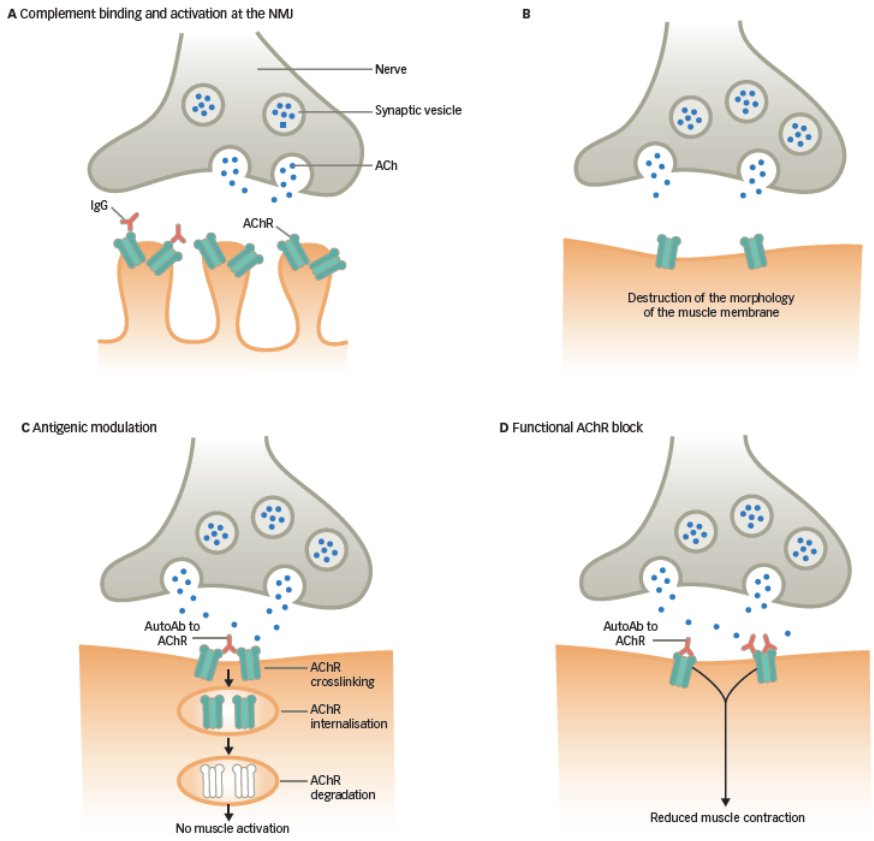

Figure 9: Schematic representation of pathogenic mechanisms of AChR MG antibodies. a) and b), antibody binding and complement activation led to the destruction of postsynaptic architecture; c) single binding led to the internalization of AChR, leading to less signal transmission; d) binding of antibodies avoid Ach binding to the receptor, blocking signal transmission. Extracted from [34].

1.4.4 Pathogenic mechanism of MuSK antibodies

MuSK antibodies appeared to belong to IgG4 subclass. Among the IgG4 characteristics, the main studied has been represented by the Fab-arm exchange. In this process every IgG4 can exchange half-molecules with other IgG4, resulting in holding two different Fab regions[82]. This process makes IgG4 antibodies unable to activate any immunocomplex or complement. Different pathogenic mechanisms have been described for MuSK antibodies, even though IgG4 subclass is still under investigation to fully understand their pathogenicity[84]. MuSK antibodies have been shown to interrupt the agrin-Lrp4-MuSK complex, thus blocking the Dok7 signal pathway and inhibiting AChR clustering[88]. In figure 10 are proposed the pathogenic mechanisms by which MuSK antibodies can affect the clustering of AChR[87]. In the first proposed mechanism, antibodies bind monovalently MuSK avoiding the formation of the Lrp4-MuSK[89] complex, inhibiting the whole clustering process. A second proposed mechanism is that bivalent binding to MuSK could lead to the independent activation of MuSK, thus activating ectopic AChR formation. However, these mechanisms are still under investigation[90,91].

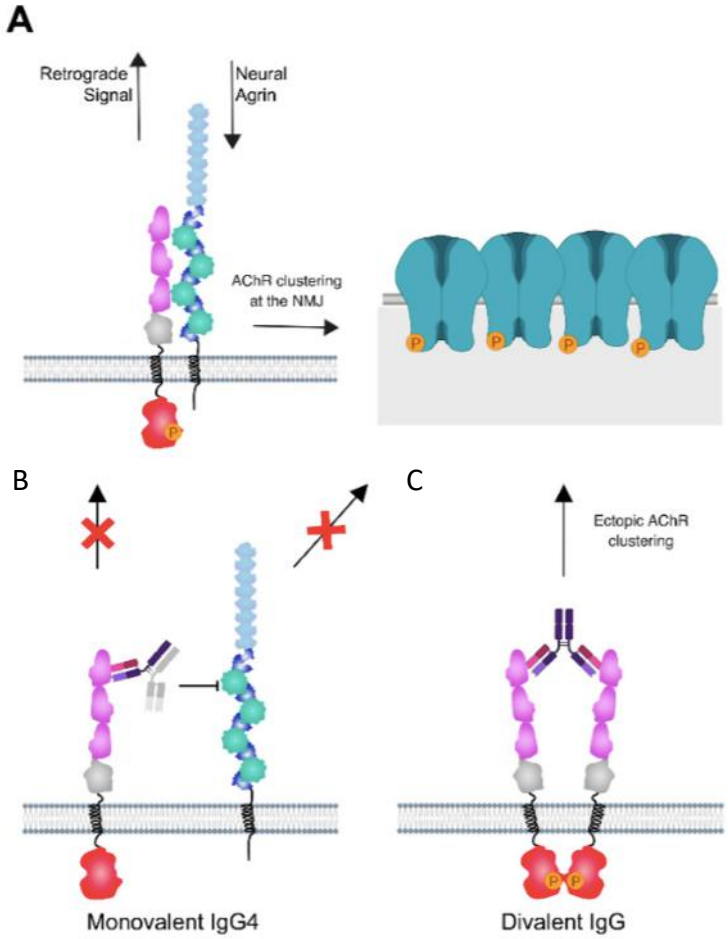

Figure 10:Schematic representation of the pathogenic mechanisms of MG autoantibodies at the NMJ; a) representation of the healthy NMJ, in which agrin/Lrp4/MuSK complex are normally activating, allowing the cluster of AChR; b) monovalent binding of IgG4 led to the interruption of clustering signal pathway. Moreover, the impossibility of a retrograde signaling from Lrp4 to the nerve is thought to influence the NMJ; c) the divalent binding of the IgG4 led to the activation of MuSK independent from the complex, thus stimulating ectopic AChR. Figure extracted from [82].

1.4.5 Seronegative MG

Seronegative myasthenia gravis (SNMG) is used to define patients with clinically diagnosed MG, but don't have detectable antibodies[92]. SNMG patients represent about 15 to 20% of total MG patients[71] and are represented predominantly by females, with a 5,5:1 female: male ratio[70]. The majority of SNMG have a late onset of the disease with mild symptoms, and the muscle group predominantly involved is the ocular muscle group[95]. However, a group of SNMG displays early onset of the disease, distinguished by more severe symptoms[96]. SNMG patients are normally treated with immunosuppression, but the response to the treatment is highly variable, and only 8% of patients showed a remission at follow-up[93,95]. Different studies assess that in approximately 10 to 20% of SNMG, neither anti-AChR nor anti-MuSK antibodies could be detected[85,92]. Autoantibodies against AChR that are isolated from the sera of SNMG patients through different diagnostic tests are considered "low affinity", since they can bind only to clustered AChR and to the native conformation protein. Low affinity antibodies have been found in approximately 66% of generalized MG patients,

which resulted to be negative with standard diagnostic AChR MG tests[72]. For the anti- MuSK antibodies[96], there is the need for a specific test due to the low titration of antibodies in the serum of the patients. The diagnosis of MG is performed by different standardized routine assays. The main used assays are radioimmunoprecipitation (RIPA) and enzyme-linked immunosorbent assay (ELISA). Cell-based assays (CBA) is a more sensitive test that has been developed to detect antibodies against AChR and MuSK after a negative result with RIPA and ELISA. In CBA for AChR, HEK293 cells are transfected with plasmids expressing the five different subunits of AChR complex and rapsyn, resembling on the surface of the cells the AChR in its native state and clustered. MuSK CBA is performed by transfecting the cells with plasmids expressing MuSK. After the transfection, there is an overexpression of the antigen in its native state, which increases the sensitivity of this assay and enables the detection of low affinity or low concentration antibodies[97]. With this test, the seronegative percentage decreases from 30% to nearly 5-10%. The use of different assays allowed the detection of antibodies against other proteins of the NMJ, such as antibodies against Lrp4, agrin, or ColQ[98]. Despite the identification of those involved molecules, MG with anti- Lrp4, agrin, ColQ antibodies still fails in the fulfilling of the Witebsky criteria. For these antibodies the pathogenic mechanism has not been understood yet[99,97]. Another feature of some seronegative patients is the presence in the serum of striational antibodies, against different epitopes of the muscle[95]. Despite the fact that their pathogenic role is still unknown; these antibodies are known to bind in a cross-striational pattern different epitopes of muscle proteins such as titin or ryanodine[102]. As of now, they are commonly used as biomarkers for thymoma or for thymectomy outcome[103]. The presence of around 15% of MG patients without known antibodies indicates that are still unknown autoantibodies involved in the pathogenesis of SNMG[94,95].

1.5 Aim of the study

SNMG patients have unknown antibodies against yet undiscovered antigens at the NMJ. The identification and the characterization of these antigens and antibodies may contribute to a better knowledge of the NMJ, but also enhance the treatment strategies for these patients. This study aims for establishing new approaches for the detection of seronegative patients' antibodies and antigens. Throughout different assays, this study has the goal to isolate from the cohort of clinically diagnosed SNMG the patients without detectable antibodies against MuSK or AChR. After the identification of SNMG patients, the presence of clustered AChR in primary human muscle cells will allow the isolation of SNMG pathogenic antibodies. Furthermore, the use of human primary muscle cell cultures can enable us to screen for the presence of those antigens at the NMJ. In conclusion, the methods should lead to the isolation of antibodies and/or antigen candidates for SNMG patients.

2 Materials and Methods

2.1 Materials

Product name	Product number	Company
DMEM	D6429	Sigma- Aldrich
DMEM	D5796	Sigma- Aldrich
Ham's F-12 Nutrient Mix	11765054	Thermo Fisher Scientific
DMEM GlutaMAX	10566016	Thermo Fisher Scientific
DPBS	14190136	Thermo Fisher Scientific
DMSO	A36720100	AppliChem GmbH
Trypsin-EDTA	25200056	Thermo Fisher Scientific
FBS	A2720801	Thermo Fisher Scientific
Penicillin-Streptomycin	15140122	Thermo Fisher Scientific
Gentamicin (10 mg/mL)	15710049	Thermo Fisher Scientific
Poly L-Lysine	P4832	Sigma- Aldrich
HEPES (1M)	15630080	Thermo Fisher Scientific
Dexamethasone	MFCD00064136	Thermo Fisher Scientific
Glutammine	25030149	Thermo Fisher Scientific
Glucose	A2494001	Thermo Fisher Scientific
Sucrose	15503022	Thermo Fisher Scientific
Lipofectamine™ 2000 Transfection Reagent	11668030	Invitrogen
Insulin	11070-73-8	Sigma - Aldrich
RIPA Lysis Buffer, 10X	20-188	MilliporeSigma
Pierce Protein A/G plus, agarose beads	8159680747	Thermo Fisher Scientific
DNA LoBind® Tubes 1.5 mL.	0030108051	Eppendorf
5x Sample Buffer	MB01015	GenScript
SurePAGE Bis-Tris 4-20% gradient Gel, precast, 10 wells	M00655	GenScript
Protease Inhibitor Cocktail	P8340	Sigma Aldrich
MOPS Gel Running Buffer powder	M00138	GenScript
Amphotericin B	A2942	Sigma Aldrich
collagenase type II	17101015	Thermo Fisher Scientific
Target2™ PVDF Syringe Filters	F2500-6	Thermo Fisher Scientific
Corning®-Zellsieb	CLS431750	Sigma Aldrich
Opti-Mem	11058021	Thermo Fischer Scientific
Aqua-Poly/Mount	18606-20	PolySciences
Escherichia coli DH5alpha	18265017	Invitrogen
QIAGEN® Plasmid Maxi Kit	12162	QUIAGEN
NanoDrop	ND-2000	Thermo Fisher Scientific

Laminin from Engelbreth-Holm-Swarm murine sarcoma basement membrane	MFCD00081739	Sigma Aldrich
Fibronectin	MFCD00131062	Sigma Aldrich
Permanox slides	160005	Thermo Fisher Scientific
Flexi-perm 8-well grid	6032039	Sarstedt
Lowry Protein Assay Kit	23240	Thermo Fisher Scientific

2.2 Antibodies

Product name	Product number	Company	Dilution	Assay
Alexa Fluor-594 conjugated bungarotoxin	B13423	Invitrogen	1:3000	TBA, Staining of AChR
Goat anti-human IgG, Alexa Fluor 488	A32723	Invitrogen	1:750	TBA
Goat anti-rabbit IgG, Alexa Fluor 488	A32731	Invitrogen	1:750	Fluorophore
Donkey anti-Mouse IgG, Alexa Fluor 594	A32744	Invitrogen	1:750	Fluorophore
Goat anti-human IgG, Alexa Fluor 594	H14101	Invitrogen	1:750	CBA
Anti-mouse IgG, HRP conjugate (anti-mouse polyclonal antibody in goat);	P 0447	Dako	1:1000	Western Blot
Purified anti-LRP4 (NH2 terminus) Antibody	MMS-5154	BioLegend	1:1000	Western blot
Monoclonal Anti-β-Actin−Peroxidase antibody produced in mouse	A3854	MilliporeSigma	1:2000	Western blot
Mouse anti-human MyoD antibody	MA1-41017	Invitrogen	1:200	Staining of Human myotubes-myoblasts
Mouse anti-human desmin antibody	MA5-16357	Invitrogen	1:100	Staining of Human myotubes
Mouse anti-human dysferlin Antibody	PA5-53546	Invitrogen	1:10	Staining of Human myotubes
Rabbit anti-human IgLON5 Antibody	Ab122763	abcam	1:200	Staining of Human myotubes

2.3 Cell Culture

All the experiments with cell lines have been performed in a laminar flow hood under aseptic conditions. For the experiments human muscle cells, HEK 293, L6C11 and C2C12 have been used.

MEDIUM RECIPES

Human growth medium stock	Ham's F12, 20% FCS ,50µg/ml Fetuin, 7mM glucose, 4mM glutamine, pen/strep 5ml, 2.5µg/ml amphotericin B
L6 growth medium	DMEM D5796 high glucose, 10% FBS, 1% pen-strep
C2C12 growth medium	DMEM D6429, 15% FBS, 1% pen-strep
HEK 293 growth medium	DMEM D6429, 10% FBS, 1% pen-strep
Human growth medium	100ml stock solution GM, Fgf 8ng/ml 8µl, Egf 20ng/ml 2µl, 400ng/ml dexamethasone (stock: 0.2mg+ 200µl sterile water), 200ng/ml insulin
Human differentiation medium	DMEM/Glutamax 10566016, 2% horse serum, 4mM glutamine (L-Glu), 100ng/ml insulin 0.1µg/ml gentamicin, 4ng/ml dexamethasone
L6/C2C12 differentiation medium	DMEM D6429, 2% horse serum, 1% pen-strep
Wash medium	DMEM D6429
Freezing medium	GM, 10% DMSO
Dissociation solution	KCl 5.4mM, glucose and sucrose 25mM, gentamycin 0.05mg/ml, trypsin 2.5 mg/ml, collagenase type II 220 U/ml, dissolved in 1x PBS (no Ca+, no Mg+) and pH 7.4.

Table 2: Recipes of the different media used in cell culture

2.3.1 Culture of HEK 293 and L6.C11

HEK293 cells were cultured in DMEM supplemented with 10% FBS and 1% pen-strep. Then, cells were incubated in an incubator at 37°C, 95% humidity and 5% CO_2. After reaching 80% confluence, the cells were split in order to maintain the culture and avoid early differentiation.

2.3.2 Culture of C2C12 cells

C2C12 mouse myoblasts were maintained in DMEM and were supplemented with 15% FBS and 1% pen-strep. They were then incubated at 37 °C in the incubator, with 95% humidity and 5% CO_2. After reaching 80% confluence, the cells were split in order to maintain the culture.

2.3.3 Isolation of Primary Muscle Cells from Muscle Biopsies

Cells were isolated from gracilis and semitendinosus muscle biopsies. Following ACL surgery, biopsies were provided a maximum of 3h post-surgery. The biopsy muscle has been placed in PBS without Ca++ and Mg++. Blood vessels and fat tissue were removed from the tissue under a dissection microscope, in a laminar flow hood. Following a proper removal, the muscle was minced

with sterile scalpels into about 0.5 mm pieces. The pieces were later transferred into a 50 ml falcon tube with 15 ml of dissociation solution, referred to as tube 1. Tube 1 was incubated in a water bath at the temperature of 37°C, slowly shaking for 1 hour. The supernatant was then aspirated and moved into a new tube (tube 2). The remaining 15ml of dissociation solution have been added to Tube 1 and incubated with the same conditions for an extra hour. Meanwhile, tube 2 was centrifuged for 5 minutes at 1200rpm. After centrifugation the supernatant has been discarded, and the pellet has been resuspended with 10 ml of PBS. After the resuspension the tube 2 was left at RT under the laminar flow. After the second incubation of tube 1 ended, the content of the two tubes was mixed. The remaining muscle pieces were triturated by pipetting against the wall of the tube approximately ten times. The tube was then filled with PBS up to 50 ml, centrifuged, and the pellet resuspended PBS. The solution was then filtered through cell strainer to remove the bigger pieces of muscle. The resulting solution has been then centrifuged for 5 min at 1200rpm, and the pellet resuspended in muscle HGM. The solution was then plated onto a cell culture dish of 60mm and incubated at 37°C. The dish has been checked every day to verify the attachment of cells. When patches of cells attached to the dish were visible, usually 7 to 10 days after the isolation, the medium containing debris was aspirated and the cells trypsinized and detached. After the trypsinization, the cells were resuspended in HGM and put back in the same plate. This process is called "spreading" and it was performed to avoid early differentiation of muscle cells.

2.3.4 Culture of Primary Muscle Cells

The human primary muscle cells were incubated at 37°C in the incubator. Cells were split when they reached 50% of confluency. Human muscle cells need to be at a density between 5000 and 7500 cells/cm^2, corresponding to 50% of confluence. This percentage has been used to avoid an early differentiation into myotubes. The seeding at the correct density allowed the cells to have a doubling time of approximately 1 to 2 days. Primary cells were trypsinized and resuspended with the protocol of paragraph 2.3.5. In order to have the correct density of cells in the dish, cells were counted after every trypsinization. The counting of the cells was performed into a Neubauer counting chamber and it was calculated the average cell count from each of the sets of 16 corner squares. Finally, the cell concentration has been calculated with the formula:

$$Number\ of\ cells\ per\ milliliter = \frac{number\ of\ counted\ cells}{number\ of\ counted\ squares} x\ chamber\ factor\ (10^4)$$

Finally, the proper dish was decided.

- Up to 2x10^4, the cells were cultured into a 24 well plate.
- Up to 7x 10^4, the cells were cultured into a 35 mm plate
- Up to 15x 10^4, the cells were cultured into a 60 mm plate
- From 4.5x 10^4 cells, were cultured into 10 cm plate
- If another amount was found during counting, cells were split on different plates.

Cells were then resuspended in HGM. Every time that cells undergo the process of trypsinization, their passage number increased. Newly isolated cells start from passage 0 (P0), after the first spreading they were P1, and so on. Cells were considered able to differentiate up to P10.

2.3.5 Splitting

When cells reached the desired confluence, the growth medium was removed and the plate was washed from residuals with 10 ml of PBS. In order to detach the cells, the dish was incubated for 5

minutes at 37°C with 5ml of trypsin-EDTA. The cells were then observed under the microscope in order to verify the detachment. The entire procedure was repeated every 5 minutes until all the cells are detached, up to a maximum time of 20 minutes. If cells result to be resistant to detaching, as it happened with human muscle cells, a first brief wash with trypsin was made before incubation with trypsin. After detaching of the cells, trypsin has been inactivated with DMEM (washing medium), centrifuged, and the cells were then resuspended in fresh GM. After this passage, the cells were counted, and the proper dish was chosen.

2.3.6 Freezing

To freeze the cells, the cell suspension after the trypsinization was resuspended in growth medium supplemented with 10% dimethyl sulfoxide (DMSO). The solution was transferred into a cryotube and placed at -80°C into a CoolCell® container. After 24h, the tube was removed from the cell container and stored in liquid nitrogen.

2.3.7 Thawing of cells

After having taken tubes from the liquid nitrogen, the cryotubes were transferred into a 37°C water bath until most of the solution was thawed and only a small part of ice was left in the tube. The entire content of the tube was transferred to a sterile 15 ml falcon tube. The cryotube was then washed with pre-warmed DMEM. The falcon tube was centrifuged for 5 min at 1200rpm RT. The supernatant, containing DMSO, was thrown and the pellet was resuspended in growth medium and plated entirely into the proper dish.

2.3.8 Differentiation of muscle cells

When cells reached 80% of confluence, the GM was switched to differentiation medium (DM- refer to table 2 for the recipes). The cells were then checked every day until myotubes were observed.

2.4 Cell-based Assays (CBA)

In the cell-based assay living HEK 293 cells were transfected to express AChR and MuSK. CBA allows the detection of anti-AChR/MuSK antibodies in the sera from SNMG patients. Sera for the CBA were available at the NeuroBiobank (Medical University of Vienna, Department of Neuropathology and Neurochemistry). These sera derived from diagnosed MG patients without detectable antibodies.

MEDIUM COMPOSITION

Blocking medium	200ml DMEM D6429, 2g BSA, 25mM HEPES
Wash medium	DMEM D6429

Table 3: Recipes of the different solutions used in CBA

2.4.1 Transfection of HEK293 with AChR and MuSK plasmids

For transfection, glass coverslips were placed into a 6-well plate, with four coverslips per well, and incubated with 0.01% Poly-L-Lysin (PLL) for 5 minutes. Following the incubation the PLL was removed and the coverslips were dry for 30 minutes in the laminar flow. Meanwhile, a plate of HEK293 cells was trypsinized and centrifuged. The pellet has been then resuspended with 10ml of HEK293 growth medium. After proper counting of the cells, a total of $2x10^5$ cells per well have been seeded and incubated at 37° for one day.
On the second day HEK293 cells were transfected using as transfection agent the lipofectamine.

- For AChR CBA, HEK cells were transfected with AChR α, β, γ, δ, ε subunits and rapsyn-GFP with the following concentrations: 2µg α,1µg β,1µg δ,1µg γ,1µg ε,1µg rapsyn-GFP per well. As a negative control, a well of HEK cells was also transfected with 1µg rapsyn- GFP.
- For MuSK CBA, HEK cells were transfected with 4µg of pIRES2-AcGFP1-MuSK per well. As a negative control, cells were transfected with 1µg of pIRES2-AcGFP1per well.

For each well, the respective amount of DNA has been added to 250µl of Opti-Mem. Simultaneously, 10µl of lipofectamine have been mixed with 250µl Opti-Mem. Both the solutions have been incubated for 5 minutes, then mixed and incubated for another 20 minutes under the laminar flow hood. Following this step, in each well were pipetted 500µl of the transfection mix and put in the incubator overnight at 37°C. On the third day, the efficacy of the transfection with GFP expressing plasmids has been verified under the microscope, checking while cells displayed a green fluorescence.

2.4.2 Incubation with human serum

If the cells show green fluorescence, the assay could be performed. On the same day, sera from MG patients, positive controls and healthy individuals were used to perform the CBA. 250 µl of the solution, composed of sera diluted 1:40 in blocking medium, were pipetted into each well. Following this a coverslip per well was added and incubated for 1 hour at 37°C. After the hour 3 steps of washing with 500µl of DMEM have been performed, with 10 minutes of incubation for each washing step. The cells have been fixed with 4% PFA, incubated for 10 minutes. After the incubation another washing has been performed. Following the fixing of the cells, the secondary antibody (goat anti-human IgG) has been pipetted. After 45 minutes of incubation in the dark, under the laminar flow, the cells were washed for 3 times with 500 µl PBS. Coverslips have been then mounted on

microscopic slides with 40µl Aqua-Poly/Mount. The analysis of the assay was then performed with fluorescent microscopy. A green signal indicates the transfection of the cells, while a red signal indicates that the patient has autoantibodies. As it is possible to see in figure 11, secondary antibody can bind to human antibodies, allowing their detection. Cells that showed both green and red signal were considered as positive, while cells expressing only the green signal were considered to be negative.

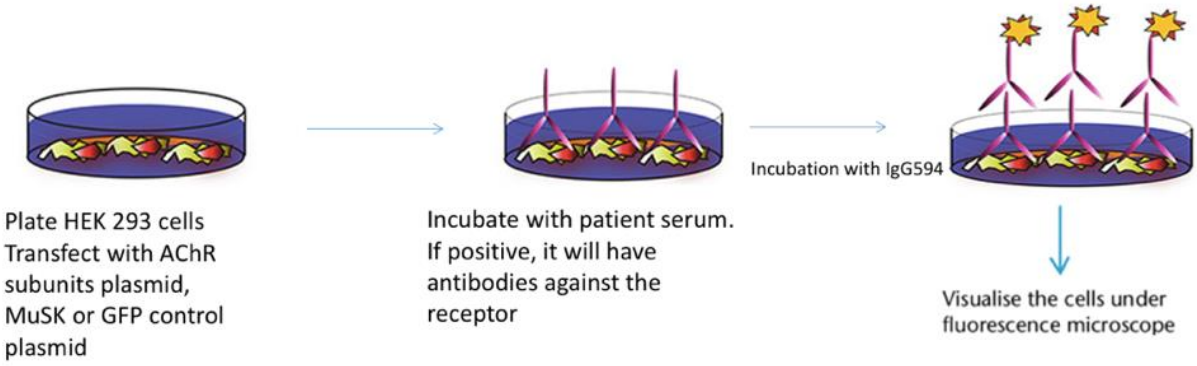

Figure 11: Schematic representation of the cell-based assay technique for the detection of autoantibodies against AChR/MuSK. In the first picture HEK293 cells were transfected with AChR subunits, MuSK or only GFP. The cells were then plated on glass coverslips and serum from SNMG patient was added and incubated with anti-human IgG594. With fluorescence microscope it was possible to visualize the green fluorescence, indicating successful transfection, and the red fluorescence, indicating the presence of autoantibodies.

2.5 Tissue-based Assays (TBA)

MEDIUM COMPOSITION

Blocking buffer	PBS, 20% normal donkey serum (NDS)
Wash medium	0.3% Triton X-100, 1% PBS

Table 4: Recipes of the different buffers for TBA

Soleus rat sections, previously snap frozen, were severed using a cryostat. Longitudinal cryosections of 8-12µm were made and following placed on microscope slides stored at -20°C. On the day of the assay, the slides were moved to a humid chamber to defrost. Afterwards, a hydrophobic pen was used to draw a fat ring surrounding the muscle section. In order to wash further fat residuals, sections were incubated in PBS for 5 minutes. Following this 200µl of blocking buffer were added onto each tissue section, with 2 hours of incubation at RT in the humid chamber. During the incubation time the sera from patients were diluted 1:50 in blocking buffer. Following the incubation, the blocking solution was removed and 200µl of the diluted sera were added to the tissue. Another hour of incubation at RT in the humid chamber has been performed. The slides were then placed into cuvettes and washed 3 times with PBS. During the wash cuvettes have been slowly shaken for 30 minutes with a buffer medium change at 10 minutes intervals. The slides have been further incubated with anti-human IgG 488, diluted 1:750 in blocking buffer, and α-bungarotoxin 594, diluted 1:3000 dilution in blocking buffer, as presented in figure 12. The incubation time has been of 30 minutes, at RT in the humid

chamber (in the dark). After this, the slides have been placed into cuvettes that were briefly rinsed 3 times with a washing buffer, while slowly shaking for 30 minutes, in the dark. The slides were then mounted using 40µl of Aqua-Poly/Mount medium. At the end, slides were analyzed with fluorescent microscopy. The red staining allowed the detection of the NMJ, while the contrasting green staining allowed the detection of human antibodies. When the two stainings colocalize at the NMJ, the patient was declared to be positive.

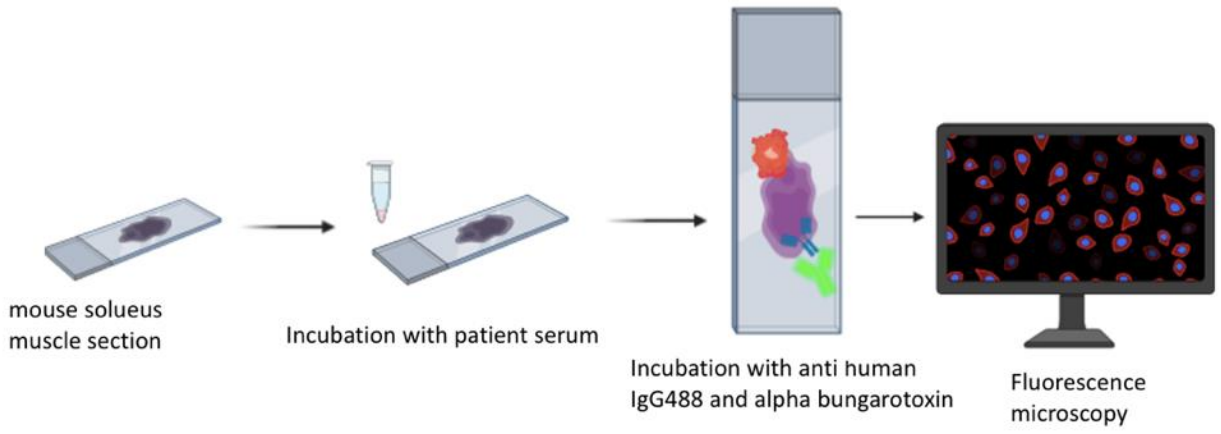

Figure 12: Schematic representation of tissue-based assay for the detection of antibodies against the NMJ. Rat soleus sections were placed on a microscope slide and incubated with serum. It was then performed an incubation with α-bungarotoxin 594 to visualize the NMJ in red and anti-human IgG488 to visualize the autoantibodies in green. The result was then analyzed with fluorescence microscopy.

2.6 Immunoprecipitation assay (IP)

BUFFER COMPOSITION

1xRIPA buffer	5ml 10x RIPA, 45ml aqua bidest
Running buffer	1 bag MOPS buffer, 1L aqua bidest

Table 5: Recipes of the buffers used in immunoprecipitation assay

2.6.1 Cell lysate

4.5x 10^4 primary human myoblasts or 1.6x10^6 L6.C11 myoblasts were seeded in each 10cm plate. Three 10 cm plates were seeded at the same time, and the cells were cultured with GM. When cells reached 90-100% confluency, it was switched to DM. The cells were checked every day. After 4 to 6 days, myotubes were visible. When early myotubes were present, further stimulation with 1:100 soluble agrin was provided, to enhance the expression of AChR on the surface of the cells. When myotubes were observed, DM medium was entirely removed except for 3ml per plate. 30µl AChR MG patient serum was pipetted to each plate and incubated for 1h in the incubator. After the incubation time, cells were washed briefly 3 times with 10ml sterile PBS. Then 1ml 1x RIPA buffer and 20µl PIC (protease inhibitor complex) were added to each plate. Plates were then incubated on a shaker at 4°C for 1h. During the incubation time, the beads were prepared. 240µl of Protein A/G

Agarose Beads were put in a 1.5 low binding Eppendorf tube. Beads were washed 3 times adding 1ml 1x RIPA buffer, centrifuging and removing the supernatant. At the third wash step, beads were resuspended in 200µl 1xRIPA buffer, pipetted into a sterile 15ml falcon tube and left under the laminar flow. After the incubation of the plates, the cell lysate was extracted. A sterile cell scraper was used to scrape off cells from the plate. The cell lysate was put in low binding 1.5 ml Eppendorf tubes and centrifuged for 1h 13200 rpm, 4°. After this step, all the supernatant was collected and mixed with the agarose beads. The tube was left at 4° rolling overnight. On the second day the complex of interest (composed of the antigen and the primary antibody) should have been bound to the beads. The tube undergoes 3 washing steps with 8ml 1xRIPA buffer. After the 3rd wash, the beads were stored at -80° until the day of the SDS page.

2.6.2 SDS-PAGE

On the day of the SDS-PAGE the beads were mixed with 40µl sample buffer, in a ratio 1:3 with the agarose beads. The solution was then heated at 95° for 5 minutes and incubated for 5 min on ice. Finally, the Eppendorf tube was centrifuged at 13200 rpm for 2 min at RT. The supernatant (without beads) was then transferred to a fresh Eppendorf tube. The proteins of interest, now, were expected to be in the supernatant. The SDS page was prepared using a SurePAGE Bis-Tris 4-20% gradient Gel, mounted in the chamber, filled with the running buffer. On the gel 1 slot was loaded with 8µl of protein marker, 1 slot with 50-60 µl of the sample. If the amount of sample was higher, it was divided into two different slots. The gel run first 20 min at 60V, then 50min at 100V. After this time the gel was taken out and cut for the entire column of the sample, as shown in figure 13, with sterile scalpels. The gel pieces were then put in sterile Eppendorf tubes and stored at -80° until Mass Spectrometry analysis. The day of the mass spectrometry analysis, the samples were taken on ice to the facility for the analysis (Medical University of Vienna, Department of laboratory medicine)

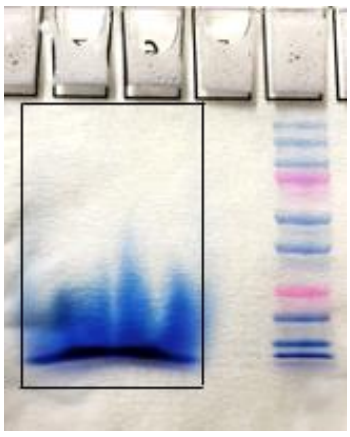

Figure 13: Size marker and cut area of the gel. The area to be cut has been identified as follows: the length of the cut area was defined by the wells in which sample was loaded, the height by the size marker.

2.7 Characterization of Myogenic Cells

2.7.1 MyoD staining for muscle cells identification

Glass coverslips were positioned in a 24 well plate and coated with 250µl of 2% gelatine in PBS. After an incubation of 20 minutes at RT under the laminar flow, the coverslips were briefly washed

with 500µl of PBS. Human myoblasts were then seeded at an early passage number (P1 or P2) with a density of $2x10^4$ per well. The myoblasts were grown in GM until they reached around 80% confluency. On the day of the staining the cells were fixed for 10 minutes with 4% PFA and, after a washing passage, incubated with mouse anti-myoD antibody for 30 minutes at 37°C. Another washing step with PBS has been performed, followed by 45 minutes of incubation with anti-mouse IgG 594 in the dark. Finally, a brief incubation of 3 minutes with 200µl of DAPI has been performed. The cells were washed again for 3 times with 500 µl of PBS. 40µl of Aqua-Poly/Mount medium have been used to mount them on microscope slides using. The analysis was then performed with fluorescence microscopy. The staining of MyoD allowed to visualize the molecule on the red channel, while nuclei appeared to be blue due to DAPI. In order to be identified as myogenic cells, red and blue staining need to colocalize in the nucleus.

2.7.2 *Identification of cells' surface markers*

Glass coverslips were positioned in a 24 well plate and coated with 250µl of 2% gelatine in PBS. After an incubation of 20 minutes at RT under the laminar flow, the coverslips were briefly washed with 500µl of PBS. Human myoblasts were seeded at a density of $2x10^4$ per well with GM at 37°C, growing until the cells reached 80% confluency. Then the GM has been replaced with DM. When myotubes were observed, the cells have been fixed with 4% PFA for 10 minutes. After the incubation, the cells were washed with PBS and incubated with mouse anti-α sarcoglycan (SG), β SG, γ SG, dysferlin and desmin antibodies. Another well was stained with rabbit anti-IgLON 5 antibodies. All the antibodies were added with a dilution of 1:100 in blocking medium for 30 minutes at 37°C. Following this passage, anti-mouse 594 or anti-mouse488 (for IgLON5 anti-rabbit 594 or 488), were added and incubated for 45 minutes at RT in the dark. The cells were then shortly incubated for 3 minutes with 200µl of DAPI. After the last washing step with 500µl of PBS, slides have been mounted on microscope slides using 40µl of Aqua-Poly/Mount medium. Analysis was then performed with fluorescence microscopy.

2.8 AChR clustering assay

Glass coverslips were placed in a 24 well plate. For the coating of the coverslips, the conditions were:

- 4µl of laminin in 250 µl PBS, incubation 37°C for 2 hours.
- Different amounts of agrin, diluted in 0.2% gelatine. Incubation 37°C for 2 hours.
- 5µl of fibronectin in 1ml of gelatine 0.2% solution. Incubation overnight at 37°C.
- 40µl of 0.2% gelatine per coverslip, incubation 20 minutes at RT.

Human myoblasts were seeded with a density of $2x10^4$cells per well and differentiated to myotubes. Myotubes were then incubated for up to 16 hours with or without soluble agrin or soluble laminin, at different concentrations. Myotubes have been firstly fixed with 10 minutes incubation with 4% PFA. The cells were then additionally incubated with AF594 conjugated alpha-bungarotoxin, diluted 1:1000 in differentiation medium for 45 minutes at 37°C. They were then washed with DMEM 3 times. After a brief incubation of 3 min with 200ul DAPI (1:40000 dilution), PBS has been used to briefly wash the cells. They were then mounted on microscope slides using 40µl of Aqua-Poly/Mount medium. Analysis was then performed with fluorescence microscopy. A-bungarotoxin allowed the staining of AChR. The observation under the microscope allowed to detect the presence of a red signal from myotubes, corresponding to AChR. When AChR were not clustered, the red signal was

diffused throughout the myotube, otherwise was possible to observe strongly red lines of around 15 µm corresponding to AChR clusters.

2.6.1 Permanox experiment

On the first day, Flexi-perm 8-well grid were sterilized by dipping in 100% ethanol and drying in the cell culture hood. Then the grids were directly attached to the permanox slides and the complex was placed in a 10cm culture dish. The wells were filled with 200 µl of 0.2% gelatine, and the surface was totally covered, as shown in figure 14. The slides were then incubated overnight at 37°C. The next day, $1x10^4$ C2C12 cells were seeded per well. At the day 4, the medium was changed with 700 µl of differentiation medium. The cells were then left in culture until day 12, when they were fixed for 10 minutes in 4% PFA, washed 3x with PBS and stained. For AChR cluster visualization, alpha BuTX has been added to the cells, and then incubated in the dark 30 minutes, then 3x PBS washing. The cells were then covered with the glass coverslips and analyzed by fluorescence microscopy.

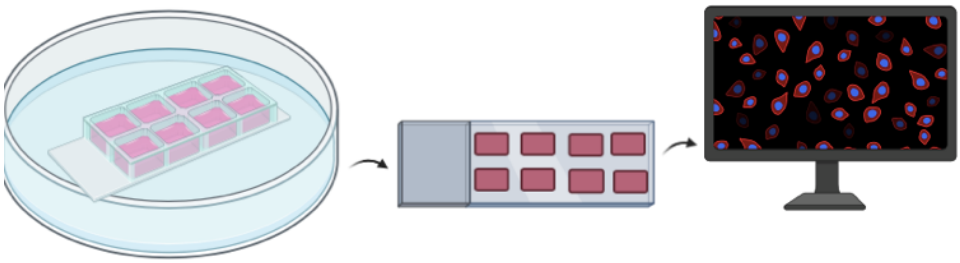

Figure 14: Schematic overview of permanox experiment. First, the slide with the grid was placed in a 10cm dish, until cells were differentiated. Finally, the grid was removed and the slide analyzed through fluorescence microscopy.

2.9 Maxiprep

Plasmids for general use in the laboratory were produced by maxiprep. A bacterial culture was inoculated from a glycerol stock of Escherichia coli DH5alpha. Each culture was then transformed with pBabe_TK-Dok7HA, pIRES2-AcGFP1-MuSK, pcDNA3.1. The amount of 1µl plasmid DNA was mixed with 25µl competent bacteria at RT. Moreover, one culture was used as a negative control and was not mixed with any DNA. Everything was first incubated on ice for 10 min, then at 42° water bath for 45 seconds and again on ice for 5 min, in order to induce the heat shock. Then, 1ml of LB medium was added to each culture and incubated for 30 min at 37°. After this, the cultures were centrifuged and the pellet resuspended in 330 µl of medium and plated on solid LB agar. The culture was then incubated overnight at 37°. The next day, it was checked if all the colonies have grown, except for the negative control in which no colony should be visible. If the transfection and the incubation time were correct, large colonies should be visible on the plates. After this check, a colony from each plate was picked by a sterile tip, and the tip was then put in a 15 ml falcon tube with 5ml of medium and 100µg/ml Ampicillin or 40µg/ml Kanamycin (depending on the plasmid). Following another incubation over night at 37°C, 1L Erlenmeyer beaker was filled with 250 ml LB medium and 100µg/ml Ampicillin or 40µg/ml Kanamycin and 5ml of bacterial culture, and incubated over night at 37°C shaking in a bacterial incubator. The last day, maxiprep was performed using the Maxi Kit

for rapid purification of transfection-grade plasmid DNA. DNA concentration was measured with NanoDrop.

2.10 MSI 1436 test

MSI solution was prepared with MSI 1436 10mM in DMSO. The stock solution has been then stored at -80° in small aliquotes.

2.10.1 MSI 1436 test with 24 well plate

16 coverslips in a 24 well plate, coated with 0.2% gelatine, were incubated at RT for 20 min and briefly washed with PBS. On day 1, $2x10^4$ cells per coverslip were seeded. Half of the wells were treated with compound (2ml medium + 2µl MSI, 250µl per well) and half with only solvent (2ml medium + 2µl DMSO, 250µl per well) as a control. The MSI-1436 stock solution was stored at -80°C. Every day for 5 days, 2 coverslips (one per treatment, one per control) were transferred to a new plate, fixed 5 min with 4% PFA, and mounted with DAPI. The coverslips were then analyzed by fluorescence microscopy: 10 random selected images at 20x were take per coverslip. Using ImageJ, the nuclei on each picture were counted. Finally, the average of the values per each coverslip were calculated, and the results were plotted on a graph to visualize the difference between MSI and the control.

2.10.2 MSI 1436 test with 35 mm dishes day counting test

On day 1, 35mm plates were prepared. Per plate, $3x10^4$ cells were seeded. The plates were treated with a different amount of MSI-1436 solution and the same amount with DMSO as a control. For every test, one plate has been used as an overall control treated only with GM. The plates were then put in the incubator at 37°. On Days 2, 3, 4, 5, a plate with DMSO, one with MSI and one with GM were trypsinized and the cells counted. The analysis was then performed with GraphPad prism. The total amount of cells was plotted, as well as the difference between cells treated with MSI and DMSO. Finally, the number of cells without any treatment was used as a standard value, in order to calculate the percentage of cells' growth with the different conditions. This process, called normalization, allowed all the experiments to be compared each other. The analysis of the results has been performed through GraphPad Prism. A one-way ANOVA analysis with Bonferroni post test has been performed to compare every column with every other column on the graph. The results have been considered statistically significant whit p value< 0.05.

2.10.3 MSI 1436 test with 35 mm dishes titration test

On day 1, 35mm plates were prepared. Per plate, $3x10^4$ cells were seeded. The plates were treated with different amount of MSI-1436 solution and the same amount with DMSO as a control. For every test, one plate has been used as an overall control treated only with GM. After 5 days in the incubator at 37°C, each plate with DMSO, compound and GM were trypsinized and the cells counted. The analysis was then performed with GraphPad prism. The total amount of cells was plotted, as well as the difference between cells treated with MSI and DMSO. Finally, the number of cells without any treatment was used as a standard value, in order to calculate the percentage of cells' growth with the different conditions. This process, called normalization, allowed to compare all the experiments.

2.11 Western blot

Western blot was performed to characterize cell lines for the expression of specific proteins. The expression of β-actin, as housekeeping gene, has been used as a positive control. In addition, it has been analyzed the expression of Lrp4 in the different cell lines.

2.11.1 Protein concentration

After having obtained the cells' lysate, the protein concentration has been detected with the Lowry protein assay. A protein standard with BSA has been prepared, from a 1:10 dilution of the stock solution (0.04g BSA in 1 ml PBS). Then, a 1:2 serial dilution has been performed from A to H, for a total of 8 samples, with the last one (H) containing only PBS. The samples were added to a 96 well plate, in order to obtain a standard curve. 5 µl of each sample were loaded in each well in duplicates. From the Lowry Protein Assay Kit, 20 µl of reagent S and 1ml of reagent A were mixed, and 25 µl of the solution were added to each well. Further 200 µl of reagent B were added to each well. After 15 min of incubation at RT, the solution has turned to a blue color. The OD640 was measured through a plate reader. The OD640 values were then plotted on the X axis of a graph, and the values of known protein concentration on the Y axis. Finally, the equation for the linear trendline displayed as Y=abcx-/+ def, in which abc represented the slope of the line. To calculate the protein concentration, the equation Y=abc*valueOD640x-/+def. Again, abc represented the slope of the line and OD640 the optical density value of the interested sample.

2.11.2 SDS-PAGE

For the preparation of the two gels, the following recipe has been followed.

	Separation gel	Collection gel
Gel concentration	10 %	4 %
A. Bidest.	3,96 mL	2,97 mL
1,5 M Tris-HCl pH 8.8	2,50 mL	-
0,5 M Tris-HCl pH 6.8	-	1250 µL
Acrylamid/Bis	3,33 mL	670 µL
10% (w/v) SDS	100 µL	50 µL
10% APS	100 µL	50 µL
TEMED	10 µL	10 µL

Table 6: SDS PAGE gels recipes

After the cassettes were mounted, the separation gel was poured between the two glass slides. On the top, ethanol was added in order to remove possible bubbles. After 45 min incubation time, the ethanol was removed and the collection gel was poured. After this passage, also the 10 wells comb was added. After 30 minutes of incubation time, the gels were loaded into the electrophoresis chamber, and everything was filled with the running buffer. The stock solution of the running buffer was prepared

with the following recipe: 30,3 g Tris-Base, 144 g Glycin, 10 g SDS, up to 1000mL with aqua bidest. Before use, the stock solution was diluted 1:10 with aqua bidest.
The samples were mixed 1:2 with the sample buffer. They were then heated for 5 minutes at 95°C, and cooled down on ice for 5 minutes. Finally, they were loaded and the gel run at 60V for 15 min and then 150V for 60 min.

2.11.3 Western blot

The gels were placed in the 1 x transfer buffer. Two membranes were incubated in methanol for 5 minutes. This will facilitate the binding of proteins to the membrane. Then two transfer sandwiches were made as shown in figure 15, from the bottom up, first a sponge, then a filter paper, then the SDS gel, then the membrane, then two filter papers, and then again a sponge in each of the two cassettes were added. Both closed cassettes were placed in the blotting chamber, with the black side of the sandwich in the direction of the electrode holder. The entire blotting chamber was filled while transfer buffer was gently agitated using a magnetic stirrer.

Figure 15: Transfer sandwiches

2.11.4 Immunodetection

The membranes were placed in a small bowl with prepared blocking buffer (recipe: 5 g Dry milk powder + 100 ml PBS), covered with parafilm and put at 4°C. Due to the blocking buffer, no undesired proteins were allowed to adhere to the membrane, reducing the risk of false signals. After the incubation time, one of the membranes (referred to as A) was incubated in primary antibody for 60 minutes. An amount of 1.5 ml of anti LRP4 antibody has been pipetted onto the parafilm and the membrane was placed with the protein side in contact with the solution. After the end of incubation time, the membrane was washed three times in PBS Tween, with changing solution every ten minutes. Then it was for 60 minutes at RT in a secondary antibody solution diluted in blocking buffer (Anti-mouse IgG, HRP Conjugate Dako). The second membrane (referred to as B) was incubated only one time in mouse anti-β-actin antibodies, dilution 1:1000. Then, 15 mL blocking buffer were mixed with 15µL of antibody, and everything was gently shacked for 60 min. Incubation was again washed three times for 10 minutes in PBS Tween. For the detection, the super signal solution was prepared by adding equal volumes (2 ml) of the Luminol/enhancer solution and the stable peroxide solution, mixed in the same box. The membranes were covered with the Super Signal solution and then incubated for 5 minutes. ChemiDoc software was used to measure the protein bands. Chemo Hi Sensitivity was chosen to include chemiluminescence. The option "Autoexposure" was chosen, following by the "Live capture" option. A time period and the number of images to take in the time spot were entered, allowing the program to take several pictures in a set time spot. Different combinations of time and number of pictures were selected. The amount of time chosen was from a

minimum of 10 minutes for beta actin detection to a maximum of 30 min for LRP4. The number of pictures per time slot was chosen with a picture every 30 sec for beta actin and for LRP4. At the end, all the pictures were analyzed. The ones showing more clear bands were then chosen.

3 Results

3.1 Identification of seronegative myasthenia gravis patients

3.1.1 Exclusion of sera with antibodies against AChR or MuSK

The CBA is a reliable tool to detect in the sera the presence of autoantibodies against AChR or MuSK with high efficiency. In each experiment, HEK 293 cells were transfected with the plasmid pG- MuSK (expressing GFP and MuSK) for the MuSK CBA. For the AChR CBA, cells were transfected with plasmids expressing AChR subunits and rapsyn-GFP. As a negative control, serum was also tested in cells transfected with GFP only. In figure 16 is shown the negative result of a healthy control tested for AChR and MuSK, and as a negative control it was tested also on cells transfected only with GFP (figure 16b.).

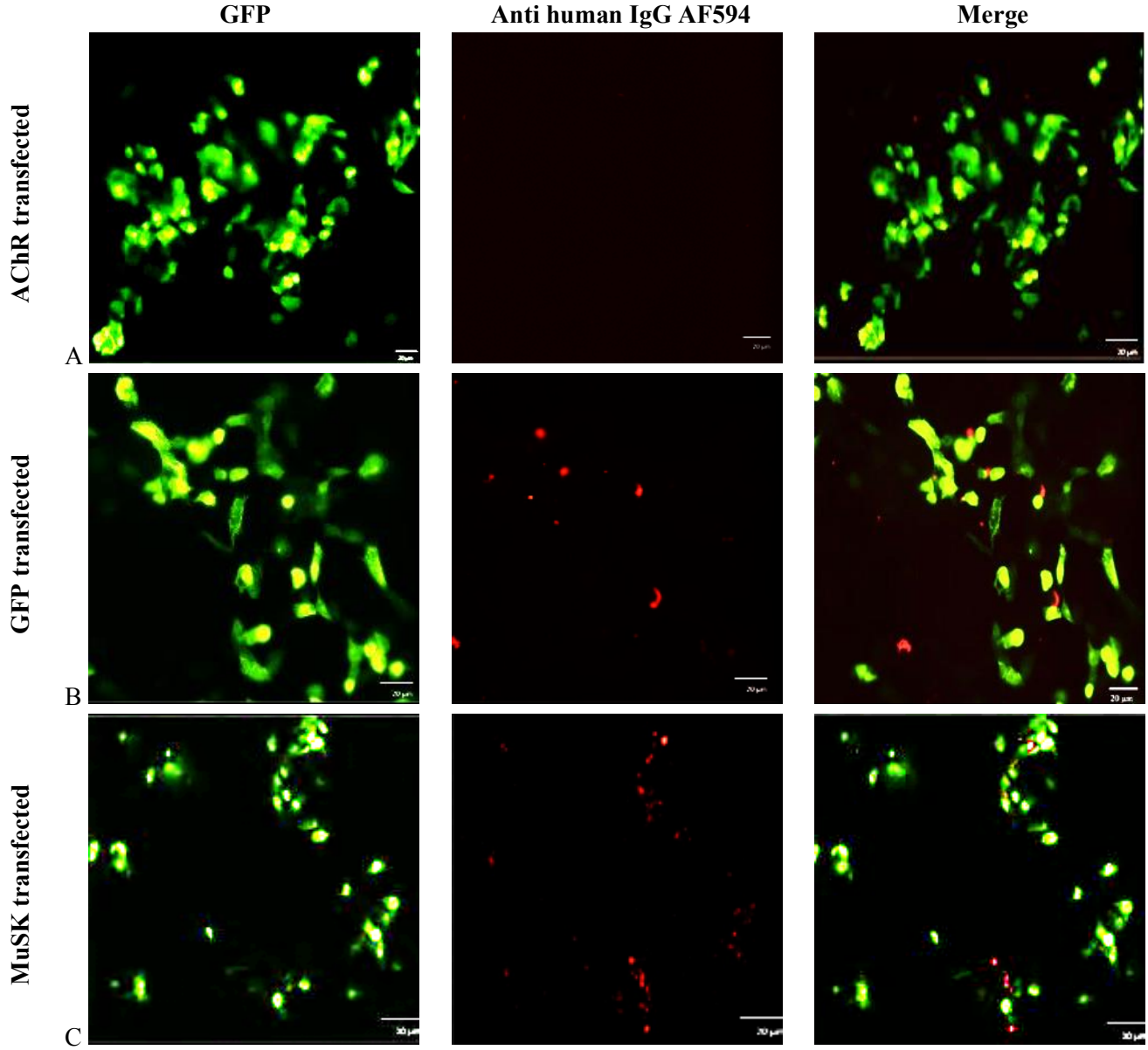

Figure 16: Results of fluorescence microscopy of cell-based assay. Transfected HEK293 cells have been incubated with a healthy control, dilution 1:40. In the left column: GFP expressed in all the transfected cells; middle column: autoantibodies detection with anti-human IgG AF594; right column: merge. a) AChR subunits transfection; b) GFP transfection; c) MuSK transfection.

Patients were considered positive for AChR and/or MuSK MG when clusters of antibodies, stained in red, were visible on the surface of the cells (Figure 17a and c). Moreover, the assay was considered valid if no clusters were visible in the negative control with GFP (figure 17b.).

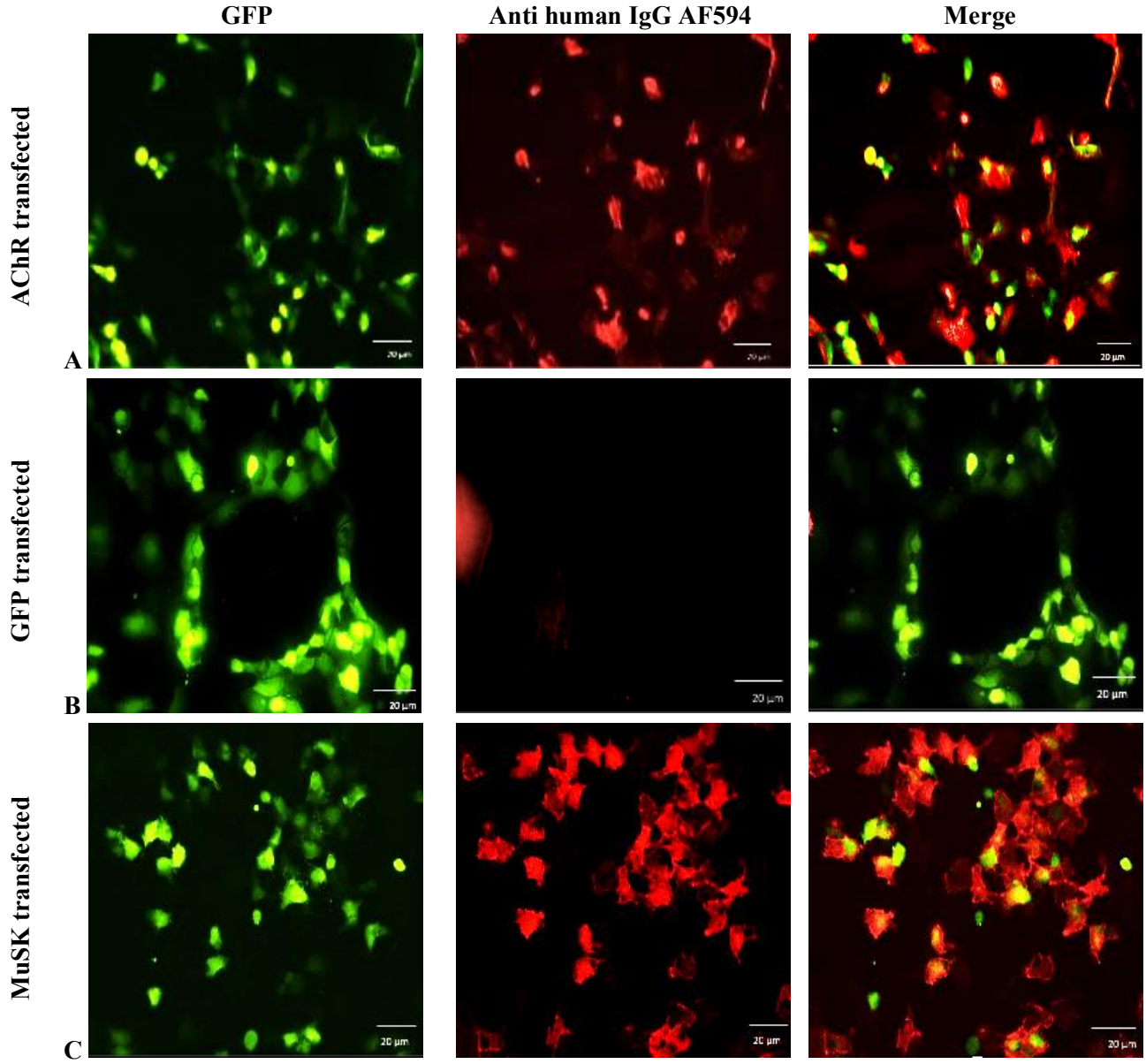

Figure 17: Results of fluorescence microscopy of cell-based assay. Transfected HEK293 cells incubated with positive control serum, dilution 1:40. Left column: GFP expressed in all the transfected cells; middle column: autoantibodies detected with anti-human IgG AF594; right column: merge. a) cells transfected with AChR subunits, incubated with AChR positive serum; b) GFP transfection, incubated with AChR positive serum; c) MuSK transfected cells incubated with MuSK positive serum;

Through CBA, it was possible to screen clinically diagnosed myasthenia gravis patients. The test allowed the detection of autoantibodies against known antigens. For the purpose of the project, those sera resulting positive to the assay have been discarded.

3.1.2 Screening for autoantibodies against NMJ with tissue-based assays

The tissue-based assay is a key feature in the process of seronegative identification. With this technique, it became possible to identify, in the pool of sera that result seronegative on the CBA, the

ones that had antibodies against the NMJ. Patient's serum was incubated on a section of a rat muscle. Then, the NMJ was visualized through α-bungarotoxin staining, while human IgG through AF488. When the antibodies staining colocalized with the NMJ, the patient was considered to be positive. Figure 18 shows the positive and negative staining at the NMJ, respectively with a positive and a negative control.

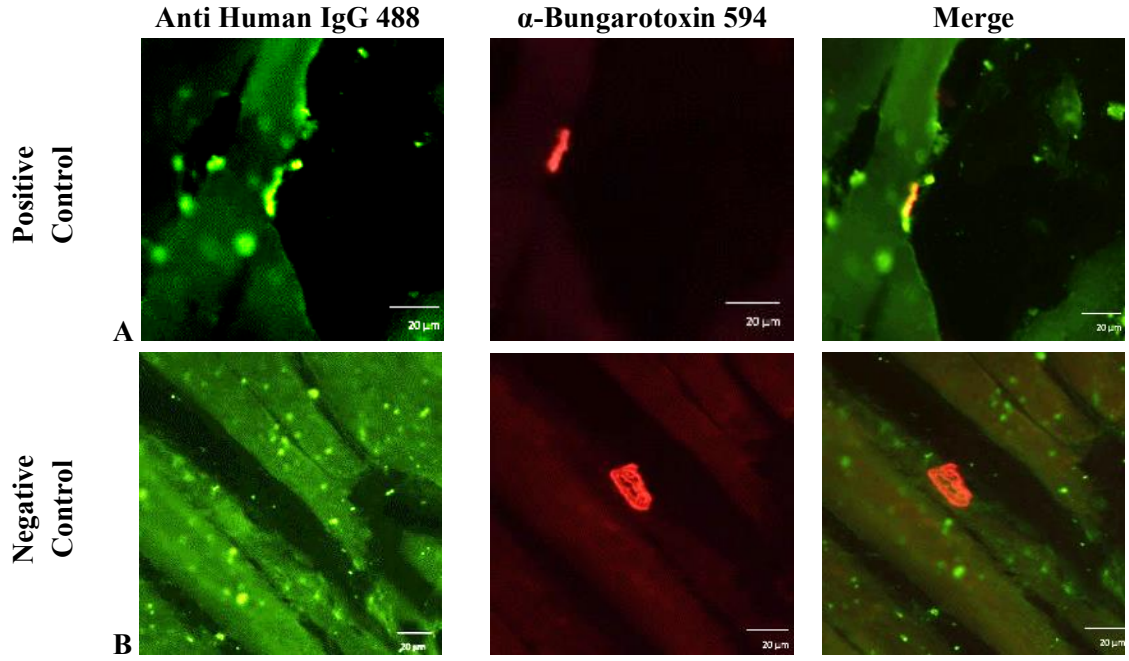

Figure 18: Fluorescent microscopy of tissue-based assay. Positive and negative control have been tested. In green, anti-human 488 antibody; in red the NMJ stained by 594 alpha-bungarotoxin. a) positive control, AChR MG patient, 1:40 dilution; b) healthy control patient serum, 1:40 dilution.

However, several tested sera did not displayed any staining at the NMJ, even though the patient was tested positive for AChR with CBA. Another result appearing several times, as it is possible to see in figure 3 a., was the presence of striational antibodies. The presence of antibodies against other muscular epitopes did not allow to use the use of serum for further studies on seronegative MG patients, and these sera had to be discarded.

3.2 Development of an *in vitro* model of the neuromuscular junction

3.2.1 Establishment of primary muscle cells culture

Primary myotubes have been used for a wide range of experiments such as immunoprecipitation assays and with the purpose of studying AChR clustering process *in vitro*. Human myogenic progenitors have been isolated through enzymatic digestion of muscle biopsies. Following the isolation process, the muscle slurry was resuspended in GM and placed in a 60mm dish and observed until cells would attach to the dish, that normally took place after 7 to 10 days (Figure 19).

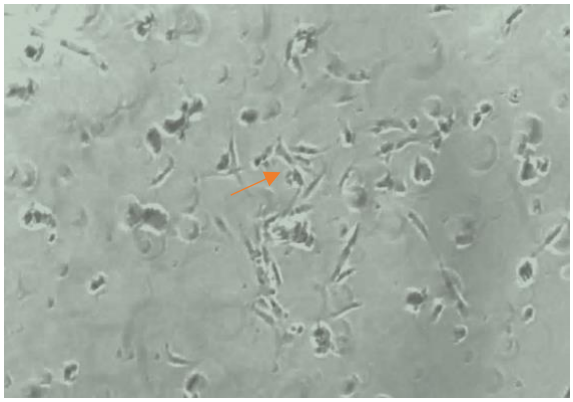

Figure 19: Patches of cells attached on the surface of the dish, 8 days after isolation.

After visualization of patches, cells had to be "sparse" when the 50% confluency was reached, in order to avoid early differentiation of myoblasts. Myoblasts (Figure 20), mononucleated cells that proliferate and fuse to form myotubes, are mostly characterized by an elongated shape.

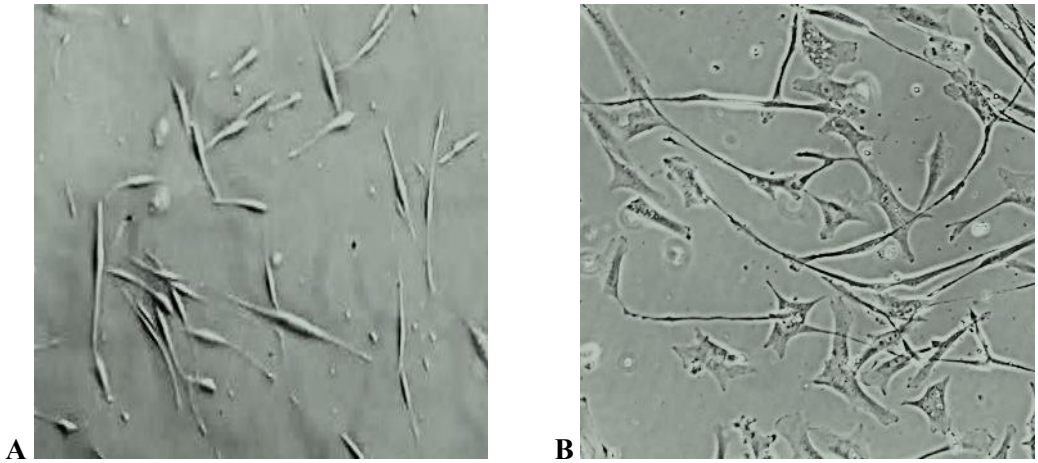

Figure 20: Human muscle cells in culture, P2, bright field microscopy; a) magnification 4x, overview of cells at 50% confluency; b) magnification 20x, overview on cells' morphology.

3.2.2 Early characterization of myogenic cells: MyoD staining

When isolating human muscle cells from muscle biopsies, one of the main challenges has been to avoid the presence of fibroblasts in culture. These kinds of cells are morphologically similar to myoblasts but have a shorter duplication time. Due to this, their presence in culture could result in the depletion of myoblasts, that have a longer duplication time compared to them. Therefore, it was necessary to perform an early analysis to verify the presence of myogenic cells in culture and to quantify the amount of non-myogenic cells. The proper removal of fat and blood vessels from the muscle during the isolation process led to the depletion of the majority of fibroblasts, resulting in almost pure myogenic cultures.

The localization of MyoD was tested in order to verify the presence, in the culture, of myogenic cells. MyoD is a transcription factor that allows differentiation of myogenic cells, and for this reason myogenic cells show a high rate of expression of MyoD at the nucleus level. In differentiated cells, as well as in non-myogenic cells, nuclei are MyoD−, but MyoD staining was observed in perinuclear regions of the cytoplasm. Immediately after the spreading or at the latest at P2, an aliquot of 2x 10^4cells were seeded on a glass coverslip. After the cells reached around 50% of confluence, they were stained with mouse anti-MyoD antibodies. In figure 21 fluorescence microscopy images are used to evaluate the presence of myogenic cells in culture. The nuclear staining in red of the cells indicated that the cell was a myoblast, while the absence of nuclear red staining was typical for non-myogenic cells.

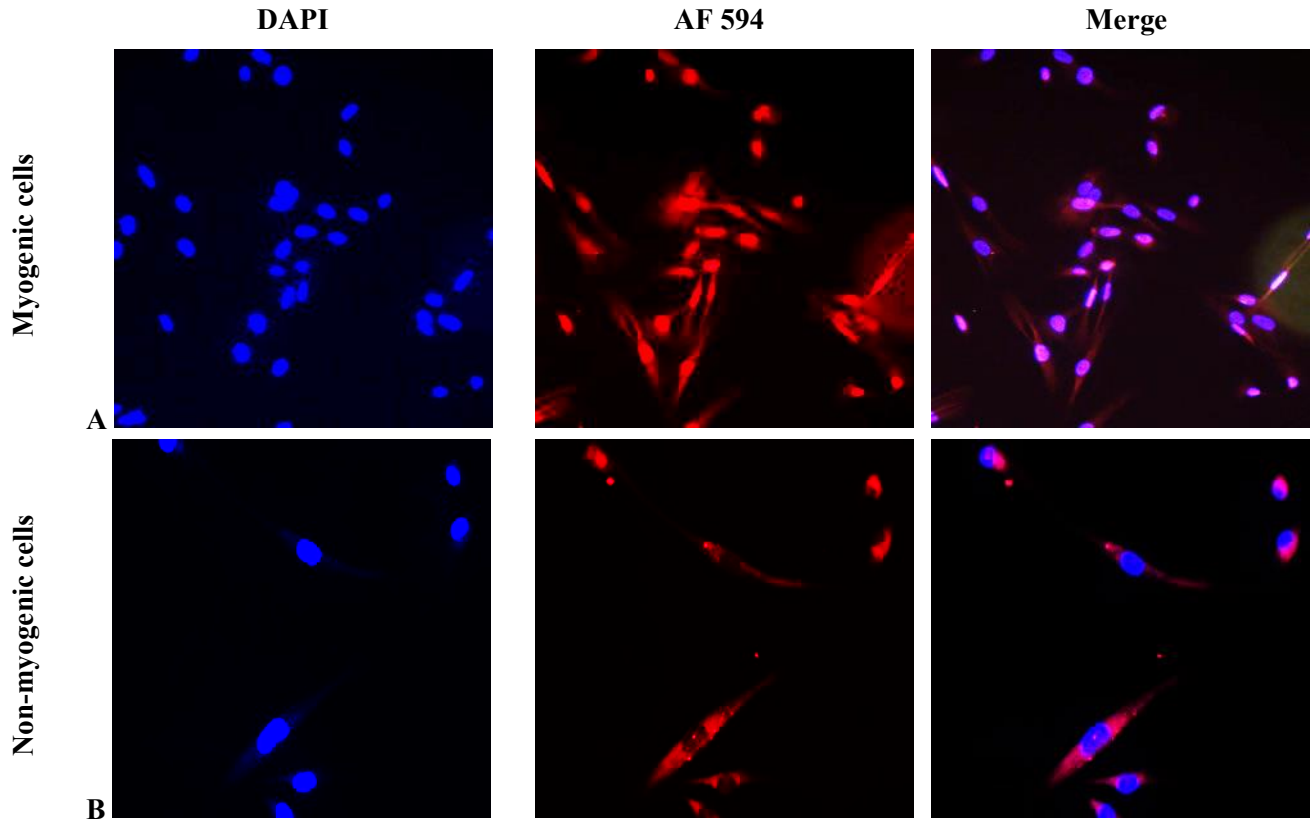

Figure 21: Comparison between myogenic and non-myogenic cells from muscle tissue. First column, cells stained with DAPI (blue). Second column, anti MyoD antibodies and AF594. Third column merged pictures; a) myoblasts; b) fibroblasts

In addition, the picture shows the purity of the culture, in which more than 90% of nuclei were stained with red.

3.2.3 Differentiation and myotubes staining

After having confirmed that the culture had myogenic cells through MyoD staining, it was possible to proceed with the differentiation of the cells. When they reached a confluency of 90 to 100%, the medium was switched to DM. Between 4 and 6 days, myotubes had become visible (figure 22).

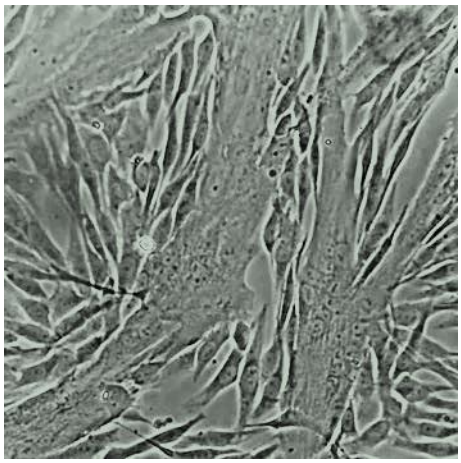

Figure 22: Differentiated human myotubes, 5 days after differentiation medium.

Despite the fact that most of the cells in culture underwent the differentiation, some cells did not differentiate as appears in figure 23. Myotubes were tested for the presence of desmin. This protein, one of the major muscle-specific proteins, can be commonly used as a biomarker for myotubes. To detect the expression of desmin, following the fixation of the cells, they were incubated with mouse anti-desmin antibodies and fluorescent anti-mouse IgG 488. The secondary antibody allowed to visualize desmin, while a brief incubation with DAPI allowed the visualization of the nuclei. In Figure 8 it is then possible to observe differentiated myotubes, in which is possible to detect elongated and multinucleated syncytia, as well as single non-differentiated cells.

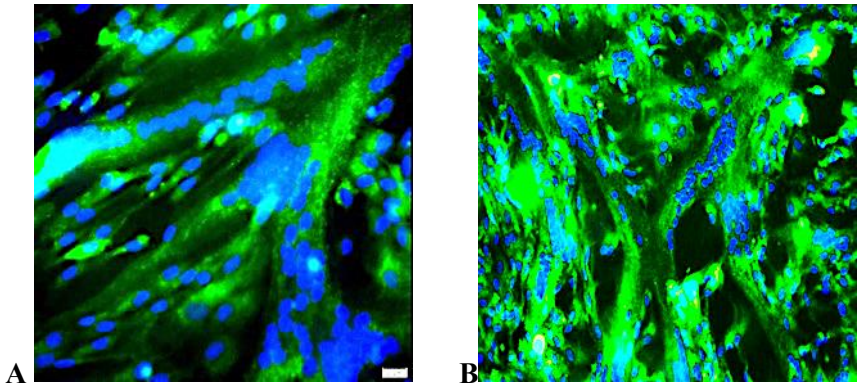

Figure 23: Staining for desmin: DAPI stained nuclei in blue, AF488 anti-desmin antibodies in green; a) desmin staining positive cells, magnification 20x. b) desmin staining positive cells, magnification 10x.

While observing myotubes, also a staining for MyoD was performed. As mentioned before, in differentiated cells nuclei became MyoD−. However, non-differentiated cultured cells resulted to be positive for the presence of MyoD in the nucleus (figure 24).

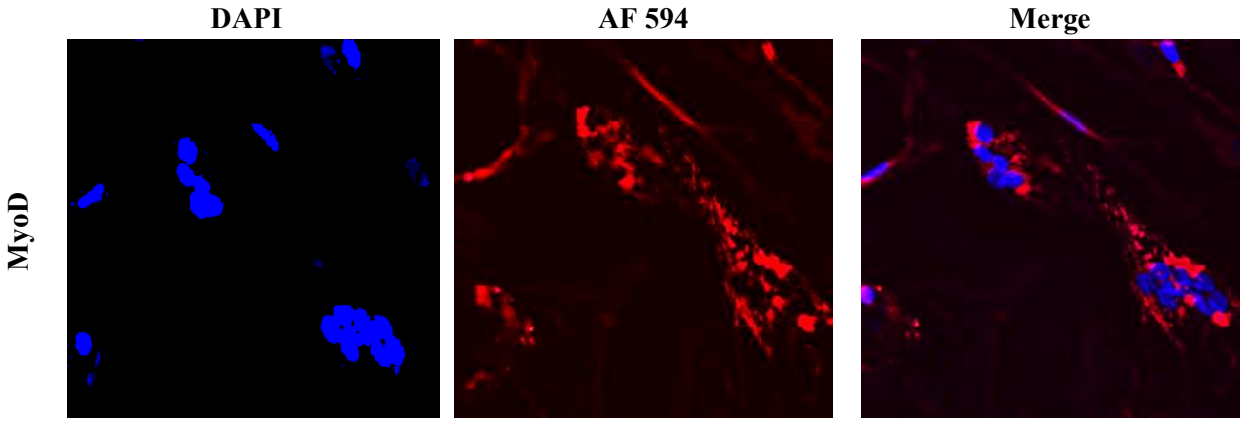

Figure 24: MyoD staining of myotubes. First column, cells stained with DAPI (blue). Second column, anti MyoD antibodies and AF594. Third column merge pictures. Magnification 20x; Nuclei of differentiated cells did not show staining for MyoD, while non differentiated cells were positive.

3.3 AChR clusters on human myotubes

As mentioned in the introduction one of the key mechanisms for the proper function of the postsynaptic apparatus is represented by the clustering of AChR. In this process several known proteins are involved, including MuSK, Lrp4 and Agrin. A proper clustering of the receptor is an indicator of a functional postsynaptic apparatus. One of the major challenges represented by human myotubes *in vitro* was the absence of a spontaneous AChR clustering. As of now, it is still not possible to induce a proper AChR clustering in human myotubes cultured *in vitro*. In addition, a functional protocol has not been developed yet. Therefore, the project aimed to test different conditions to induce an efficient AChR clustering. The cells were seeded in a 24 well plate on coated glass coverslips, and the AChR were then stained with α bungarotoxin. The first experiment aimed at assessing the level of expression and clustering of AChR without external stimulations. The coverslips were coated with 2% gelatine allowing better attachment of the cells and cultured until myotubes were visible. Figure 25 shows that without external stimulation, the expression of AChR in human myotubes was really low, and there only a diffuse expression of receptors on myotubes' surface could be observed here.

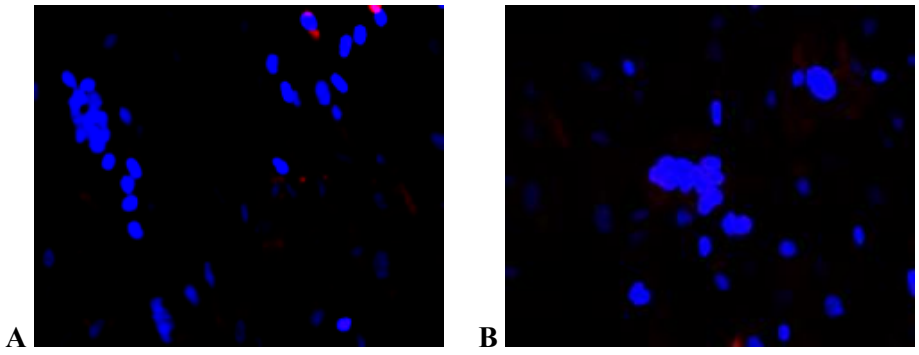

Figure 25: Human myotubes without stimulation. Nuclei stained with DAPI in blue, AChR stained with α bungarotoxin in red . a) and b) human myotubes on gelatine coated coverslips.

3.3.1 Soluble stimulation

It has been demonstrated that molecules from the extracellular matrix were able to induce clustering even when supplemented to the medium[122,123]. When myotubes were visible, soluble agrin (1:5 to 1:1000 dilution) and/or laminin (4 µg/ml) were supplemented to the medium. After 16 or 24 hours, the cells were stained with α-bungarotoxin to visualize AChR.

3.3.2 Soluble agrin for stimulation

Different concentrations of soluble agrin were used, to evaluate their effect on the clustering process. Only gelatine was used as coating agent allowing the comparison with the previous results. In table 7 it is possible to see the various combinations tested.

Soluble stimulation
agrin 1:1000
agrin 1:500
agrin 1:200
agrin 1:100
agrin 1:50
agrin 1:20
agrin 1:10
agrin 1:5

Table 7: Different agrin dilutions to stimulate AChR clustering on gelatine coated coverslips.

The most representative pictures of the experiment, in figure 26, showed no significant difference of AChR expression with none of the conditions tested. However, in figure S1 all the conditions have been presented.

A 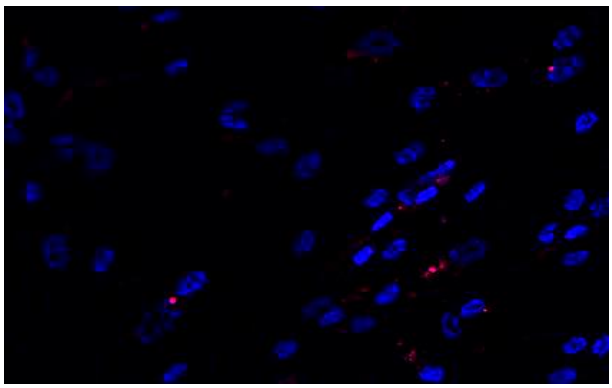 **B** 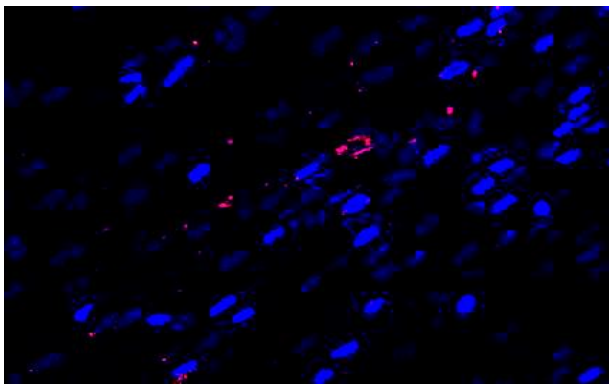

Figure 26: Agrin stimulated myotubes. Nuclei stained with DAPI, blue; AChR stained with α bungarotoxin, in red; a) 1:1000 titration b) 1:5 titration.

Another factor worth mentioning is that the myotubes were still at an early stage of maturation which could explain the low amount of AChR expressed. For this reason, only mature myotubes were taken in consideration in the following experiments.

3.3.3 Coating

In order to enhance the ability of the cells to induce AChR clusters, glass coverslips were coated with different molecules of the muscle extracellular matrix. The cells were then seeded and differentiation was induced. After myotubes appeared, the cells were stained with α-bungarotoxin, in order to have AChR visualized by a red fluorescent signal.

3.3.4 Soluble agrin and fibronectin coating

Following the previous experiment, soluble stimulation has been used in combination with different coating conditions. The cells have been seeded and differentiated on fibronectin coated coverslips, the myotubes have been stimulated with soluble agrin at 1:500, 1:100, 1:50,1:10 and 1:5 dilutions. The staining was performed 16h after stimulation. As appears from figure 27, the different conditions tested led to an upregulation of the expression of receptors. Nonetheless, only a diffuse expression of AChR has been detected. The only exception has been the 1:50 dilution, in which a "spot-like" staining pattern has been observed, that may indicate the presence of microclusters.

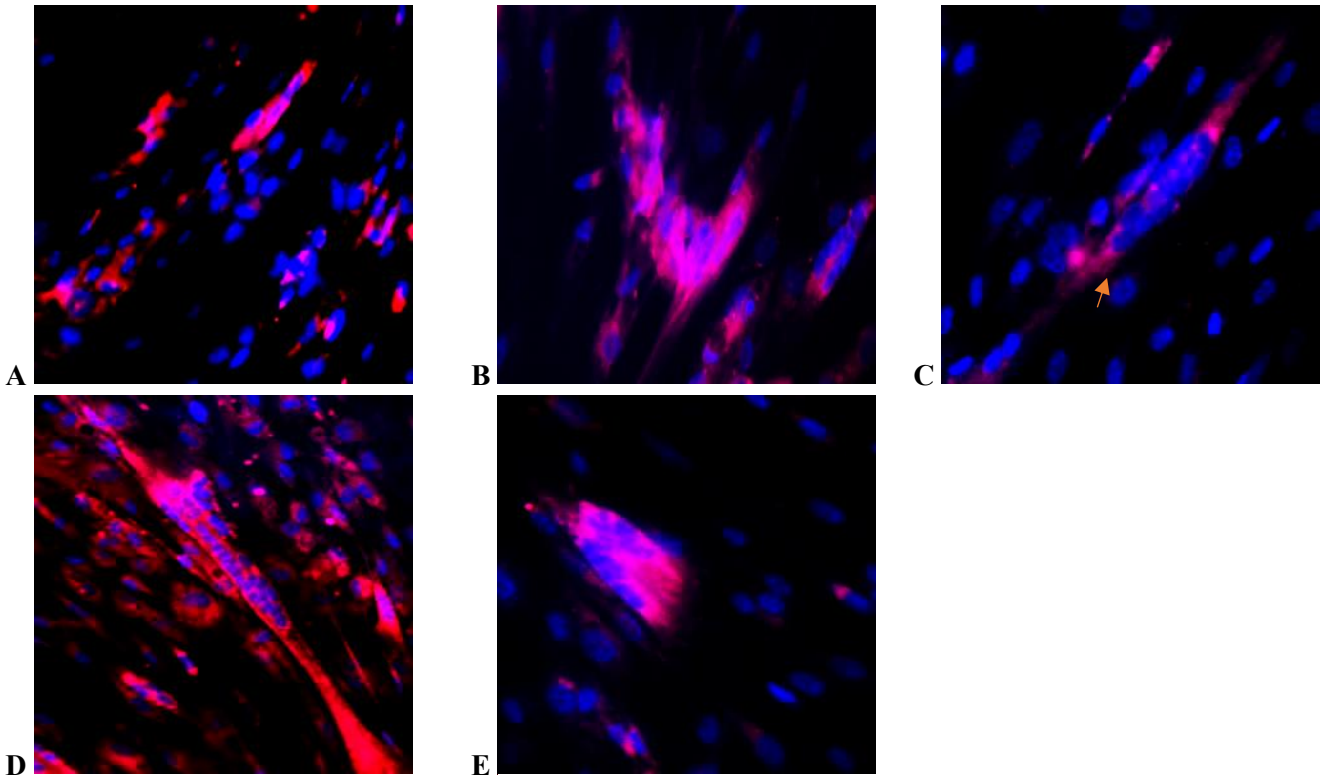

Figure 27: Agrin stimulated myotubes on fibronectin coating. Nuclei stained with DAPI, blue; AChR stained with α bungarotoxin, in red; a) 1:500 dilution; b) 1:100 dilution; c)1:50 dilution; d) 1:20 dilution; e) 1:10 dilution. The arrow indicates an area of possible AChR clustering.

The results indicated that for AChR clustering a coating may be required in addition to soluble stimulation.

3.3.5 Soluble agrin and laminin coating

Together with fibronectin, also laminin is a molecule highly expressed in extracellular matrix. As a control, one well was treated without agrin, in order to assess the sole ability of laminin of increasing the expression of AChR by itself. Glass coverslips have been coated with laminin 1:100, and table 8

summarized the tested conditions of soluble stimulation. Out of the condition tested, the results in figure 28 highlighted that four conditions gave structures compatible with a beginning of a clustering process.

Soluble stimulation
agrin 1:1000
agrin 1:500
agrin 1:200
agrin 1:100
agrin 1:50
agrin 1:10
agrin 1:5
No agrin

Table 8: different agrin dilutions on laminin coated coverslips

In figure S2 are presented the results confirming that myotubes, which were treated without agrin and with the titrations 1:1000,1:500 and 1:200, did not show any sign of an upregulation of AChR, neither of a clustering effect.

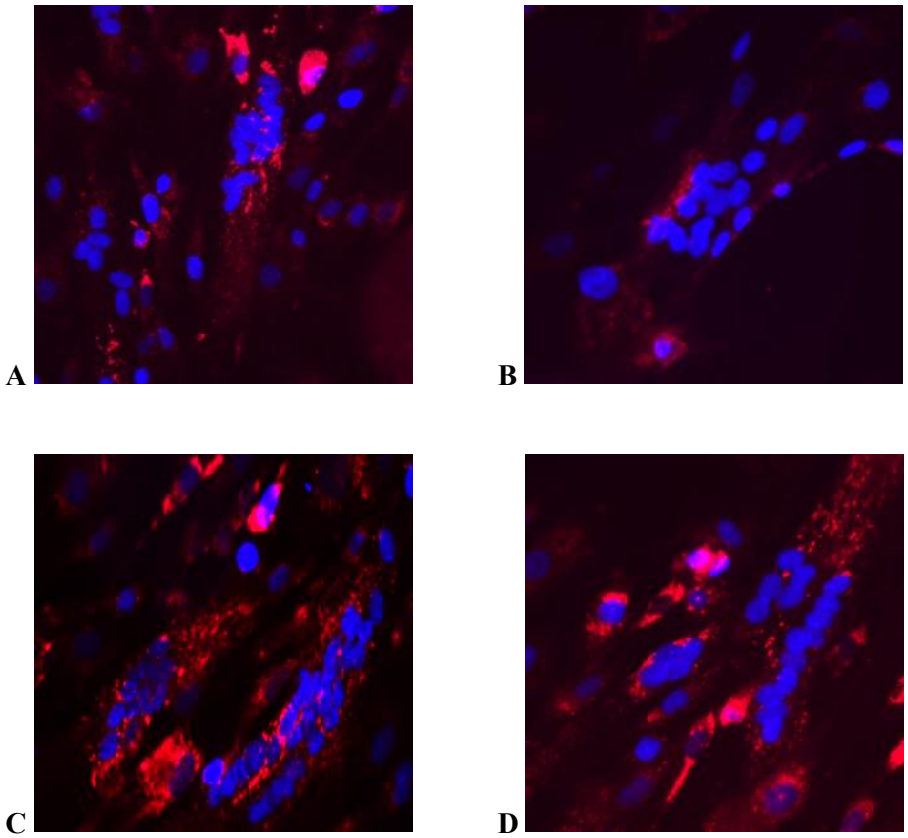

Figure 28: Agrin stimulated myotubes on laminin coated coverslips. Nuclei stained with DAPI, blue; AChR stained with α bungarotoxin, in red; a) 1:100 dilution; b) 1:50 dilution; c) 1:10 dilution; d) 1:5 dilution;

Due to the results obtained with these conditions, the experiment has been repeated to confirm the presence of complex clusters, and the cells have been stained only with α-bungarotoxin . Out of the conditions tested, in 1:100 and 1:50 agrin stimulation it was possible to detect structures that might resemble a more advanced clustering of the receptors, as visible in figure 29 a. and b. The other tested conditions, in figure S3, showed a diffuse expression of AChR, indicating a possible background effect in the previous experiment.

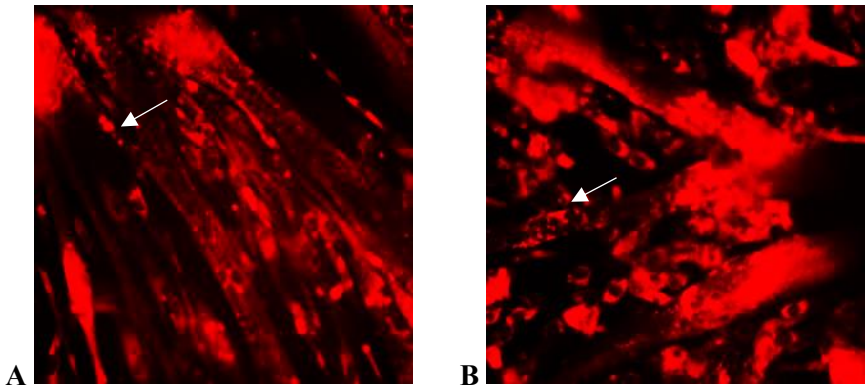

Figure 29: A-bungarotoxin stained myotubes a) 1:50 agrin stimulation; b) 1:100 agrin stimulation. The arrows indicate regions in which may be present a clustering of AChR.

These conditions have been taken into consideration for further studies.

3.3.6 Soluble agrin in combination with agrin-laminin coating

Glass coverslips have been coated with laminin 1:100 and agrin 1:100, 1:50, 1:10, 1:5 dilution. The same dilutions of agrin have been used for the soluble stimulation of myotubes (figure 30). The experiment aimed to test if soluble agrin at the same dilution of the coating, together with the growth of myotubes directly on both agrin and laminin, it would have been able to increase the clustering process.

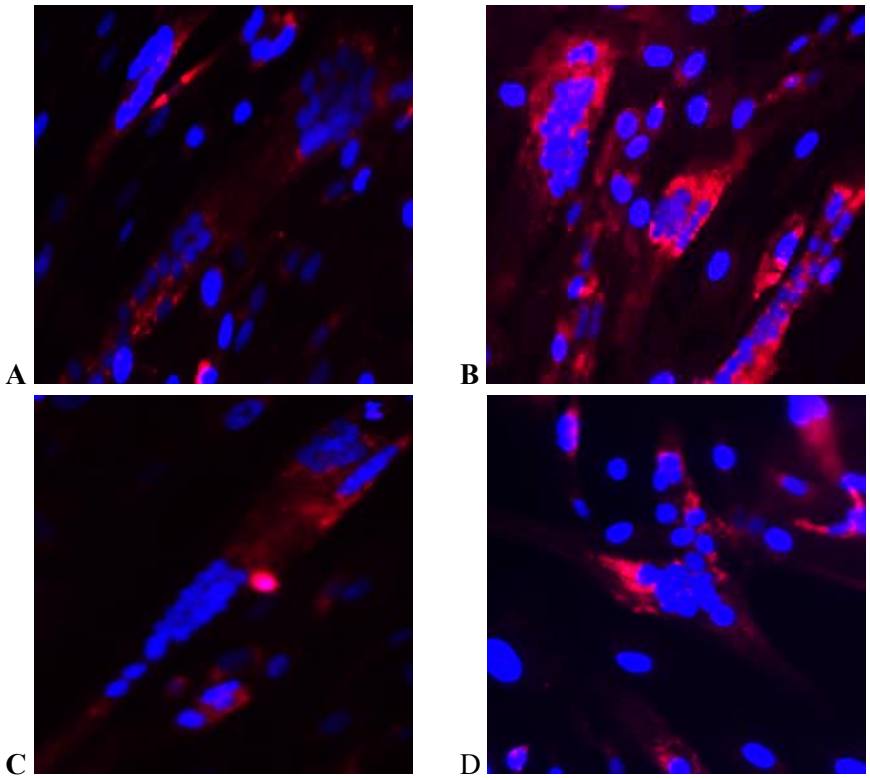

Figure 30: Agrin stimulated myotubes on laminin and agrin coated coverslips. Nuclei stained with DAPI, blue; AChR stained with α bungarotoxin, in red; a) 1:100 agrin dilution; b) 1:50 agrin dilution; c)1:10 agrin dilution; d) 1:5 agrin dilution.

All the conditions resulted in a clustered expression of AChR, but no complex postsynaptic apparatus was detected.

3.3.7 Soluble laminin on different coating

Due to the results obtained with the previous experiments, it has been tried to verify if soluble stimulation with laminin 1:100 could have had the same effect of agrin on AChR clustering. In figure 31a. a coverslip was coated with gelatine, laminin 1:100 and agrin 1:100 and soluble laminin has been used to stimulate the clustering. In figure 31b., the coverslip was treated with agrin 1:100 coating and soluble laminin. Both the conditions resulted in an upregulation of AChR, and in structures compatible with an early clustering process.

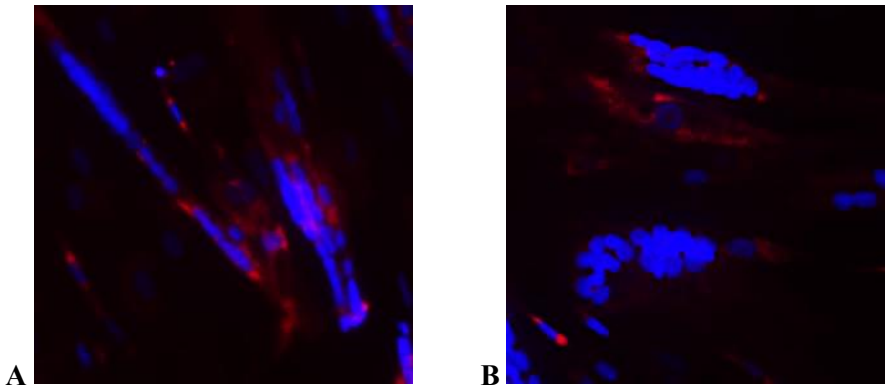

Figure 31: Laminin stimulated myotubes on coated coverslips. Nuclei stained with DAPI, blue; AChR stained with α-bungarotoxin, in red; a) laminin and agrin coated coverslips, 1:100 laminin; b) gelatine and agrin 1:100 coated coverslip, laminin 1:100 stimulation

Another tested condition has been the coating with laminin and 1:100,1:50, 1:10 and 1:5 agrin. Myotubes have been then stimulated with 1:100 laminin. However, these conditions, in figure S4, did not show any significant AChR upregulation nor a clustering effect, and were discarded.

3.3.8 Soluble agrin and laminin

Finally, it has been tested whether soluble agrin and laminin together could increase the previous results. In one of the wells the soluble stimulation has been repeated for two times, one at day 2 and one at day 3 after switching to differentiation medium. As appears from figure 32 a. and b., stimulation with laminin and agrin together and the double stimulation every 24h showed an increased level of AChR expression and a "spot like" staining pattern. However, no significant difference with the only agrin stimulation has been observed. All the conditions have been tested with a 16h incubation time with the soluble molecule. Another tested condition, for this reason, included coating with gelatine, laminin 1:100 and agrin 1:100, and treatment with soluble agrin or laminin stimulation, 1:100 dilution, for 24 hours. The stimulation of 1:100 agrin did not give any different result from the previous experiments with 16h incubation (Figure 32 c.). However, figure 32 d. showed that stimulation with laminin for 24h resulted in lower expression of AChR compared to the incubation for 16h.

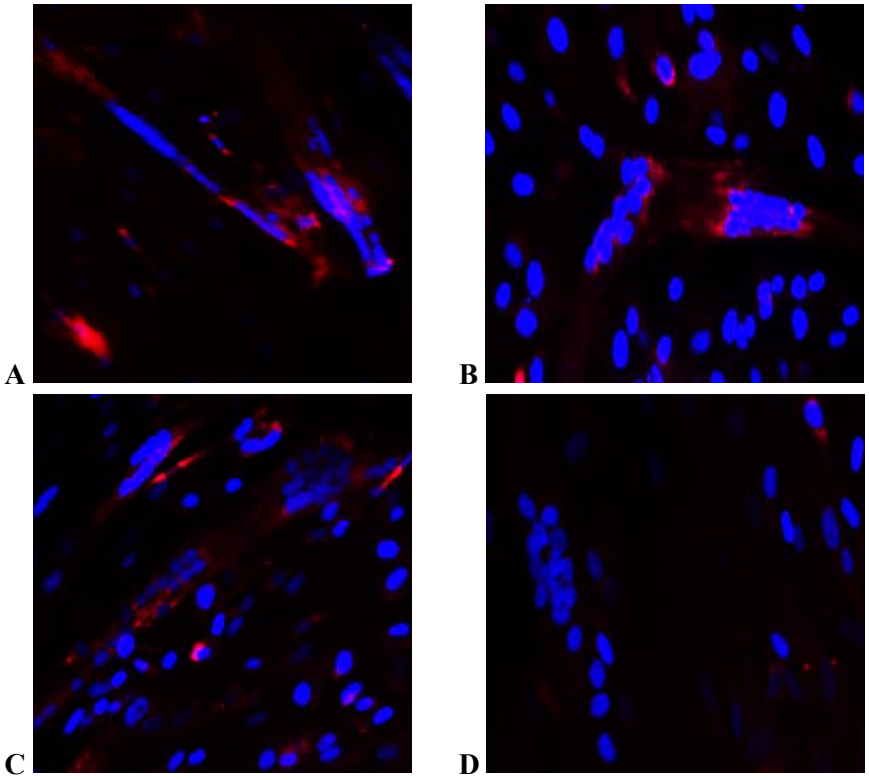

Figure 32: Agrin and laminin soluble stimulation. Nuclei stained with DAPI, blue; AChR stained with α bungarotoxin, in red; a) 1:100 agrin and laminin stimulation, glass coverslips coated with agrin and laminin; b) 1:100 agrin and laminin double stimulation, glass coverslips coated with agrin and laminin c) 1:100 agrin stimulation for 24 hours, on agrin and laminin coated coverslips; d) laminin 24h stimulation, on agrin and laminin coated coverslip.

In table 9, below, are presented all the conditions tested and the results. The ones that appeared to be promising have been kept in consideration for further studies.

Coating	**Soluble stimulation**	**Result**
2% gelatine	agrin 1:1000	-
2% gelatine	agrin 1:500	-
2% gelatine	agrin 1:200	-
2% gelatine	agrin 1:100	-
2% gelatine	agrin 1:50	-
2% gelatine	agrin 1:20	-
2% gelatine	agrin 1:10	-
2% gelatine	agrin 1:5	-
2% gelatine + fibronectin	agrin 1:500	-
2% gelatine + fibronectin	agrin 1:100	-
2% gelatine + fibronectin	agrin 1:50	-
2% gelatine + fibronectin	agrin 1:10	-
2% gelatine + fibronectin	agrin 1:5	-
2% gelatine +laminin 1:100	agrin 1:1000	-
2% gelatine +laminin 1:100	agrin 1:500	-
2% gelatine +laminin 1:100	agrin 1:200	-
2% gelatine +laminin 1:100	agrin 1:100	X
2% gelatine +laminin 1:100	agrin 1:50	X
2% gelatine +laminin 1:100	agrin 1:10	X
2% gelatine +laminin 1:100	agrin 1:5	X
2% gelatine +laminin 1:100	No agrin	-
2% gelatine +laminin 1:100+agrin1:100	agrin 1:100	Y
2% gelatine +laminin 1:100+ agrin 1:50	agrin 1:50	Y
2% gelatine +laminin 1:100+agrin1:10	agrin 1:10	X
2% gelatine +laminin 1:100+agrin1:5	agrin 1:5	X
2% gelatine +laminin 1:100+agrin1:100	laminin 1:100	Y
2% gelatine +laminin 1:100	laminin 1:100	-
2% gelatine +agrin1:100	laminin1:100	Y
2% gelatine +agrin1:50	laminin1:100	-
2% gelatine +agrin1:10	laminin1:100	-
2% gelatine +laminin 1:100+agrin1:100	agrin 1:100+laminin 1:100	X

2% gelatine +laminin 1:100+agrin1:100	agrin 1:100+laminin 1:100 (x2 stimul)	X
2% gelatine +laminin 1:100+agrin1:100	Agrin 1:100 for 24h	-
2% gelatine +laminin 1:100+agrin1:100	Laminin 1:100 for 24h	-

Table 9: Coating and stimulation molecules used to induce AChR clustering on human myotubes. The "Y" in the results section indicates results comparable with early clustering. The "X" indicates a that showed an upregulation of AChR and possible microclusters. The "-" indicates no upregulation of AChR nor a clustering effect.

3.3.9 Permanox slides

A published protocol[123] has highlighted a method to improve myotubes culturing on laminins. The protocol suggested the use of permanox slides, microscope slides are made by a special moulding resin, and covered with a plastic grid. The conditions have been proved to offer a better attachment of the cells and to avoid detaching, that might happen on glass coverslips. The cells were seeded directly on the permanox slide coated with 2% gelatine and surrounded by a plastic well grid, as previously mentioned in paragraph 2.6.1. A slide without gelatine coating has been used as a control. The medium was switched to differentiation medium when the cells reached 90% confluency. The cells on gelatine coating, figure 33 a., died the day after switching to differentiation medium. The ones grown without gelatine, on the other hand, were able to differentiate (figure 33 b. and c.).

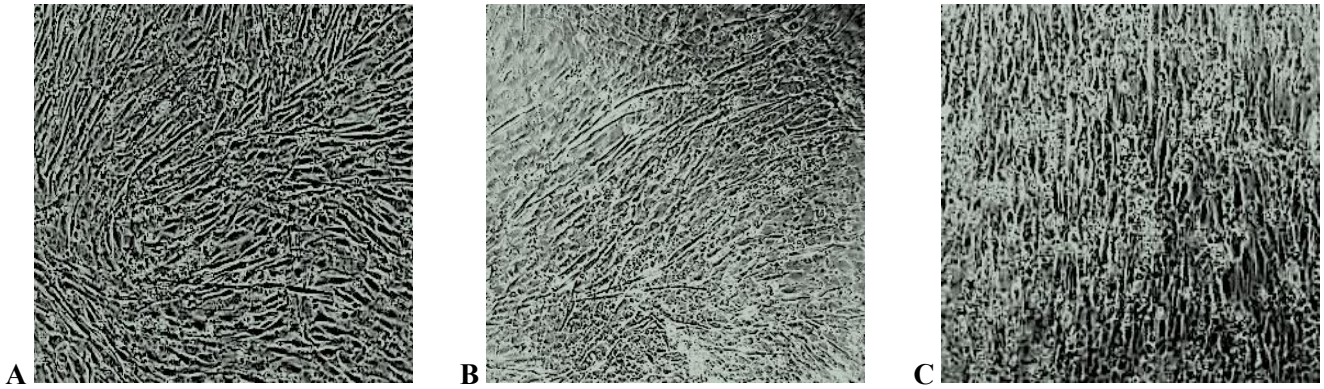

Figure 33: C2C12 cells on permanox slides. a) well without gelatine; b) well with gelatine; c) cells without gelatine after differentiation.

However, it was not possible to stain the cells due to their inability to properly attach to the slide. The experiment has been repeated with the same conditions. And again, cells did not show any adherence to the plastic slide. Due to the inability to induce a proper attachment of the cells to the slide, the method was discarded.

3.4 Immunoprecipitation

Immunoprecipitation is an assay that can be used for the isolation of unknown autoantibodies in seronegative MG patients. Through the beads used in the immunoprecipitation assay, it is possible to isolate the unknown antibody of the patient and the antigen at the postsynaptic apparatus simultaneously. A mass spectrometry analysis after the assay gives then the possibility to identify the isolated molecules. A total of four different sera, all strongly positive for AChR MG, have been tested both on human myotubes and L6 myotubes. In order to increase the amount of AChR present on the surface of myotubes, cells have been stimulated with 1:100 soluble agrin about 16 hour prior the assay, in order to increase the expression of AChR (figure 34).

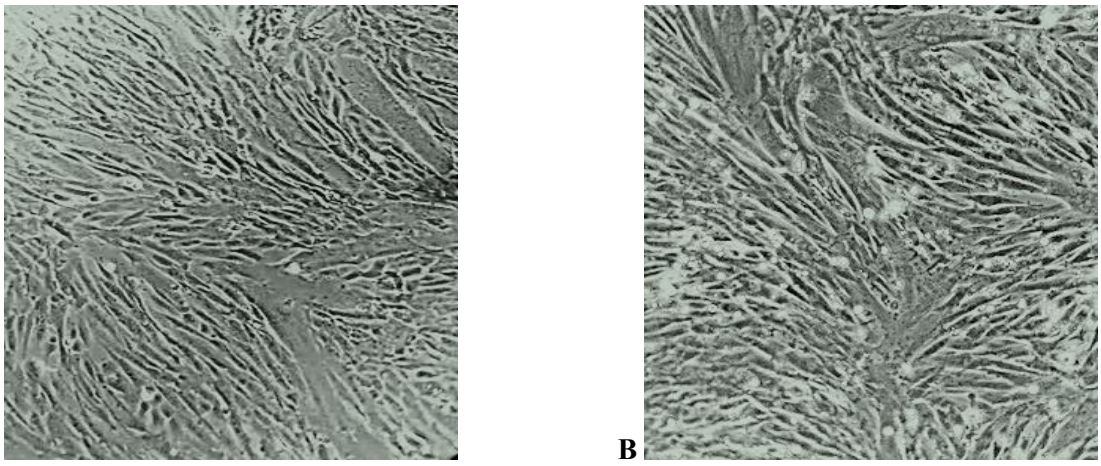

Figure 34: Myotubes after soluble agrin stimulation; a) human myotubes; b) L6 myotubes.

After incubation with patient serum, a cell lysate has been obtained and a SDS PAGE have been performed to further purify it. As already mentioned, the entire area containing the sample have been cut and sent for the mass spectrometry analysis. The first mass spectrometry analysis, performed on a human myotubes extract, did not show the presence of any molecule related to AChR subunits or human IgG, but only factors related to the complement signaling. For this reason, the SDS PAGE of a cell lysate from both human and L6 myotubes, incubated with the same serum, has been stained with Coomassie. Through this staining, it has been possible to verify the presence in the elute of molecules with the same molecular weight of human IgG and/or α subunit of the AChR, prior to the mass spectrometry. The staining appeared very weak, and the obtained bands were not completely distinguishable from their background, leading to difficulties in the gel analysis (figure 35). It was possible, though, to observe a staining at 50kDa and 25kDa, corresponding to a human IgG heavy and light chain. Additionally, in the sample of human cells, there was a band at the molecular weight of 60 kDa, corresponding to the weight of the AChR α subunit. The arrows have been inserted for an easier analysis of the picture, due to the really low staining that the gel allowed. Due to the high possibility that the bands could have been a background effect, the results have to be further confirmed by mass spectrometry.

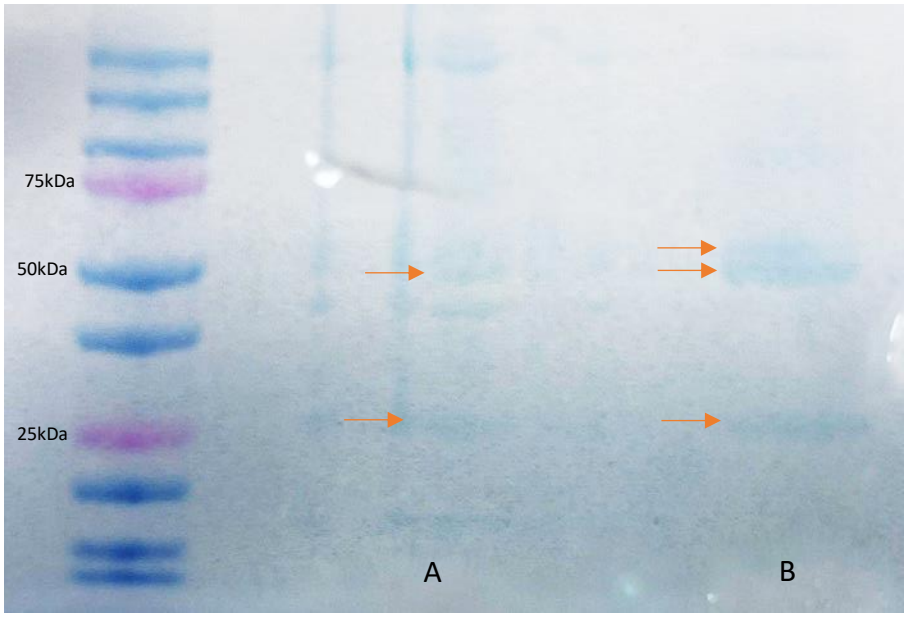

Figure 35: Coomassie staining of the SDS PAGE gel; a) L6 myotubes lysate, incubated with 6325/18 serum; b) human myotubes lysate, incubated with 6325/18 serum.

The results of immunoprecipitation, together, showed that this method still needs an improvement for the isolation of the molecules prior to mass spectrometry, in order to not lose the samples.

3.5 Cell surface markers identification

Together with AChR, myotubes express a wide range of other muscle-specific transmembrane proteins. As a side project, the presence of these molecules on the surface of myotubes has been tested. The analyzed protein were different molecules involved in the muscular maintenance *in vivo*. Antibodies against α, β and γ sarcoglycan, transmembrane proteins involved in the protein complex that connects the muscle fiber to extracellular matrix, has been used to detect these proteins on myotube's surface. It has also been tried with antibodies anti-dysferlin, a protein linked with skeletal muscle repair, and anti- IgLON 5, a cell-adhesion molecule. Incubation with antibodies, AF594 conjugated, against the molecule of interest allowed the visualization of the molecules of interest in the red channel. In figure 36 the results from the fluorescence microscopy allowed the assessment of all the molecules expressed on the surface of early myotubes with a pointed expression. Among all, γ-sarcoglycan was the one that showed the lowest level of expression.

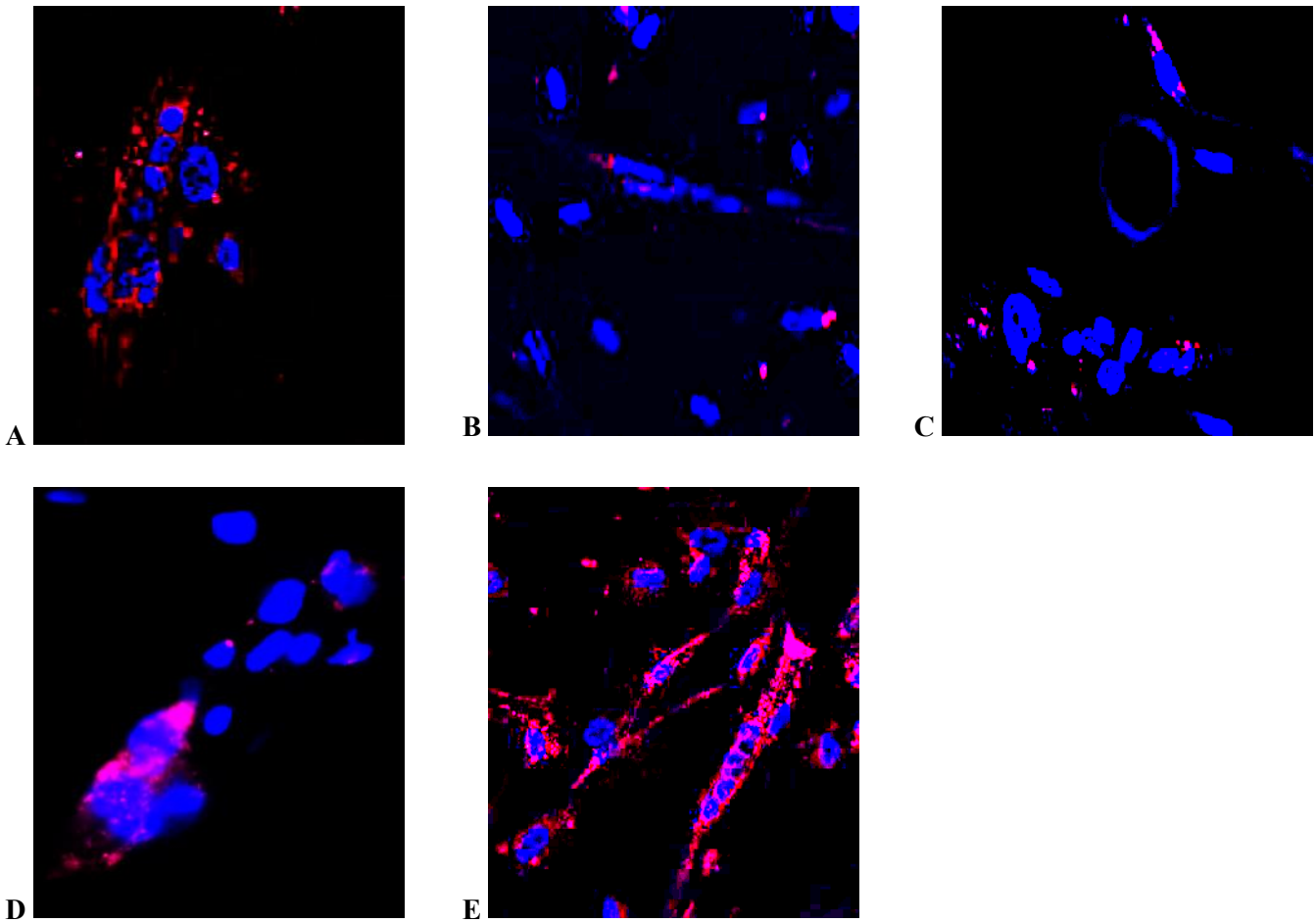

Figure 36: Early myotubes stained with antibodies against the protein of interest, AF594 in red and nuclei stained with DAPI in blue; a) α-sarcoglycan; b) β-sarcoglycan; c) γ-sarcoglycan; d) IgLON5; e) dysferlin.

Due to the "spot like" staining obtained, the experiment has been repeated with the same antibodies but with a different fluorophore, AF488, to exclude a background effect from the previous results. In figure 37 the results of the experiments are presented. The second staining confirmed the low expression of the molecules, as well as their "spot like" expression on the membrane of the myotubes.

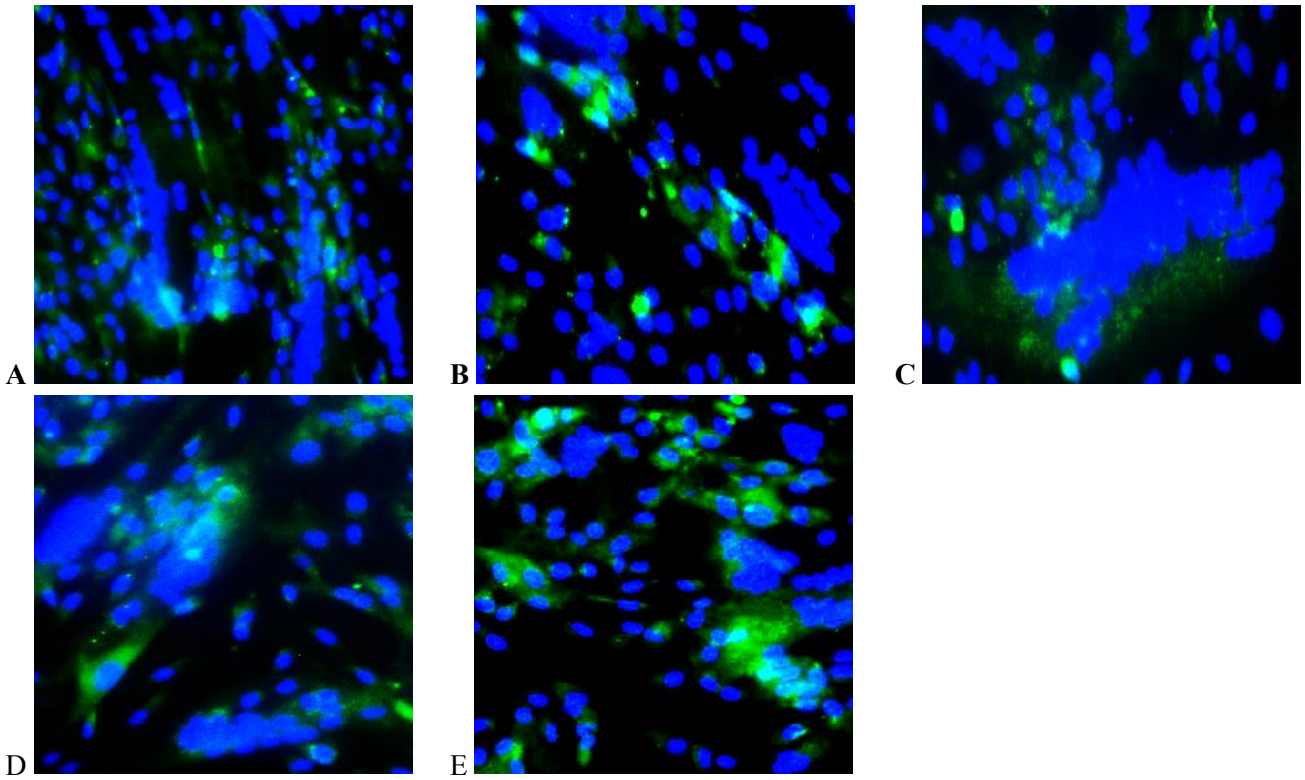

Figure 37: Myotubes stained with antibodies against the protein of interest, AF488 in green and nuclei stained with DAPI in blue; a) α-sarcoglycan; b) β-sarcoglycan; c) γ-sarcoglycan; d) IgLON5; e) dysferlin.

3.6 MSI-1436

MSI-1436 is a novel drug candidate that is currently under investigation for its effect on skeletal muscle repair. After studies have highlighted its potential in mouse and zebrafish, it has been decided to test the efficiency on human muscle stem cells. The aim of the experiment was to test if the molecule was able to increase myoblast proliferation and if DMSO, in which the drug is dissolved, could have a toxic effect on the cells.

3.6.1 Effect of different MSI concentrations

To test whether MSI was able to increase the cell growth, and if DMSO could have a toxic effect on cells, they have been monitored over a period of 5 days. Every day, cells treated with MSI and cells treated with DMSO were trypsinized and counted. Each well of a 24 well plate received 250uM of growth medium with 2 μM concentration of MSI or DMSO. The results graph, in S5a, showed no significant cell growth over the 5 days. However, it has been observed a higher number of cells in wells treated with MSI compared to the DMSO ones. The experiment has been repeated on 35 mm dishes, that allowed easier and shorter cell counting. In the beginning, cells were treated with 2 μM and 1 μM concentration of MSI or DMSO. In figure 38 both the graph shows an increased number of cells in samples treated with MSI, compared to the ones treated with DMSO.

A

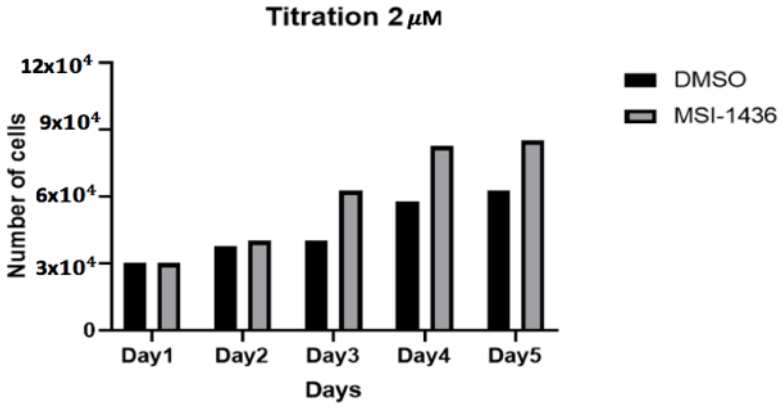

B

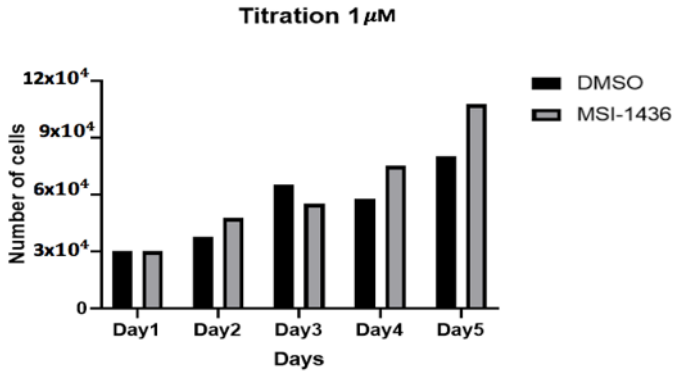

Figure 38: MSI and DMSO treated cell number. a) 2 μM titration; b) 1 μM titration.

To assess the possibility of a dose dependent effect, different concentrations of MSI and DMSO have been tested (1, 2 μM and the 4 μM) in the same experiment. In addition to this, a sample was treated only with growth medium, in order to test the differences with the normal cell growth level. The number of cells have been evaluated only at the last day, in order to see the effect on each plate of the compound used. The result, in figure S6, showed a potential dose-dependent effect, with cell numbers decreasing when increasing the concentration. When calculating the difference between cell numbers of wells treated with MSI compared to the ones treated with DMSO, it also confirmed that the difference between cells increased with the increasing of the dose. The lower concentrations (1 and 2 μM) showed to have similar number of cells, with a strong difference compared to the higher concentration (4 μM).

With the purpose of further studying the possibility of a dose-dependent effect, the concentrations of 3 μM and 5 μM have also been included in the study. Each condition, moreover, has been tested in triplicates in order to assess a statistically valid result. Finally, the results of each experiment have been normalized in order to allow the comparison between the experiments. The values of cell growth were calculated as a percentage compared to the control with no treatment.

The graphs in figure S7 show the cell growth with different concentrations of MSI and DMSO, calculated every day over a period of 5 days. In figure 39, the final growth number has been resumed for each titration compared to the control, at day 5. The results highlighted the higher number of cells treated with MSI, but also the number of cells highly decreased with an increasing of the amount of both MSI and DMSO. We hypothesized that the toxicity of DMSO at higher concentrations could be damaging for the cells, covering the growing stimulation effect of MSI in the treated samples.

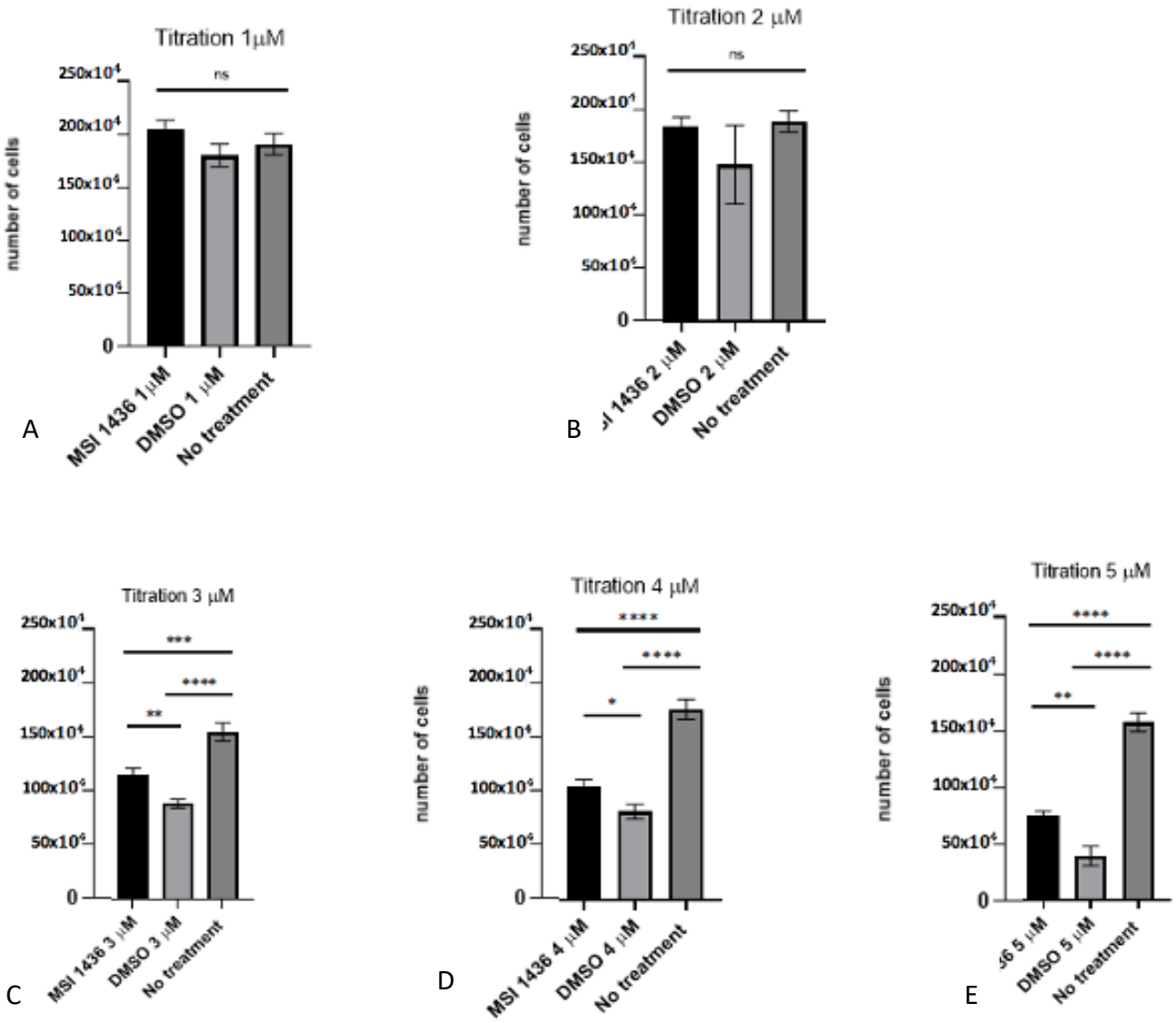

*Figure 39: Overall growth results of cells at day 5 for each condition, compared to the untreated control. A) 1µM concentration; b) 2 µM concentration; c) 3 µM concentration; d) 4 µM concentration; e) 5 µM concentration. * for P value <0.05; ** for P value <0.005; *** for P value <0.0005; **** for P value < 0.0001. All the P values > 0.05 have been considered not statistically significant.*

The difference between cells treated with MSI and DMSO has been calculated after 5 days in order to assess the efficacy of the compound. The final result in figure 40, that sum all the experiments with normalized data, show a dose dependent increase of the difference between cells treated with MSI and the ones with DMSO. However, the difference at the concentration of 5 µM did not show a correlation with the previous results.

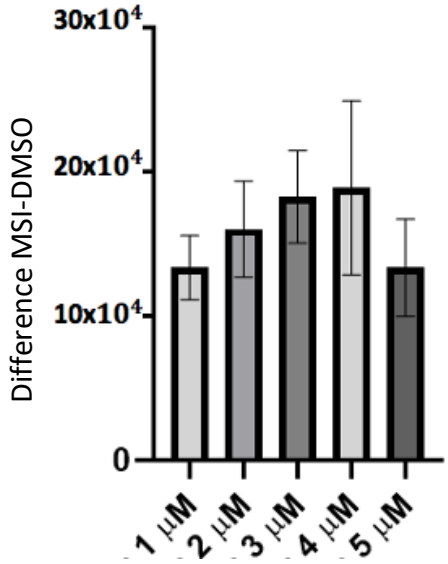

Figure 40: Overall growth difference between the conditions after 5 days. Up to 5 µM it is possible to see an increasing difference between the 2 treatments. Nevertheless, at 5 µM the difference decreases again. Cells incubated with MSI/DMSO for 5 days.

3.6.2 MSI effects on the morphology of cells

After having performed a quantitative analysis on cell growth, it has been tested whether MSI could have an effect on the morphology of the cells. The observation of the cells was performed in three independent experiments, with cells at a different passage number, in order to exclude possible variables between cells lines in the evaluation of the MSI effects. The observation of cells has been performed with bright field microscopy, at different magnifications, to evaluate the overall effect on the culture and on the single cell morphology. Figure 41 shows representative images of MSI and DMSO treated cells compared to the control sample, and no significant difference has been detected. When observing all the pictures at different magnifications, as figure S8 demonstrates, it has been confirmed that MSI did not change the morphology or other characteristics of cells.

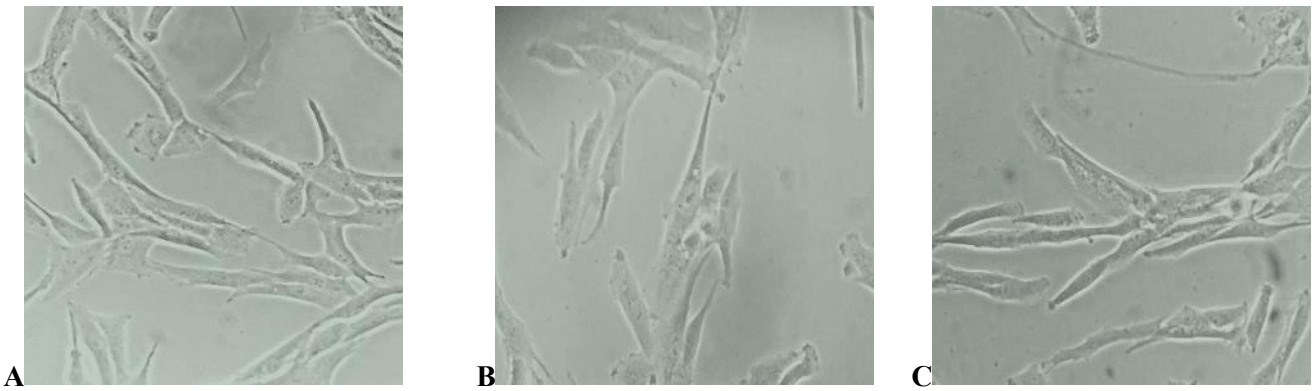

Figure 41: Overview on the morphology of the cells with different treatments; a) MSI 1 µM treated cells; b) DMSO 1 µM treated cells; c) no treatment control

When increasing the concentration of MSI/DMSO, the cells appeared to be sparser in culture, and it was possible to see an increasing number of detached cells with the increase of the concentration. In conclusion, these results could explain the difference in the number of cells treated with different

concentrations of MSI and DMSO with a major number of dead cells in the conditions with lower numbers of cells.

3.6.3 MSI effects on differentiation of human muscle cells

When switched to differentiation medium, in one of the experiments the cells died the following day, so no pictures were recorded. In the other experiments cells survived. However, 3 days after switching to differentiation medium myotubes had become visible only in cells treated with DMSO and the control, while in cells treated with MSI there wasn't any differentiation of cells (Figure 25). Moreover, cells treated with higher concentrations of MSI died immediately, while cells with the same amount DMSO underwent the differentiation process, but showed an high number of dead cells in culture. The only exception has been represented by cells treated with DMSO at 5μM concentration, which did not die but did not undergo the differentiation process. In figure 42 only a representative picture is shown, however the pictures of all the conditions have been recorded and documented in Figure S10.

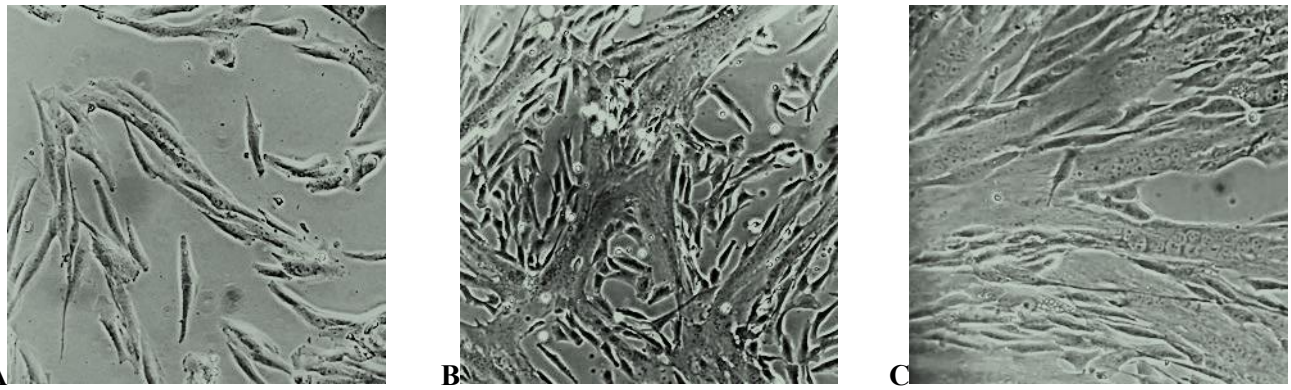

Figure 42: Human muscle cells three days after switching to differentiation medium; a) MSI 1 μM treated cells; b) DMSO 1 μM treated cells; c) control

3.7 Cell line characterization

The presence of NMJ machinery specific proteins has been evaluated in different cell lines. The cells lines that have been tested were: human myotubes, human myoblasts, C2C12 myotubes, C2C12 myoblasts, L6 myotubes, L6 myoblasts and T37 myoblasts. The expression of β-actin, a housekeeping gene, has been used as a positive control to ensure the validity of the western blot assay. As reported in figure 43 a., β-actin signal has been obtained in all cell lines and thus confirming the accuracy of the assay and the fact that no errors in the procedure have been performed. Then the presence of LRP4 protein in the different cell lines has been evaluated. Two positive controls of LRP4 antigen, which normally are used for ELISA assays in the host lab, have been used in addition to the samples. In figure 43 b. the result of the western blot analysis. The results showed that LRP4 signal has been found only in L6 myoblasts, further confirming previous results indicating the absence of a functional neural synapse *in vitro*.

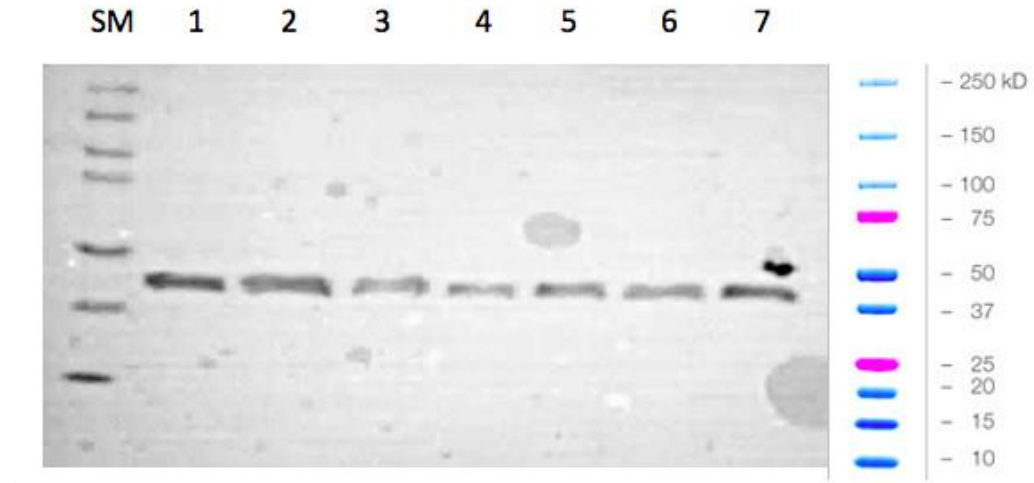

A

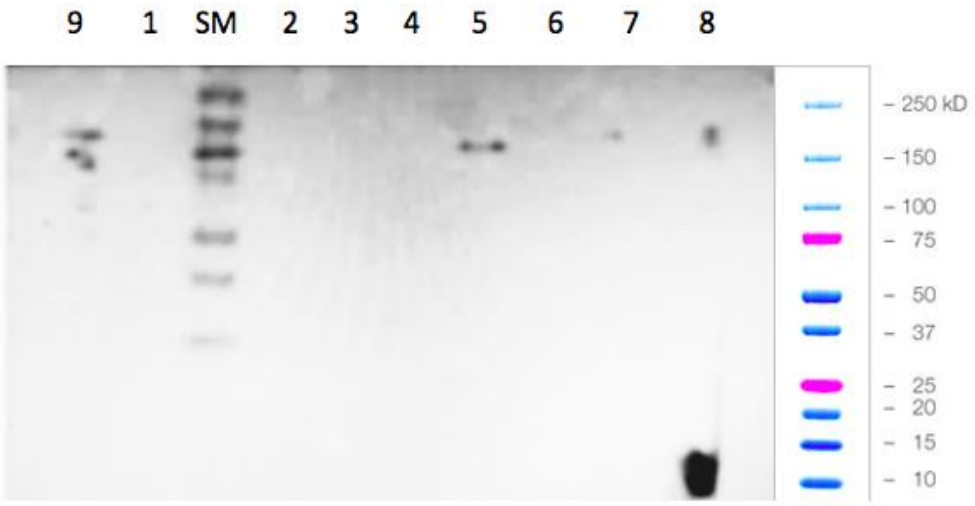

B

Figure 43: SM, size marker; 1, C2C12 myoblasts; 2, C2C12 myotubes; 3, human myoblasts; 4, human myotubes; 5, L6 myotubes; 6, L6 myoblasts; 7, T37 myoblasts; 8, LRP4 antigen 1; 9, LRP4 antigen 2; a) western blot immunodetection of β-actin. All the samples tested showed the band for β-actin protein; b) western blot immunodetection of LRP4. Only L6 myoblasts showed an expression in addition to the positive controls.

4 Discussion

SNMG are a subgroup of MG patients clinically diagnosed with myasthenia gravis lacking detectable antibodies. The goal of the project the establishment of new methods for the detection of autoantibodies involved in SNMG using different primary cell cultures.
The CBA allowed the isolation of SNMG sera in the cohort of diagnosed MG patients, and the exclusion from the study of sera with detectable antibodies against AChR and MuSK. The TBA, then, has been used to assess the presence of antibodies against NMJ in the serum.
Myogenic stem cells, isolated from routine surgery biopsies, have been cultured and differentiated to perform a wide range of experiments. The experiments aimed at the establishment of a functional model of the human postsynaptic apparatus. Different stainings confirmed the ability of the cells to express different muscle specific proteins such as MyoD and desmin on their surface. However, human myotubes presented only a diffuse expression of AChR and lack of a developed postsynaptic apparatus of clustered AChR. The clustering of AChR is an essential process for the study of NMJ diseases and has been necessary for isolation of SNMG antibodies through the immunoprecipitation assay. For this reason, different conditions have been tested to establish a protocol for AChR clustering in vitro. Agrin, laminin and fibronectin have displayed the ability to induce an upregulation of receptors and a beginning of clustering, indicating a possibility for inducing this phenomenon in in vitro cultures.
As a side project, stem cells culture were used to test the effects of a novel drug candidate for tissue regeneration, called MSI 1436. This drug, known to inhibit the PTB1B protein, has been tested to evaluate the effects on proliferation and differentiation of human stem cells in vitro. The results indicate the potentiality of MSI to increase stem cell proliferation, but also the primary culture potential to be a reliable model for studying new drug targets.

4.1 Identification of SNMG patients

For the isolation of SNMG autoantibodies, it was necessary to exclude from the cohort of diagnosed MG patients the ones showing antibodies against AChR and MuSK. These antibodies are the most common in MG patients, and are normally detected with radioimmunoprecipitation assay or ELISA[105,106]. These assays however do not always allow the detection of antibodies[105], mainly due to low affinity of the antibodies to recombinant or soluble antigens. Through the CBA, it was possible to screen patient serum on a more sensitive and specific test. In the assay, HEK293 cell line was transfected with MuSK or AChR subunits and rapsyn, that stimulates the clustering of AChR. Through the expression of clustered AChR on the membrane, it was possible to isolate antibodies that bind only to high density AChR, or antibodies which cannot recognize AChR antigen due to the destruction of the epitopes by the process to isolate the antigen[107]. For the antibodies against MuSK, the largest limitation of the common assays is the low concentration of antibodies in the serum, that do not allow the detection by standard methods[107]. In the CBA, this problem has been overcome by the high expression of the antigen on the cell membrane that improves the binding of the antibody at cell surface. Through CBA a large part of the sera identified as seronegative have been classified as AChR or MuSK positive, and several studies on this technique show that a large part of SNMG patients are normally represented by MuSK positive MG [108,109]. However, one of the major limitations of the CBA as a diagnostic test is that it is a qualitative and a not-quantitative test[5]. The evaluation of fluorescence, and sequent diagnosis as MuSK/AChR positive, is highly subjective. Moreover, the presence of a background may alter the interpretation of results. For this reason, each CBA result

have been evaluated by two different people before assessing positivity to avoid any observer bias. Additionally, several samples had to be analyzed several times due to the high level of the background.

4.2 Detection of autoantibodies against NMJ with TBA

In the cohort of patients indicated as seronegative autoantibodies against other components of the NMJ postsynaptic cleft, such as Lrp4 or ColQ[110,111], were described. However, even though a CBA for Lrp4 is currently under investigation and some laboratories presented a valid protocol[89], the absence of a CBA for the other proteins did not allow for an identification of the SNMG antibodies through this test[110,111]. The TBA could be used as a tool for a screening of patients that result SNMG after the CBA. This assay allows to detect antibodies from patients against unknown components of the NMJ, but similar to CBA is a qualitative analysis. The test was performed on rat muscle because human biopsies were derived from the extremity of the muscles and might not have enough NMJ to perform the analysis. With rat, it was possible to obtain a larger amount of muscle section with higher probability of obtaining at least one NMJ per each section. The TBA protocol has been the same used for routine diagnosis of other diseases [113] and has been improved during other NMJ disease studies.
Rat skeletal muscle have been snap frozen to preserve the NMJ morphology and the protein structures, and then cut using a cryostat to prepare the sections for the TBA. The tested serum dilution has been 1:40 and the muscle section thickness was 8 μm. Different sera which were strongly positive for AChR MG, have been tested, as well as healthy controls. All the positive samples tested have shown a staining at the NMJ. However most of them resulted to have striational antibodies[111] against epitopes of the muscle proteins. Striational antibodies are really common: they are being found in 30% of MG patients and 74% of patients with thymoma associated MG[100,101]. Their pathogenic role is still unknown although they are commonly used as biomarkers for thymoma and some studies highlight the efficacy as biomarkers to predict an unsatisfactory outcome of thymectomy[103]. The sera showing striational antibodies have to be discarded from the analysis, due to the high level of background produced. Patients showing striational antibodies, in fact, have a fluorescent signal on the whole the section and not only on the neuromuscular junction, making the interpretation of the TBA result not reliable.

4.3 Culture of primary muscle cells

Human satellite cells have been isolated by the enzymatic digestion of a skeletal muscle biopsy. To reach the aim of the project, cultures of primary human muscle cells have been established. In comparison with immortalized cell lines, primary muscle cell cultures are derived directly from the tissue, reflecting the variability and the *in vivo* state. For this reason, primary cultures have been suggested as a physiologically relevant model for studying myogenesis *in vitro*[115]. Due to the low abundance of primary myogenic cells in adult skeletal muscle, the process of isolation of primary myoblasts still represents a technical challenge[114,115]. One of the major problems in isolation of cells from biopsies is represented by the risk of fibroblasts presence in the culture. The proper removal of fat and blood vessels from the muscle, however, led to high purity cultures[114].
After the isolation, it was not possible to characterize the cultured cells through morphological characteristics, due to their high similarity to fibroblasts [117]. Fibroblasts did not undergo the process of differentiation into myotubes. The culture had to be discarded if its quantity was high. The number of fibroblasts in primary cultures had to be really low and this because of a risk for the depletion of myogenic cells due to their lower doubling time[117]. Primary cell culture purity have been identified

by the presence of MyoD staining in the nucleus of the cells. MyoD is a transcription factor expressed by cells committed to skeletal muscle cell faith. For this reason, it is largely abundant in the nucleus of proliferating myogenic cells, and widely detectable in the nucleus of non-myogenic and differentiated cells[61,64]. MyoD staining showed high levels of purity in human primary cells culture, at 90 to 95%, and therefore no additional steps for depleting fibroblasts have been performed. MyoD positive cells in culture further differentiate into myotubes, when medium was switched to DM. Myotubes have been then further characterized for the expression of desmin, a muscle specific protein. Desmin, an intermediate filament protein, has been used as a biomarker for cells that are terminally differentiated[119,120] in several studies. The positive staining for desmin indicates the presence of terminally differentiated muscle cells in culture[66]. The staining of the cultures resulted to be approximately 90% desmin positive, indicating that almost all the cells have undergone the process of differentiation to muscle cells. Myotubes have been further characterized by another MyoD staining, that showed the nuclei of differentiated cells to be MyoD negative. Previous studies have already mentioned that nuclei become MyoD- in differentiated cells, further confirming that the cells have exited the cell cycle[120,121].

4.4 AChR clusters on human myotubes

Human myoblasts were cultured on glass coverslips in a 24-well-plate and differentiated. The presence of AChR clusters have been evaluated by staining with α-bungarotoxin[122,123]. The results then showed that without external stimulation no AChR clustering was observed, and only a low expression of clusters could be observed, confirming previous results[122]. A study [127] highlighted the possibility that clustering on non-innervated myotubes appear, but only in a diffuse manner and tend to disappear rapidly. For this reason, in all the tested conditions cells have been fixed with 4% PFA and stained after, to avoid the internalization of receptors.

Neural rat agrin has been used to stimulate myotubes, but despite an upregulation of AChR compared with the previous conditions, no clusters could be observed. The double stimulation of the cells with glass coverslips coating and soluble agrin or laminin stimulation, presented in [20], has been tested to assess the level of clustering with different conditions. Different molecules have been tested, as suggested in several different studies [124,125,126] that have confirmed that proteins expressed in the ECM enhance the process of clustering of AChR. One important point to be discussed is that almost all the studies on AChR clustering have been performed on C2C12 cells and this with good results. Within the few treating human muscle cell models [124,128] only a few results have been obtained, and none of the studies obtained a complex postsynaptic development and remodeling as in mouse models. Following the experiments reported in [124] about efficacy of coating, human muscle cells were stimulated with coated laminin and soluble agrin, and a strong upregulation of AChR has been observed, together with some structures that were compatible with early clusters. As it was observed in different experiments[124], the conditions did not induce the presence of a complex postsynaptic cleft in none of the experiments. The coating of coverslip with fibronectin displayed a strong upregulation of AChR, and the same result has been obtained with stimulation through soluble laminin only.

To sum it up, these results further confirm that neural agrin is required for the proper development of the NMJ postsynaptic apparatus [125,126]. When coverslips were coated with laminin and agrin, a major amount of possible early clusters has been detected compared with the previous conditions. This result partially confirms the results obtained in other studies and highlight the ability of the components of the basal lamina in enhancing AChR cluster formation[123,124]. In several studies, however, the possibility to increase the process of clustering has been represented with a coating that

expresses the majority of molecules which are present *in vivo* [124,128,129], mimicking the conditions *in vivo*. The studies altogether indicate that the clustering process requires several proteins and growth factors and, furthermore, a complex extracellular matrix may favor the clustering of AChR.
Another point that has been analyzed has been the culturing of the cells. The [124] study, which obtained good results with human muscle cells, highlighted also how the culturing conditions may affect the AChR clustering. Another study suggested[124] that the permanox slides have been tested for increasing cell's attachment to the surface of the slide, mimicking the *in vivo* condition. Despite the good results obtained with C2C12 in that study, the protocol did not work in the laboratory and cells did not show any attachment to the surface of the slide. Due to the poor results obtained with human cells in the same study, and due to the poor results obtained with this protocol in the laboratory, the experiment has been discarded.
Consequently, the different protocols presented may be optimized with the use of a coating that includes more molecules of the ECM and different surfaces. A culture of human myotubes displaying clustered AChR could be used sequent for the isolation of unknown antigens against the NMJ but also for studies on other NMJ diseases.

4.5 Immunoprecipitation

Immunoprecipitation assay allow the isolation of an unknown antibody and an unknown antigen in SNMG. Intact differentiated cells have been incubated with MG positive sera in order to allow the binding of the antibodies to their antigens. After the incubation the precipitation of these immunocomplexes should allow the isolation of both the antigen and the antibody. The sequent mass spectrometry analysis allows the characterization of the antigen-antibody complex. One of the major limitations of this assay is the absence of a fully developed postsynaptic membrane in human myotubes *in vitro* cultures, that could led to the absence of autoantibodies binding. In order to test the effect of AChR clustering absence on the results of the test, L6 myotubes cultures have been used in parallel and tested with the same sera.
L6 myotubes have been shown to express AChR clusters in culture, thus overcoming the problem of a human muscle cell model [130,131]. To test the difference in efficiency of the two different models, four sera strongly positive for AChR MG have been tested. Lysates have been incubated with protein A/G agarose beads to capture IgG and bound target antigen, and both have been then separated by SDS-PAGE. The following step of the analysis consisted in the identification of proteins by mass spectrometry, a standard method in biochemical research and for the characterization of unknown molecules. Prior to identification by mass spectrometry the gel could not be stained because the protein de-staining protocols[132,133], as they prolong the sample preparation for mass spectrometry, increase the risks of sample contaminations[132]. For this reason, the entire band of the gel has been excised and analyzed. However, due to the absence of staining a high amount of gel pieces have been analyzed and by doing so, problems with the analysis of the samples appeared. Neither AChR subunits nor of human IgG have been found in the mass spectrometry results.
To further confirm the presence of the interested proteins in another sample, a staining of the gel with Coomassie has been performed and the respective bands have been then cut and sent for mass spectrometry analysis. However, the gel did not show a strong staining and the bands were almost not detectable. Moreover, as already mentioned in [132], Coomassie staining is not completely compatible with mass spectrometry analysis, leading to a high probability of losing the sample prior to analysis.

An implementation of this assay could be represented by silver staining, that is more time consuming and toxic compared to the current methods but allow immediately and very specifically the presence of proteins with the desired weight in the gel[133,134]. Immunoprecipitation is a practical and efficient tool for antigen and antibody isolation in SNMG but the absence of a complex postsynaptic machinery in human muscle cell culture may interfere with the efficacy of the analysis. For this reason, different cell lines expressing complex AChR clustering may be used instead while improving the current method. Nevertheless, the use of only some muscle cell lines may represent a limitation in this type of study, as the cells might not express all the protein involved in SNMG. This might, at the end, decrease the possibilities of isolating the antigens involved in the pathogenicity of this disease.

4.6 Cell surface markers identification

Different cell surface proteins have been correlated to a wide range of neurodegenerative diseases [135,137,139], and their expression on *in vitro* culture has been tested. The sarcoglycans are proteins which are part of the dystrophin-glycoprotein complex. This complex is thought to link the cytoskeleton to the extracellular matrix in muscle fibers[140] and their alterated expression has been associated to dystrophy[135]. A study has highlighted that the sarcolycan complex, formed by α-, β-, γ- and δ-sarcoglycan [140,141], is expressed on the membrane of the muscle. The results of the staining performed in the laboratory showed, by means of two different experiments, a weak and "spot-like" staining on the cell membrane of the myotubes, coherent with other published results[142]. However, the weak staining results may be caused by the absence of an association of myotubes with the plasma membrane[142,143]. The alteration of another gene, dysferlin, lead to a specific type of muscular dystrophy, referred to as dysferlinopathy. Diagnosis is complex due to the high clinical variability of the symptoms, and several electrophysiological and muscle imaging tests are required[139]. However, new protocols present different methods to detect dysferlin deficiency in monocytes for the diagnosis of dysferlin myopathies[139]. The [139] study highlighted the upregulation of dysferlin in activated satellite cells, with increasing levels of expressed dysferlin in differentiated myotubes, which was further confirmed by another study in C2C12 cell line [140]. The staining with anti-dysferlin antibodies detects the presence of dysferlin on myotubes, indicating the possibility of developing an essay to detect human IgG against dysferlin in primary cultures. In addition to the previously mentioned proteins, IgLON5 expression on human myotubes has been tested for an unrelated project. IgLON5, and the IgLON family of proteins, are neuronal cell adhesion proteins with an unknown function. The staining confirmed the expression of IgLON5 protein in the myotubes, even though the staining was weak and "spot-like".

4.7 MSI 1436

Regenerative medicine represents a promise in regenerating tissues damaged by diseases or injury[145]. In this field, small molecules represent an emerging area of study. Using model organisms such as zebrafish or mouse, a novel candidate has been identified. MSI 1436, an inhibitor of the enzyme protein-tyrosine phosphatase 1B (PTB1B)[150,151]. We have tried to test the regenerative potentiality of this molecule on proliferation of human stem cells in culture, following the previous results obtained in mouse that showed an increase in cell proliferation and tissue regeneration [145]. The results have shown an increase of the cell proliferation in cells treated with MSI compared with the ones treated with DMSO, partially confirming the results obtained with mouse in [145]. Furthermore the difference between cells treated with MSI and DMSO has been calculated, showing a dose

dependent increase. However, contrary to the results presented in a previous study [145,] the difference within the cells did not result to be statistically relevant. An explanation for this result may be the lower number of cells compared to the number of cells in an organ and the shorter time of observation in the study (5 days compared to the 28 in the study). It has been subsequently observed if MSI could have an effect on cell's morphology, and no deformation of the shape of the cells have been observed. However, with higher amounts of MSI a lower number of cells has been observed, and the observation allowed to explain the result with an increasing rate of cell's death. MSI seemed to display a dose dependent toxicity, confirming previous results of different studies which have already highlighted the toxicity of DMSO[145,146]. The studies confirmed a toxicity of the compound in a dose dependent manner after the concentration of 1%[147]. Experiments showed that MSI treated cells were not able to differentiate and, after switching to a differentiation medium, the cells treated with a higher amount of MSI immediately died, while the lower amount of MSI was able to inhibit differentiation of the cells.

It is difficult to explain this element due to the fact that the results of the DMSO controls did not show any toxic effect. Therefore, we hypothesized that MSI was able to strongly inhibit the differentiation by blocking some signal pathways and at a higher concentration this inhibition could led to the death of the cells. However, studies of MSI on clinical trials did not show effects of toxicity of the compound [145,150]. The explanation of this phenomenon could be that in *in vitro* cultures the growth medium has a high presence of growth factors and nutrients, while in a differentiation medium the growth factors (such as FBF) are replaced by differentiation factors (such as HS)[150]. Whitout proliferation factors, cells are pushed to differentiation that has been inhibited by MSI, and this might explain the high amount of dead cells. This might explain also why this phenomenon has not been observed in *in vivo* studies.

In conclusion, the results highlight the high potentiality of MSI in regenerating tissues[145], but open several questions on its effects on stem cells[146], indicating that more studies on this have to be performed.

4.8 Western blot

Cell lysates of human myotubes, human myoblasts, C2C12 myotubes, C2C12 myoblasts, L6 myotubes, L6 myoblasts and T37 myoblasts were prepared. Protein concentration was measured by nanodrop and the samples were subjected to SDS-PAGE and Western Blotting. The obtained results show that the β-actin, an housekeeping gene used as a control[153], was expressed in all the cell lines. In the other gel, two positive controls of commercial Lrp4 antigens were added, and the membrane was incubated with anti-Lrp4 antibody. The results showed a band on both the positive controls and in L6 myoblasts. As presented in figure 43, a slight band could be visible also on a T37 sample, but it was not possible to exclude the possibility that the slight band could be only the background. The absence of a staining in the majority of the samples, but not in the controls, indicates that a higher concentration of protein could be required for the detection of Lrp4 in the different cell lines. Moreover, the analysis should be repeated with all the proteins expressed in the NMJ to assess the ability of the cell lines to express the different proteins required for AChR clustering. Confirming the presence of all the proteins in the different cell lines could be a first step towards developing new methods for AChR clustering and complex postsynaptic development[126,127].

4.9 Antigen discovery in Myasthenia gravis

After the identification of the pathogenic effects of AChR and MuSK antibodies[48], several other antibodies against the NMJ have been detected in myasthenia gravis patients, such as anti- Lrp4, agrin and ColQ[7,8] antibodies. ELISA, CBA and immunoprecipitation studies have been used for the detection of these autoantibodies, however the results showed that there is an high variability in the results due to the detection assay used and the source of the antigen[104]. Moreover, for all of these molecules, their role in MG, their diagnostic value and the specificity for MG have not been understood yet[104].

One of the major limitations of the standardized diagnostic test, such as ELISA, is the low affinity of some kind of antibodies to the commercial and recombinant antigens. This has been shown to strongly affect the diagnosis and the detection of different antigens, including MuSK[4,5]. The different methods tested in the project aimed for isolating and characterizing the SNMG antibodies and antigens. In this method, as opposed to the previous experiments, the combination of different techniques allowed the isolation of SNMG sera positive for antibodies against components of the NMJ. One of the major limitations of working with primary muscle cells has been the absence of a fully developed and remodeled postsynaptic machinery, as already mentioned in former studies[20,21]. This made the isolation of seronegative antibodies still impossible, due to the absence of all the proteins of NMJ expressed. Different studies have highlighted the possibility to use mouse models with the same scope, but seronegative serum might not react with animal protein, despite the high similarity with the human ones. Nevertheless, the use of only a single cell line may be a limitation, due to the genetic variation and the possible absence of all the NMJ antigens. Here we have proposed a new approach for the identification of the factors involved in SNMG using both tissue sections and myogenic progenitors from different species, including human ones. Primary cell cultures, resembling the physiological conditions *in vivo*, ensured that the cells displayed all the antigens required for the isolation of unknown antibodies. The use of tissue sections, at the same time, ensured the incubation of sera with a fully developed NMJ. The herewith methods presented have been shown to have great potentiality but still need an improvement to really be able to isolate antigens or antibodies. Despite this, the presented approach allows the analysis of both antibodies and antigens increasing the chances of isolating new candidates for SNMG. Moreover, the experiments on primary cell cultures highlighted them as a useful diagnostic and study tool for a wide range of other diseases.

4.10 Final considerations

In conclusion, our work has confirmed the CBA as a reliable tool to identify seronegative MG within a cohort of patients. At the same time, TBA and immunoprecipitation might represent a key tool for the identification of antibodies SNMG patients, but both the test showed the need for further improvements to the current protocol to allow the isolation of SNMG antibodies. Besides, the studies performed on human muscle stem cell culture highlighted their potential as a possible diagnostic tool for a wide range of other diseases, not limited to MG. In summary the approach presented in this project could be employed not solely for the detection and identification of unknown antigens at the NMJ, but additionally to study the molecules involved in other muscular pathologies and develop new drug targets.

4.11 Outlook

The isolation of new antigents responsible for SNMG would represent an important improvement in the comprehension of the disease. One of the major problems raised during the project has been the absence of a functional AChR clustering and postsynaptic development. In the future, it would be helpful to introduce a co-culture or an electric stimulation to myotubes in order to achieve this goal. Other experiments have shown that also the transfection of human cells with proteins from the NMJ, such as Dok7, resulted in a clustering of the receptors. It would be worth trying to reproduce the protocol, to assess the possibility of inducing a complete development of AChR receptors also in the human model. In addition to this, the mouse model for NMJ, C2C12 cell line, have also shown to express a fully developed postsynaptic membrane and it would be helpful to perform the immunoprecipitation assay with this model as well, in order to assess the possibility of isolating antigens.
Finally, different protocols reported functional CBA with different antigens from the NMJ, such as Lrp4. Performing this kind of experiments on the sera that have resulted negative for AChR and MuSK would increase the comprehension and the knowledge of these antibodies.

5 BIBLIOGRAPHY

1 Margo CE, Harman LE. Autoimmune disease: Conceptual history and contributions of ocular immunology. Surv Ophthalmol. 2016 Sep-Oct;61(5):680-8. doi: 10.1016/j.survophthal.2016.04.006. Epub 2016 Apr 27. PMID: 27131478.

2 Wang L, Wang FS, Gershwin ME. Human autoimmune diseases: a comprehensive update. J Intern Med. 2015 Oct;278(4):369-95. doi: 10.1111/joim.12395. Epub 2015 Jul 25. PMID: 26212387.

3 Rosenblum MD, Remedios KA, Abbas AK. Mechanisms of human autoimmunity. J Clin Invest. 2015;125(6):2228-2233. doi:10.1172/JCI78088

4 Smith DA, Germolec DR. Introduction to immunology and autoimmunity. Environ Health Perspect. 1999;107 Suppl 5(Suppl 5):661-665. doi:10.1289/ehp.99107s5661

5 Rose NR, Bona C. Defining criteria for autoimmune diseases (Witebsky's postulates revisited). Immunol Today. 1993 Sep;14(9):426-30. doi: 10.1016/0167-5699(93)90244-F. PMID: 8216719.

6 Descotes J, Choquet-Kastylevsky G. Gell and Coombs's classification: is it still valid? Toxicology. 2001 Feb 2;158(1-2):43-9. doi: 10.1016/s0300-483x(00)00400-5. PMID: 11164991.

7 Gell P.G.H. , Coombs R.R.A. The classification of allergic reactions underlying disease.in: Coombs R.R.A. Gell P.G.H. Clinical Aspects of Immunology. Blackwell Science

8 Bukantz SC. Clemens von Pirquet and the concept of allergie. J Allergy Clin Immunol. 2002 Apr;109(4):724-6. PMID: 11980437.

9 Drachman DB. How to recognize an antibody-mediated autoimmune disease: criteria. Res Publ Assoc Res Nerv Ment Dis. 1990;68:183-6. PMID: 2183310.

10 Ludwig RJ, Vanhoorelbeke K, Leypoldt F, et al. Mechanisms of Autoantibody-Induced Pathology. Front Immunol. 2017;8:603. Published 2017 May 31. doi:10.3389/fimmu.2017.00603

11 Tozzoli R. Receptor autoimmunity: diagnostic and therapeutic implications. Auto Immun Highlights. 2020;11(1):1. Published 2020 Jan 7. doi:10.1186/s13317-019-0125-5

12 Vincent A. ANTIBODIES AND RECEPTORS: From Neuromuscular Junction to Central Nervous System. Neuroscience. 2020 Jul 15;439:48-61. doi: 10.1016/j.neuroscience.2020.03.009. Epub 2020 Mar 17. PMID: 32194225.

13 Rizo J, Rosenmund C. Synaptic vesicle fusion. Nat Struct Mol Biol. 2008;15(7):665-674. doi:10.1038/nsmb.1450

14 Omar A, Marwaha K, Bollu PC. Physiology, Neuromuscular Junction. [Updated 2020 May 24]. In: StatPearls [Internet]. Treasure Island (FL): StatPearls Publishing; 2020 Jan-. Available from: https://www.ncbi.nlm.nih.gov/books/NBK470413/

15 Slater CR. The Structure of Human Neuromuscular Junctions: Some Unanswered Molecular Questions. Int J Mol Sci. 2017;18(10):2183. Published 2017 Oct 19. doi:10.3390/ijms18102183

16 Ivicic T. Myasthenia gravis-a review. Gyrus Vol III No 3, 2015; DOI: http://dx.doi.org/10.17486/gyr.3.1036

17 Zhang B, Luo S, Wang Q, Suzuki T, Xiong WC, Mei L. LRP4 serves as a coreceptor of agrin. Neuron. 2008;60(2):285-297. doi:10.1016/j.neuron.2008.10.006

18 Apel ED, Roberds SL, Campbell KP, Merlie JP. Rapsyn may function as a link between the acetylcholine receptor and the agrin-binding dystrophin-associated glycoprotein complex. Neuron. 1995 Jul;15(1):115-26. doi: 10.1016/0896-6273(95)90069-1. PMID: 7619516.
19 Sanes JR, Lichtman JW. Development of the vertebrate neuromuscular junction. Annu Rev Neurosci. 1999;22:389-442. doi: 10.1146/annurev.neuro.22.1.389. PMID: 10202544.
20 Valenzuela DM, Stitt TN, DiStefano PS, Rojas E, Mattsson K, et al. 1995. Receptor tyrosine kinase specific for the skeletal muscle lineage: expression in embryonic muscle, at the neuromuscular junction, and after injury. Neuron 15:573–84
21 Martin PT, Sanes JR. 1997. Integrins mediate adhesion to agrin and modulate agrin signaling. Development 124:3909–17
22 Mukund K, Subramaniam S. Skeletal muscle: A review of molecular structure and function, in health and disease. Wiley Interdiscip Rev Syst Biol Med. 2020 Jan;12(1):e1462. doi: 10.1002/wsbm.1462. Epub 2019 Aug 13. PMID: 31407867; PMCID: PMC6916202.
23 Witzemann, V. Development of the neuromuscular junction. Cell Tissue Res 326, 263–271 (2006). https://doi.org/10.1007/s00441-006-0237-x
24 Buckingham M, Bajard L, Chang T, Daubas P, Hadchouel J, Meilhac S, Montarras D, Rocancourt D, Relaix F. The formation of skeletal muscle: from somite to limb. J Anat. 2003 Jan;202(1):59-68. doi: 10.1046/j.1469-7580.2003.00139.x. PMID: 12587921; PMCID: PMC1571050.
25 Campagna JA, Rüegg MA, Bixby JL. Agrin is a differentiation-inducing "stop signal" for motoneurons in vitro. Neuron. 1995 Dec;15(6):1365-74. doi: 10.1016/0896-6273(95)90014-4. PMID: 8845159.
26 Kelly AM, Zacks SI. The fine structure of motor endplate morphogenesis. J Cell Biol. 1969;42(1):154-169. doi:10.1083/jcb.42.1.154
27 McNally EM. The Sarcoglycans. In: Madame Curie Bioscience Database [Internet]. Austin (TX): Landes Bioscience; 2000-2013. Available from: https://www.ncbi.nlm.nih.gov/books/NBK6317
28 Covault J, Sanes JR. 1985. Neural cell adhesion molecule (N-CAM) accumulates in denervated and paralyzed skeletal muscles. Proc. Natl. Acad. Sci. USA 82:4544–48
29 Sealock R, Wray BE, Froehner SC. 1984. Ultrastructural localization of the Mr 43,000 protein and the acetylcholine receptor in Torpedo postsynaptic membranes using monoclonal antibodies. J. Cell Biol. 98:2239–44
30 Hack AA, Groh ME, McNally EM. Sarcoglycans in muscular dystrophy. Microsc Res Tech. 2000 Feb 1-15;48(3-4):167-80. doi: 10.1002/(SICI)1097-0029(20000201/15)48:3/4<167::AID-JEMT5>3.0.CO;2-T. PMID: 10679964.
31 Matsumura K, Saito F, Yamada H, Hase A, Sunada Y, Shimizu T. Sarcoglycan complex: a muscular supporter of dystroglycan-dystrophin interplay? Cell Mol Biol (Noisy-le-grand). 1999 Sep;45(6):751-62. PMID: 10541473.
32 Hoffman, E. P., Brown, R. H., Jr., & Kunkel, L. M. (1987). Dystrophin: The protein product of the Duchenne muscular dystrophy locus. Cell, 51(6), 919–928.
33 Zhao K, Shen C, Li L, Wu H, Xing G, Dong Z, Jing H, Chen W, Zhang H, Tan Z, Pan J, Xiong L, Wang H, Cui W, Sun XD, Li S, Huang X, Xiong WC, Mei L. Sarcoglycan Alpha Mitigates Neuromuscular Junction Decline in Aged Mice by Stabilizing LRP4. J Neurosci. 2018 Oct 10;38(41):8860-8873. doi: 10.1523/JNEUROSCI.0860-18.2018. Epub 2018 Aug 31. PMID: 30171091; PMCID: PMC6181315.

34 Liu J, Aoki M, Illa I, Wu C, Fardeau M, Angelini C, Serrano C, Urtizberea JA, Hentati F, Hamida MB, Bohlega S, Culper EJ, Amato AA, Bossie K, Oeltjen J, Bejaoui K, McKenna-Yasek D, Hosler BA, Schurr E, Arahata K, de Jong PJ, Brown RH Jr. Dysferlin, a novel skeletal muscle gene, is mutated in Miyoshi myopathy and limb girdle muscular dystrophy. Nat Genet. 1998 Sep;20(1):31-6. doi: 10.1038/1682. PMID: 9731526.
35 Bansal D, Miyake K, Vogel SS, Groh S, Chen CC, Williamson R, McNeil PL, Campbell KP. Defective membrane repair in dysferlin-deficient muscular dystrophy. Nature. 2003 May 8;423(6936):168-72. doi: 10.1038/nature01573. PMID: 12736685.
36 Goebel HH, Bornemann A. Desmin pathology in neuromuscular diseases. Virchows Arch B Cell Pathol Incl Mol Pathol. 1993;64(3):127-35. doi: 10.1007/BF02915105. PMID: 8242173.
37 Yue B. Biology of the extracellular matrix: an overview. J Glaucoma. 2014;23(8 Suppl 1):S20-S23. doi:10.1097/IJG.0000000000000108
38 Rahimov F, Kunkel LM. The cell biology of disease: cellular and molecular mechanisms underlying muscular dystrophy. J Cell Biol. 2013 May 13;201(4):499-510. doi: 10.1083/jcb.201212142. PMID: 23671309; PMCID: PMC3653356.
39 Burden SJ, Yumoto N, Zhang W. The role of MuSK in synapse formation and neuromuscular disease. Cold Spring Harb Perspect Biol. 2013 May 1;5(5):a009167. doi: 10.1101/cshperspect.a009167. PMID: 23637281; PMCID: PMC3632064.
40 Hubbard SR, Gnanasambandan K. Structure and activation of MuSK, a receptor tyrosine kinase central to neuromuscular junction formation. Biochim Biophys Acta. 2013 Oct;1834(10):2166-9. doi: 10.1016/j.bbapap.2013.02.034. Epub 2013 Mar 5. PMID: 23467009; PMCID: PMC3923368.
41 Burden SJ, Huijbers MG, Remedio L. Fundamental Molecules and Mechanisms for Forming and Maintaining Neuromuscular Synapses. Int J Mol Sci. 2018 Feb 6;19(2):490. doi: 10.3390/ijms19020490. PMID: 29415504; PMCID: PMC5855712
42 Rodríguez Cruz, P. M., Cossins, J., Cheung, J., Maxwell, S., Jayawant, S., Herbst, R., Waithe, D., Kornev, A. P., Palace, J., & Beeson, D. (2020). Congenital myasthenic syndrome due to mutations in MUSK suggests that the level of MuSK phosphorylation is crucial for governing synaptic structure. Human mutation, 41(3), 619–631. https://doi.org/10.1002/humu.23949
43 Buyan A, Kalli AC, Sansom MS. Multiscale Simulations Suggest a Mechanism for the Association of the Dok7 PH Domain with PIP-Containing Membranes. PLoS Comput Biol. 2016;12(7):e1005028. Published 2016 Jul 26. doi:10.1371/journal.pcbi.1005028
44 Li L, Cao Y, Wu H, et al. Enzymatic Activity of the Scaffold Protein Rapsyn for Synapse Formation. Neuron. 2016;92(5):1007-1019. doi:10.1016/j.neuron.2016.10.023
45 Huebsch KA, Maimone MM. Rapsyn-mediated clustering of acetylcholine receptor subunits requires the major cytoplasmic loop of the receptor subunits. J Neurobiol. 2003 Feb 15;54(3):486-501. doi: 10.1002/neu.10177. PMID: 12532399.
46 Zhang H, Sathyamurthy A, Liu F, et al. Agrin-Lrp4-Ror2 signaling regulates adult hippocampal neurogenesis in mice. Elife. 2019;8:e45303. Published 2019 Jul 3. doi:10.7554/eLife.45303
47 Vilmont V, Cadot B, Ouanounou G, Gomes ER. A system for studying mechanisms of neuromuscular junction development and maintenance. Development. 2016;143(13):2464-2477. doi:10.1242/dev.130278

48 Tang, J., He, A., Yan, H. et al. Damage to the myogenic differentiation of C2C12 cells by heat stress is associated with up-regulation of several selenoproteins. Sci Rep 8, 10601 (2018). https://doi.org/10.1038/s41598-018-29012-6
49 Yap A, Nishiumi S, Yoshida K, Ashida H. Rat L6 myotubes as an in vitro model system to study GLUT4-dependent glucose uptake stimulated by inositol derivatives. Cytotechnology. 2007;55(2-3):103-108. doi:10.1007/s10616-007-9107-y
50 Weston C, Yee B, Hod E, Prives J. Agrin-induced acetylcholine receptor clustering is mediated by the small guanosine triphosphatases Rac and Cdc42. J Cell Biol. 2000;150(1):205-212. doi:10.1083/jcb.150.1.205
51 Liu L, Zhang C, Wang W, Xi N, Wang Y. Regulation of C2C12 Differentiation and Control of the Beating Dynamics of Contractile Cells for a Muscle-Driven Biosyncretic Crawler by Electrical Stimulation. Soft Robot. 2018 Dec;5(6):748-760. doi: 10.1089/soro.2018.0017. Epub 2018 Oct 18. PMID: 30277855.
52 Lautaoja JH, Pekkala S, Pasternack A, Laitinen M, Ritvos O, Hulmi JJ. Differentiation of Murine C2C12 Myoblasts Strongly Reduces the Effects of Myostatin on Intracellular Signaling. Biomolecules. 2020;10(5):695. Published 2020 Apr 30. doi:10.3390/biom10050695
53 Lawson MA, Purslow PP. Differentiation of myoblasts in serum-free media: effects of modified media are cell line-specific. Cells Tissues Organs. 2000;167(2-3):130-7. doi: 10.1159/000016776. PMID: 10971037.
54 Afshar Bakooshli M, Lippmann ES, Mulcahy B, et al. A 3D culture model of innervated human skeletal muscle enables studies of the adult neuromuscular junction. Elife. 2019;8:e44530. Published 2019 May 14. doi:10.7554/eLife.44530
55 Ostrovidov S, Ahadian S, Ramon-Azcon J, Hosseini V, Fujie T, Parthiban SP, Shiku H, Matsue T, Kaji H, Ramalingam M, Bae H, Khademhosseini A. Three-dimensional co-culture of C2C12/PC12 cells improves skeletal muscle tissue formation and function. J Tissue Eng Regen Med. 2017 Feb;11(2):582-595. doi: 10.1002/term.1956. Epub 2014 Nov 13. PMID: 25393357.
56 Perry RL, Rudnick MA. Molecular mechanisms regulating myogenic determination and differentiation. Front Biosci. 2000 Sep 1;5:D750-67. doi: 10.2741/perry. PMID: 10966875.
57 Asfour HA, Allouh MZ, Said RS. Myogenic regulatory factors: The orchestrators of myogenesis after 30 years of discovery. Exp Biol Med (Maywood). 2018 Jan;243(2):118-128. doi: 10.1177/1535370217749494. Epub 2018 Jan 7. PMID: 29307280; PMCID: PMC5788151.
58 Musarò A, Carosio S. Isolation and Culture of Satellite Cells from Mouse Skeletal Muscle. Methods Mol Biol. 2017;1553:155-167. doi: 10.1007/978-1-4939-6756-8_12. PMID: 28229414.
59 Stern-Straeter J, Bonaterra GA, Kassner SS, Zügel S, Hörmann K, Kinscherf R, Goessler UR. Characterization of human myoblast differentiation for tissue-engineering purposes by quantitative gene expression analysis. J Tissue Eng Regen Med. 2011 Aug;5(8):e197-206. doi: 10.1002/term.417. Epub 2011 Mar 3. PMID: 21370490.
60 Morgan JE, Partridge TA. Muscle satellite cells. Int J Biochem Cell Biol. 2003 Aug;35(8):1151-6. doi: 10.1016/s1357-2725(03)00042-6. PMID: 12757751.
61 Ishibashi J, Perry RL, Asakura A, Rudnicki MA. MyoD induces myogenic differentiation through cooperation of its NH2- and COOH-terminal regions. J Cell Biol. 2005;171(3):471-482. doi:10.1083/jcb.200502101

62 Schmidt, M., Schüler, S.C., Hüttner, S.S. et al. Adult stem cells at work: regenerating skeletal muscle. Cell. Mol. Life Sci. 76, 2559–2570 (2019). https://doi.org/10.1007/s00018-019-03093-6
63 Fu X, Wang H, Hu P. Stem cell activation in skeletal muscle regeneration. Cell Mol Life Sci. 2015;72(9):1663-1677. doi:10.1007/s00018-014-1819-5
64 Koishi K, Zhang M, McLennan IS, Harris AJ. MyoD protein accumulates in satellite cells and is neurally regulated in regenerating myotubes and skeletal muscle fibers. Dev Dyn. 1995 Mar;202(3):244-54. doi: 10.1002/aja.1002020304. PMID: 7780174.
65 Ma Y, Peng J, Liu W, et al. Proteomics identification of desmin as a potential oncofetal diagnostic and prognostic biomarker in colorectal cancer. Mol Cell Proteomics. 2009;8(8):1878-1890. doi:10.1074/mcp.M800541-MCP200
66 Yablonka-Reuveni, Z, and M Nameroff. "Temporal differences in desmin expression between myoblasts from embryonic and adult chicken skeletal muscle." Differentiation; research in biological diversity vol. 45,1 (1990): 21-8. doi:10.1111/j.1432-0436.1990.tb00452.x
67 Adams GR, Haddad F, Baldwin KM. Time course of changes in markers of myogenesis in overloaded rat skeletal muscles. J Appl Physiol (1985). 1999 Nov;87(5):1705-12. doi: 10.1152/jappl.1999.87.5.1705. PMID: 10562612.
68 Boldrin L, Muntoni F, Morgan JE. Are human and mouse satellite cells really the same? J Histochem Cytochem. 2010 Nov;58(11):941-55. doi: 10.1369/jhc.2010.956201. Epub 2010 Jul 19. PMID: 20644208; PMCID: PMC2958137.
69 Linda L. Kusner, Henry J. Kaminski, Chapter 10 - Myasthenia Gravis, Editor(s): Michael J. Zigmond, Lewis P. Rowland, Joseph T. Coyle, Neurobiology of Brain Disorders, Academic Press, 2015.Pages 135-150,
70 Jayam Trouth A, Dabi A, Solieman N, Kurukumbi M, Kalyanam J. Myasthenia gravis: a review. Autoimmune Dis. 2012;2012:874680. doi:10.1155/2012/874680
71 Pekmezović T, Lavrnić D, Jarebinski M, Apostolski S. [Epidemiology of myasthenia gravis]. Srp Arh Celok Lek. 2006 Sep-Oct;134(9-10):453-6. Serbian. PMID: 17252917.
72 Meriggioli MN, Sanders DB. Muscle autoantibodies in myasthenia gravis: beyond diagnosis?. Expert Rev Clin Immunol. 2012;8(5):427-438. doi:10.1586/eci.12.34
73 Gilhus NE, Verschuuren JJ. Myasthenia gravis: subgroup classification and therapeutic strategies. Lancet Neurol. 2015 Oct;14(10):1023-36. doi: 10.1016/S1474-4422(15)00145-3. PMID: 26376969.
74 Harrison's Neurology in Clinical Medicine, 3rd Edition CHAPTER 47. MYASTHENIA GRAVIS AND OTHER DISEASES OF THE NEUROMUSCULAR JUNCTION, Daniel B. Drachman
75 Meriggioli MN. Myasthenia gravis with anti-acetylcholine receptor antibodies. Front Neurol Neurosci. 2009;26:94-108. doi: 10.1159/000212371. Epub 2009 Apr 6. PMID: 19349707.
76 Wang W, Chen YP, Wei DN. [The clinical characteristics of early-onset versus late-onset types of myasthenia gravis]. Zhonghua Nei Ke Za Zhi. 2011 Jun;50(6):496-8. Chinese. doi: 10.3760/cma.j.issn.0578-1426.2011.06.013. PMID: 21781535.
77 Aarli JA. Late-Onset Myasthenia Gravis: A Changing Scene. Arch Neurol. 1999;56(1):25–27. doi:10.1001/archneur.56.1.25
78 Mygland Å, Vincent A, Newsom-Davis J, et al. Autoantibodies in Thymoma-Associated Myasthenia Gravis With Myositis or Neuromyotonia. Arch Neurol. 2000;57(4):527–531. doi:10.1001/archneur.57.4.527

79 Rodolico C, Bonanno C, Toscano A, Vita G. MuSK-Associated Myasthenia Gravis: Clinical Features and Management. Front Neurol. 2020;11:660. Published 2020 Jul 23. doi:10.3389/fneur.2020.00660
80 Oh SJ. Muscle-specific receptor tyrosine kinase antibody positive myasthenia gravis current status. J Clin Neurol. 2009;5(2):53-64. doi:10.3988/jcn.2009.5.2.53
81 Myasthenia gravis with antibodies to MuSK: an update. Evoli A, Alboini PE, Damato V, Iorio R, Provenzano C, Bartoccioni E, Marino M, Ann N Y Acad Sci. 2018 Jan; 1412(1):82-89.
82 Koneczny I, Herbst R. Myasthenia Gravis: Pathogenic Effects of Autoantibodies on Neuromuscular Architecture. Cells. 2019;8(7):671. Published 2019 Jul 2. doi:10.3390/cells8070671
83 Gilhus, N. E. et al. Myasthenia gravis - Autoantibody characteristics and their implications for therapy. Nat. Rev. Neurol. 12, 259–268 (2016).
84 Vidarsson G, Dekkers G, Rispens T. IgG subclasses and allotypes: from structure to effector functions. Front Immunol. 2014;5:520. Published 2014 Oct 20. doi:10.3389/fimmu.2014.00520
85 Angela Vincent, John Bowen, John Newsom-Davis, John McConville, Seronegative generalised myasthenia gravis: clinical features, antibodies, and their targets, The Lancet Neurology,Volume 2, Issue 2,2003,Pages 99-106,
86 Vincent A, Newsom Davis J. Anti-acetylcholine receptor antibodies. J Neurol Neurosurg Psychiatry. 1980;43(7):590-600. doi:10.1136/jnnp.43.7.590
87 Bindu PS, Nirmala M, Patil SA, Taly AB. Myasthenia gravis and acetylcholine receptor antibodies: a clinico immunological correlative study on South Indian patients. Ann Indian Acad Neurol. 2008;11(4):242-244. doi:10.4103/0972-2327.44560
88 Bergamin, E., Hallock, P. T., Burden, S. J. & Hubbard, S. R. The Cytoplasmic Adaptor Protein Dok7 Activates the Receptor Tyrosine Kinase MuSK via Dimerization. Mol. Cell 39, 100–109 (2010).
89 Rivner, MH, Quarles, BM, Pan, J-X, et al. Clinical features of LRP4/agrin-antibody–positive myasthenia gravis: A multicenter study. Muscle & Nerve. 2020; 62: 333– 343. https://doi.org/10.1002/mus.26985
90 Conti-Fine BM, Milani M, Kaminski HJ. Myasthenia gravis: past, present, and future. J Clin Invest. 2006;116(11):2843-2854. doi:10.1172/JCI29894
91 Hong, Y., Liang, X. & Gilhus, N.E. AChR antibodies show a complex interaction with human skeletal muscle cells in a transcriptomic study. Sci Rep 10, 11230 (2020). https://doi.org/10.1038/s41598-020-68185-x
92 Kaminski HJ. Seronegative Myasthenia Gravis-A Vanishing Disorder? JAMA Neurol. 2016 Sep 1;73(9):1055-6. doi: 10.1001/jamaneurol.2016.2277. PMID: 27380019.
93 Rodriguez Cruz PM, Al-Hajjar M, Huda S, et al. Clinical Features and Diagnostic Usefulness of Antibodies to Clustered Acetylcholine Receptors in the Diagnosis of Seronegative Myasthenia Gravis. JAMA neurology. 2015;72(6):642-649.
94 Hong Y, Zisimopoulou P, Trakas N, Karagiorgou K, Stergiou C, Skeie GO, Hao HJ, Gao X, Owe JF, Zhang X, Yue YX, Romi F, Wang Q, Li HF, Gilhus NE, Tzartos SJ. Multiple antibody detection in 'seronegative' myasthenia gravis patients. Eur J Neurol. 2017 Jun;24(6):844-850. doi: 10.1111/ene.13300. Epub 2017 May 4. PMID: 28470860.

95 Cortés-Vicente E, Gallardo E, Martínez MÁ, et al. Clinical Characteristics of Patients With Double-Seronegative Myasthenia Gravis and Antibodies to Cortactin. JAMA Neurol. 2016;73(9):1099–1104. doi:10.1001/jamaneurol.2016.2032
96 Dang T, Macwan S, Dasanu CA. Late-onset double-seronegative myasthenia gravis syndrome and myasthenic crisis due to nivolumab use for Hodgkin's lymphoma. J Oncol Pharm Pract. 2020 Dec 8:1078155220976797. doi: 10.1177/1078155220976797. Epub ahead of print. PMID: 33292071.
97 Ohta M, Ohta K, Itoh N, Kurobe M, Hayashi K, Nishitani H. Anti-skeletal muscle antibodies in the sera from myasthenic patients with thymoma: identification of anti-myosin, actomyosin, actin, and alpha-actinin antibodies by a solid-phase radioimmunoassay and a western blotting analysis. Clin Chim Acta. 1990;187(3):255–264.
98 Otsuka, K., Ito, M., Ohkawara, B. et al. Collagen Q and anti-MuSK autoantibody competitively suppress agrin/LRP4/MuSK signaling. Sci Rep 5, 13928 (2015). https://doi.org/10.1038/srep13928
99 Zoltowska Katarzyna M, Belaya K, Leite M, Patrick W, Vincent A, Beeson D. Collagen Q--a potential target for autoantibodies in myasthenia gravis. J Neurol Sci. 2015;348(1-2):241-244. doi:10.1016/j.jns.2014.12.015
100. Cikes N, Momoi MY, Williams CL, et al: Striational autoantibodies: quantitative detection by enzyme immunoassay in myasthenia gravis, thymoma, and recipients of D-penicillamine or allogeneic bone marrow. Mayo Clin Proc 1988 May;63(5):474-481
101 Vernino S, Lennon VA: Muscle and neuronal autoantibody markers of thymoma: neurological correlations. Ann NY Acad Sci 2003 Sep;998:359-361
102 Romi F, Skeie GO, Gilhus NE, Aarli JA. Striational Antibodies in Myasthenia Gravis: Reactivity and Possible Clinical Significance. Arch Neurol. 2005;62(3):442–446. doi:10.1001/archneur.62.3.442
103 Lazaridis K, Tzartos SJ. Autoantibody Specificities in Myasthenia Gravis; Implications for Improved Diagnostics and Therapeutics. Front Immunol. 2020;11:212. Published 2020 Feb 14. doi:10.3389/fimmu.2020.00212
104 Zisimopoulou P, Brenner T, Trakas N, Tzartos SJ. Serological diagnostics in myasthenia gravis based on novel assays and recently identified antigens. Autoimmun Rev. 2013 Jul;12(9):924-30. doi: 10.1016/j.autrev.2013.03.002. Epub 2013 Mar 26. PMID: 23537507.
105 Trakas N, Tzartos SJ. Immunostick ELISA for rapid and easy diagnosis of myasthenia gravis. J Immunol Methods. 2018 Sep;460:107-112. doi: 10.1016/j.jim.2018.06.016. Epub 2018 Jul 2. PMID: 30056940.
106 Lazaridis K, Tzartos SJ. Autoantibody Specificities in Myasthenia Gravis; Implications for Improved Diagnostics and Therapeutics. Front Immunol. 2020;11:212. Published 2020 Feb 14. doi:10.3389/fimmu.2020.00212
107 Rodríguez Cruz PM, Al-Hajjar M, Huda S, Jacobson L, Woodhall M, Jayawant S, Buckley C, Hilton-Jones D, Beeson D, Vincent A, Leite MI, Palace J. Clinical Features and Diagnostic Usefulness of Antibodies to Clustered Acetylcholine Receptors in the Diagnosis of Seronegative Myasthenia Gravis. JAMA Neurol. 2015 Jun;72(6):642-9. doi: 10.1001/jamaneurol.2015.0203. PMID: 25894002; PMCID: PMC6044422.
108 Chang T, Leite MI, Senanayake S, Gunaratne PS, Gamage R, Riffsy MT, Jacobson LW, Adhikari M, Perera S, Vincent A. Clinical and serological study of myasthenia gravis using both radioimmunoprecipitation and cell-based assays in a South Asian population. J Neurol

Sci. 2014 Aug 15;343(1-2):82-7. doi: 10.1016/j.jns.2014.05.037. Epub 2014 May 27. PMID: 24929651.

109Shen C, Lu Y, Zhang B, Figueiredo D, Bean J, Jung J, Wu H, Barik A, Yin DM, Xiong WC, Mei L. Antibodies against low-density lipoprotein receptor-related protein 4 induce myasthenia gravis. J Clin Invest. 2013 Dec;123(12):5190-202. doi: 10.1172/JCI66039. Epub 2013 Nov 8. PMID: 24200689; PMCID: PMC3859418.

110Gilhus NE, Aarli JA, Matre R. Myasthenia gravis. Antibodies to skeletal muscle cell surface antigens. J Neuroimmunol. 1983 Dec;5(3):239-49. doi: 10.1016/0165-5728(83)90044-9. PMID: 6361067.

111Park KH, Waters P, Woodhall M, Lang B, Smith T, et al. (2018) Correction: Myasthenia gravis seronegative for acetylcholine receptor antibodies in South Korea: Autoantibody profiles and clinical features. PLOS ONE 13(6): e0200225.https://doi.org/10.1371/journal.pone.0200225

112Bien CI, Nehls F, Kollmar R, Weis M, Steinke W, Woermann F, Dalmau J, Bien CG. Identification of adenylate kinase 5 antibodies during routine diagnostics in a tissue-based assay: Three new cases and a review of the literature. J Neuroimmunol. 2019 Sep 15;334:576975. doi: 10.1016/j.jneuroim.2019.576975. Epub 2019 May 29. PMID: 31177032.

113Hindi L, McMillan JD, Afroze D, Hindi SM, Kumar A. Isolation, Culturing, and Differentiation of Primary Myoblasts from Skeletal Muscle of Adult Mice. Bio Protoc. 2017 May 5;7(9):e2248. doi: 10.21769/BioProtoc.2248. PMID: 28730161; PMCID: PMC5515488.

114Hong, Y., Liang, X. & Gilhus, N.E. AChR antibodies show a complex interaction with human skeletal muscle cells in a transcriptomic study. Sci Rep 10, 11230 (2020). https://doi.org/10.1038/s41598-020-68185-x

115Rao N, Evans S, Stewart D, et al. Fibroblasts influence muscle progenitor differentiation and alignment in contact independent and dependent manners in organized co-culture devices. Biomed Microdevices. 2013;15(1):161-169. doi:10.1007/s10544-012-9709-9

116Alberts B, Johnson A, Lewis J, et al. Molecular Biology of the Cell. 4th edition. New York: Garland Science; 2002. Fibroblasts and Their Transformations: The Connective-Tissue Cell Family. Available from: https://www.ncbi.nlm.nih.gov/books/NBK26889/

117 Yablonka-Reuveni Z, Nameroff M. Temporal differences in desmin expression between myoblasts from embryonic and adult chicken skeletal muscle. Differentiation. 1990;45(1):21-28. doi:10.1111/j.1432-0436.1990.tb00452.x

118Gard DL, Lazarides E. The synthesis and distribution of desmin and vimentin during myogenesis in vitro. Cell. 1980 Jan;19(1):263-75. doi: 10.1016/0092-8674(80)90408-0. PMID: 7188890.

119Koishi K, Zhang M, McLennan IS, Harris AJ. MyoD protein accumulates in satellite cells and is neurally regulated in regenerating myotubes and skeletal muscle fibers. Dev Dyn. 1995 Mar;202(3):244-54. doi: 10.1002/aja.1002020304. PMID: 7780174.

120 Lingbeck JM, Trausch-Azar JS, Ciechanover A, Schwartz AL. Determinants of nuclear and cytoplasmic ubiquitin-mediated degradation of MyoD. J Biol Chem. 2003 Jan 17;278(3):1817-23. doi: 10.1074/jbc.M208815200. Epub 2002 Oct 22. PMID: 12397066.

121 Mazhar S, Herbst R. The formation of complex acetylcholine receptor clusters requires MuSK kinase activity and structural information from the MuSK extracellular domain. Mol Cell Neurosci. 2012;49(4):475-486. doi:10.1016/j.mcn.2011.12.007

122Sugiyama JE, Glass DJ, Yancopoulos GD, Hall ZW. Laminin-induced acetylcholine receptor clustering: an alternative pathway. J Cell Biol. 1997;139(1):181-191. doi:10.1083/jcb.139.1.181

123 Pęziński, M., Daszczuk, P., Pradhan, B.S. et al. An improved method for culturing motubes on laminins for the robust clustering of postsynaptic machinery. Sci Rep 10, 4524 (2020). https://doi.org/10.1038/s41598-020-61347-x

124Godfrey, E. W., Nitkin, R. M., Wallace, B. G., Rubin, L. L. & McMahan, U. J. Components of Torpedo electric organ and muscle that cause aggregation of acetylcholine receptors on cultured muscle cells. J. Cell Biol. 99, 615–627 (1984).

125 Schmidt, N., Basu, S., Kroger, S. & Brenner, H. R. A Cell Culture System to Investigate the Presynaptic Control of Subsynaptic Membrane Differentiation at the Neuromuscular Juction. Methods Mol. Biol.1538, 3–11 (2017).

126Frank E. Fischbach G.D. Early events in neuromuscular junction formation in vitro: induction of acetylcholine receptor clusters in the postsynaptic membrane and morphology of newly formed synapses. J. Cell Biol. 1979; 83: 143-158

127 Bakooshli, M. A. et al. A 3d culture model of innervated human skeletal muscle enables studies of the adult neuromuscular junction. Elife 8, 1–29 (2019).

128Bayne EK, Anderson MJ, Fambrough DM. Extracellular matrix organization in developing muscle: correlation with acetylcholine receptor aggregates. J Cell Biol. 1984 Oct;99(4 Pt 1):1486-501. doi: 10.1083/jcb.99.4.1486. PMID: 6480700; PMCID: PMC2113317.

129Land BR, Podleski TR, Salpeter EE, Salpeter MM. Acetylcholine receptor distribution on myotubes in culture correlated to acetylcholine sensitivity. J Physiol. 1977;269(1):155-176. doi:10.1113/jphysiol.1977.sp011897

130 Ortiér GL, Benders AG, Oosterhof A, Veerkamp JH, van Kuppevelt TH. Differentiation markers of mouse C2C12 and rat L6 myogenic cell lines and the effect of the differentiation medium. In Vitro Cell Dev Biol Anim. 1999 Apr;35(4):219-27. doi: 10.1007/s11626-999-0030-8. PMID: 10478802.

131 Scuderi, F., Marino, M., Colonna, L. et al. Anti-P110 Autoantibodies Identify a Subtype of “Seronegative” Myasthenia Gravis with Prominent Oculobulbar Involvement. Lab Invest 82, 1139–1146 (2002). https://doi.org/10.1097/01.LAB.0000028144.48023.9B

132 Mata-Gómez MA, Yasui MT, Guerrero-Rangel A, Valdés-Rodríguez S, Winkler R. Accelerated identification of proteins by mass spectrometry by employing covalent pre-gel staining with Uniblue A. PLoS One. 2012;7(2):e31438. doi:10.1371/journal.pone.0031438

133Stochaj WR, Berkelman T, Laird N. Mass spectrometry-compatible silver staining. CSH Protoc. 2007 May 1;2007:pdb.prot4742. doi: 10.1101/pdb.prot4742. PMID: 21357083.

134Irina Gromova, Julio E. Celis, Chapter 27 - Protein Detection in Gels by Silver Staining: A Procedure Compatible with Mass Spectrometry,Editor(s): Julio E. Celis, Cell Biology (Third Edition),Academic Press,2006,Pages 219-223,ISBN 9780121647308, https://doi.org/10.1016/B978-012164730-8/50212-4.

135 Duggan DJ, Gorospe JR, Fanin M, Hoffman EP, Angelini C. Mutations in the sarcoglycan genes in patients with myopathy. N Engl J Med. 1997 Feb 27;336(9):618-24. doi: 10.1056/NEJM199702273360904. PMID: 9032047.

136 Gallardo E, de Luna N, Diaz-Manera J, et al. Comparison of dysferlin expression in human skeletal muscle with that in monocytes for the diagnosis of dysferlin myopathy. PLoS One. 2011;6(12):e29061. doi:10.1371/journal.pone.0029061

137Gaig C, Graus F, Compta Y, et al. Clinical manifestations of the anti-IgLON5 disease. Neurology. 2017;88(18):1736-1743. doi:10.1212/WNL.0000000000003887

138Noemí de Luna, PHD, Eduard Gallardo, PHD, Isabel Illa, MD, PHD, In Vivo and In Vitro Dysferlin Expression in Human Muscle Satellite Cells, Journal of Neuropathology & Experimental Neurology, Volume 63, Issue 10, October 2004, Pages 1104–1113, https://doi.org/10.1093/jnen/63.10.1104

139Davis DB, Doherty KR, Delmonte AJ, McNally EM. Calcium-sensitive phospholipid binding properties of normal and mutant ferlin C2 domains. J Biol Chem. 2002 Jun 21;277(25):22883-8. doi: 10.1074/jbc.M201858200. Epub 2002 Apr 16. PMID: 11959863.

140Anastasi G, Cutroneo G, Sidoti A, Santoro G, D'Angelo R, Rizzo G, Rinaldi C, Giacobbe O, Bramanti P, Navarra G, Amato A, Favaloro A. Sarcoglycan subcomplex in normal human smooth muscle: an immunohistochemical and molecular study. Int J Mol Med. 2005 Sep;16(3):367-74. PMID: 16077941.

141Noguchi S, Wakabayashi E, Imamura M, Yoshida M, Ozawa E. Formation of sarcoglycan complex with differentiation in cultured myocytes. Eur J Biochem. 2000 Feb;267(3):640-8. doi: 10.1046/j.1432-1327.2000.00998.x. PMID: 10651799

142M. Vainzof, M. R. Passos-Bueno, M. Canovas, E. S. Moreira, R. C. M. Pavanello, S. K. Marie, L. V. B. Anderson, C. G. Bonnemann, E. M. McNally, V. Nigro, L. M. Kunkel, M. Zatz, The Sarcoglycan Complex in the Six Autosomal Recessive Limb-Girdle Muscular Dystrophies, Human Molecular Genetics, Volume 5, Issue 12, December 1996, Pages 1963–1969, https://doi.org/10.1093/hmg/5.12.1963

143Honorat JA, Komorowski L, Josephs KA, Fechner K, St Louis EK, Hinson SR, Lederer S, Kumar N, Gadoth A, Lennon VA, Pittock SJ, McKeon A. IgLON5 antibody: Neurological accompaniments and outcomes in 20 patients. Neurol Neuroimmunol Neuroinflamm. 2017 Jul 18;4(5):e385. doi: 10.1212/NXI.0000000000000385. PMID: 28761904; PMCID: PMC5515599.

144 Smith, Ashley M., Katie Maguire-Nguyen, T. Rando, M. Zasloff, K. Strange and V. Yin. “The protein tyrosine phosphatase 1B inhibitor MSI-1436 stimulates regeneration of heart and multiple other tissues.” NPJ Regenerative Medicine 2 (2017): n. pag.

145Da Violante G, Zerrouk N, Richard I, Provot G, Chaumeil JC, Arnaud P. Evaluation of the cytotoxicity effect of dimethyl sulfoxide (DMSO) on Caco2/TC7 colon tumor cell cultures. Biol Pharm Bull. 2002 Dec;25(12):1600-3. doi: 10.1248/bpb.25.1600. PMID: 12499647.

146Verheijen, M., Lienhard, M., Schrooders, Y. et al. DMSO induces drastic changes in human cellular processes and epigenetic landscape in vitro. Sci Rep 9, 4641 (2019). https://doi.org/10.1038/s41598-019-40660-0

147 de Abreu Costa L, Henrique Fernandes Ottoni M, Dos Santos MG, Meireles AB, Gomes de Almeida V, de Fátima Pereira W, Alves de Avelar-Freitas B, Eustáquio Alvim Brito-Melo G. Dimethyl Sulfoxide (DMSO) Decreases Cell Proliferation and TNF-α, IFN-γ, and IL-2 Cytokines Production in Cultures of Peripheral Blood Lymphocytes. Molecules. 2017 Nov 10;22(11):1789. doi: 10.3390/molecules22111789. PMID: 29125561; PMCID: PMC6150313.

148Ben Trivedi A, Kitabatake N, Doi E. Toxicity of dimethyl sulfoxide as a solvent in bioassay system with HeLa cells evaluated colorimetrically with 3-(4,5-dimethylthiazol-2-yl)-2,5-diphenyl-tetrazolium bromide. Agric Biol Chem. 1990 Nov;54(11):2961-6. PMID: 1368650.

149Perni M, Flagmeier P, Limbocker R, Cascella R, Aprile FA, Galvagnion C, Heller GT, Meisl G, Chen SW, Kumita JR, Challa PK, Kirkegaard JB, Cohen SIA, Mannini B, Barbut D, Nollen EAA, Cecchi C, Cremades N, Knowles TPJ, Chiti F, Zasloff M, Vendruscolo M, Dobson CM. Multistep Inhibition of α-Synuclein Aggregation and Toxicity in Vitro and in Vivo by Trodusquemine. ACS Chem Biol. 2018 Aug 17;13(8):2308-2319. doi: 10.1021/acschembio.8b00466. Epub 2018 Jun 28. PMID: 29953201

150Zasloff M, Williams JI, Chen Q, Anderson M, Maeder T, Holroyd K, Jones S, Kinney W, Cheshire K, McLane M. A spermine-coupled cholesterol metabolite from the shark with potent appetite suppressant and antidiabetic properties. Int J Obes Relat Metab Disord. 2001 May;25(5):689-97. doi: 10.1038/sj.ijo.0801599. PMID: 11360152

151Lindstrom JM, Seybold ME, Lennon VA, Whittingham S, Duane DD. Antibody to acetylcholine receptor in myasthenia gravis. Prevalence, clinical correlates, and diagnostic value. Neurology. 1976 Nov;26(11):1054-9. doi: 10.1212/wnl.26.11.1054. PMID: 988512.

152Nie X, Li C, Hu S, Xue F, Kang YJ, Zhang W. An appropriate loading control for western blot analysis in animal models of myocardial ischemic infarction. Biochem Biophys Rep. 2017;12:108-113. Published 2017 Sep 12. doi:10.1016/j.bbrep.2017.09.001

LIST OF FIGURES

Figure 1: A schematic representation of the neuromuscular junction. Each branch of the motor neuron innervates more muscle fibers. At the NMJ, the end of the nerve has a button shape, in which Ach-loaded vesicles are accumulated. The nerve and the postsynaptic membrane are separated by the area referred as to the synaptic cleft. The NMJ postsynaptic membrane has several folds, containing many ion Na+ channels. On the top of the folds, AChR is densely clustered. When the nerve action potential arrives, the increase of Ca2+ causes the fusion of the vesicles with the membrane and the following release of Ach in the synaptic cleft. Ach binds to the clustered AChR on the muscle membrane, and this phenomenon triggers the opening of the ion Na+ channels. The following influx of Na+ ions allows the muscle to contract. The additional proteins in the picture are rapsyn, MuSK, and agrin[14,15]. These proteins are located in the closeness of AChR due to their role in clustering and maintenance of the postsynaptic area. MASC, myotube-associated specificity component, proposed to be a binding site for agrin[17]; RATL, rapsyn-associated transmembrane linker, proposed to be associate with the clustering machinery for AChR[18]. Extracted from [16].....9

Figure 2: Schematic overview of the principal cytoskeletal and extracellular matrix proteins. The dystrophin-associated protein complex represents is a group of heterogeneous proteins. The main sarcoplasmic proteins are α-dystrobrevin, syntrophins, and nNOS; the transmembrane ones are represented by β-dystroglycan, sarcoglycans, caveolin-3, and sarcospan and some of them have an extracellular location, such as α-dystroglycan. These proteins are involved in the link of dystrophin to the extracellular matrix. Dystrophin complex is also liked to desmin, via α-dystrobrevin-syncoilin, providing a mechanical link to the fiber. Finally, dysferlin and caveolin are implied in injury repair of the muscle. Extracted from [38]. 11

Figure 3:Schematic representation of the proteins involved in clustering of AChR. The clustering process promoted by the agrin-Lrp4-MuSK complex; AChR is linked to rapsyn, which connects the clusters to the cytoskeleton. Image extracted from [40]. 12

Figure 4: Schematic representation of the muscle fiber structure highlighting the satellite cell niche. Image from [62].....13

Figure 5: Schematic representation of the myogenic lineage progression. Satellite cells, when quiescent, are characterized from the expression of Pax7 and Myf5. Following activation, the cells express MyoD and Myf5, and proliferate. The pool of muscle precursor cells (MPC) represents the committed muscle cells. MPC start then to express MRF4 and myogenin, fusing and differentiating into myotubes. The pool of cells that do not divide, and come back to the satellite niche, downregulate MyoD and come back to the quiescent state. Figure from[68].....14

Figure 6:Human myoblast in culture, 2D classical technique and 3D technique. Nuclei in blue, AChR in green and membrane in red; a) human primary myotubes culture without external innervation; b) co-culture with nerve cells, fully developed postsynaptic membrane. Extracted from [54]. Arrows indicates broken muscle fibers in the 2D culture, indicating that the muscle without proper postsynaptic development is additionally more fragile compared to the innervated one. 15

Figure 7: Schematic representation of normal and myasthenic neuromuscular junctions; a) the normal neuromuscular transmission, described in 1.2; b) reduced number of AChR, flattened folds. Image extracted from [74].....16

Figure 8: Schematic representation of the structure of IgG antibodies. Extracted from [82].....18

Figure 9: Schematic representation of pathogenic mechanisms of AChR MG antibodies. a) and b), antibody binding and complement activation led to the destruction of postsynaptic architecture; c) single binding led to the internalization of AChR, leading to less signal transmission; d) binding of antibodies avoid Ach binding to the receptor, blocking signal transmission. Extracted from [34].....19

Figure 10:Schematic representation of the pathogenic mechanisms of MG autoantibodies at the NMJ; a) representation of the healthy NMJ, in which agrin/Lrp4/MuSK complex are normally activating, allowing the cluster of AChR; b) monovalent binding of IgG4 led to the interruption of clustering signal pathway. Moreover, the impossibility of a retrograde signaling from Lrp4 to the nerve is thought to influence the NMJ; c) the divalent binding of the IgG4 led to the activation of MuSK independent from the complex, thus stimulating ectopic AChR. Figure extracted from [82].....20

Figure 11: Schematic representation of the cell-based assay technique for the detection of autoantibodies against AChR/MuSK. In the first picture HEK293 cells were transfected with AChR subunits, MuSK or only GFP. The cells were then plated on glass coverslips and serum from SNMG patient was added and incubated with anti-human IgG594. With fluorescence microscope it was possible to visualize the green fluorescence, indicating successful transfection, and the red fluorescence, indicating the presence of autoantibodies. 28

Figure 12: Schematic representation of tissue-based assay for the detection of antibodies against the NMJ. Rat soleus sections were placed on a microscope slide and incubated with serum. It was then performed an incubation with α-bungarotoxin 594 to visualize the NMJ in red and anti-human IgG488 to visualize the autoantibodies in green. The result was then analyzed with fluorescence microscopy. 29

Figure 13: Size marker and cut area of the gel. The area to be cut has been identified as follows: the length of the cut area was defined by the wells in which sample was loaded, the height by the size marker. 30

Figure 14: Schematic overview of permanox experiment. First, the slide with the grid was placed in a 10cm dish, until cells were differentiated. Finally, the grid was removed and the slide analyzed through fluorescence microscopy. 32

Figure 15: Transfer sandwiches 35

Figure 16: Results of fluorescence microscopy of cell-based assay. Transfected HEK293 cells have been incubated with a healthy control, dilution 1:40. In the left column: GFP expressed in all the transfected cells; middle column: autoantibodies detection with anti-human IgG AF594; right column: merge. a) cells transfected with AChR subunits; b) GFP transfection; c) MuSK transfected cells. 37

Figure 17: Results of fluorescence microscopy of cell-based assay. Transfected HEK293 cells incubated with positive control serum, dilution 1:40. Left column: GFP expressed in all the transfected cells; middle column: autoantibodies detected with anti-human IgG AF594; right column: merge. a) cells transfected with AChR subunits, incubated with AChR positive serum; b) GFP transfection, incubated with AChR positive serum; c) MuSK transfected cells incubated with MuSK positive serum; 38

Figure 18: Fluorescent microscopy of tissue-based assay. Positive and negative control have been tested. In green, anti-human 488 antibody; in red the NMJ stained by 594 alpha-bungarotoxin. a) positive control, AChR MG patient, 1:40 dilution; b) healthy control patient serum, 1:40 dilution. 39

Figure 19: Patches of cells attached on the surface of the dish, 8 days after isolation. 40

Figure 20: Human muscle cells in culture, P2, bright field microscopy; a) magnification 4x, overview of cells at 50% confluency; b) magnification 20x, overview on cells' morphology. 40

Figure 21: Comparison between myogenic and non-myogenic cells from muscle tissue. First column, cells stained with DAPI (blue). Second column, anti MyoD antibodies and AF594. Third column merged pictures; a) myoblasts; b) fibroblasts 41

Figure 22: Differentiated human myotubes, 5 days after differentiation medium. 42

Figure 23: Staining for desmin: DAPI stained nuclei in blue, AF488 anti-desmin antibodies in green; a) desmin staining positive cells, magnification 20x. b) desmin staining positive cells, magnification 10x.....42

Figure 24: MyoD staining of myotubes. First column, cells stained with DAPI (blue). Second column, anti MyoD antibodies and AF594. Third column merge pictures. Magnification 20x; Nuclei of differentiated cells did not show staining for MyoD, while non differentiated cells were positive. .43

Figure 25: Human myotubes without stimulation. Nuclei stained with DAPI in blue, AChR stained with α bungarotoxin in red . a) and b) human myotubes on gelatine coated coverslips. 43

Figure 26: Agrin stimulated myotubes. Nuclei stained with DAPI, blue; AChR stained with α bungarotoxin, in red; a) 1:1000 titration b) 1:5 titration. 44

Figure 27: Agrin stimulated myotubes on fibronectin coating. Nuclei stained with DAPI, blue; AChR stained with α bungarotoxin, in red; a) 1:500 dilution; b) 1:100 dilution; c)1:50 dilution; d) 1:20 dilution; e) 1:10 dilution. The arrow indicates an area of possible AChR clustering. 45

Figure 28: Agrin stimulated myotubes on laminin coated coverslips. Nuclei stained with DAPI, blue; AChR stained with α bungarotoxin, in red; a) 1:100 dilution; b) 1:50 dilution; c) 1:10 dilution; d) 1:5 dilution; 46

Figure 29: A-bungarotoxin stained myotubes a) 1:50 agrin stimulation; b) 1:100 agrin stimulation. The arrows indicate regions in which may be present a clustering of AChR. 47

Figure 30: Agrin stimulated myotubes on laminin and agrin coated coverslips. Nuclei stained with DAPI, blue; AChR stained with α bungarotoxin, in red; a) 1:100 agrin dilution; b) 1:50 agrin dilution; c)1:10 agrin dilution; d) 1:5 agrin dilution.....48

Figure 31: Laminin stimulated myotubes on coated coverslips. Nuclei stained with DAPI, blue; AChR stained with α-bungarotoxin, in red; a) laminin and agrin coated coverslips, 1:100 laminin; b) gelatine and agrin 1:100 coated coverslip, laminin 1:100 stimulation 48

Figure 32: Agrin and laminin soluble stimulation. Nuclei stained with DAPI, blue; AChR stained with α bungarotoxin, in red; a) 1:100 agrin and laminin stimulation, glass coverslips coated with agrin and laminin; b) 1:100 agrin and laminin double stimulation, glass coverslips coated with agrin and laminin c) 1:100 agrin stimulation for 24 hours, on agrin and laminin coated coverslips; d) laminin 24h stimulation, on agrin and laminin coated coverslip. 49

Figure 33: C2C12 cells on permanox slides. a) well without gelatine; b) well with gelatine; c) cells without gelatine after differentiation. 51

Figure 34: Myotubes after soluble agrin stimulation; a) human myotubes; b) L6 myotubes. 52

Figure 35: Coomassie staining of the SDS PAGE gel; a) L6 myotubes lysate, incubated with 6325/18 serum; b) human myotubes lysate, incubated with 6325/18 serum. 53

Figure 36: Early myotubes stained with antibodies against the protein of interest, AF594 in red and nuclei stained with DAPI in blue; a) α-sarcoglycan; b) β-sarcoglycan; c) γ-sarcoglycan; d) IgLON5; e) dysferlin. 54

Figure 37: Myotubes stained with antibodies against the protein of interest, AF488 in green and nuclei stained with DAPI in blue; a) α-sarcoglycan; b) β-sarcoglycan; c) γ-sarcoglycan; d) IgLON5; e) dysferlin. 55

Figure 38: MSI and DMSO treated cell number. a) 2 μM titration; b) 1 μM titration. 56

Figure 39: Overall growth results of cells at day 5 for each condition, compared to the untreated control. A) 1μM concentration; b) 2 μM concentration; c) 3 μM concentration; d) 4 μM concentration; e) 5 μM concentration. * for P value <0.05; ** for P value <0.005; *** for P value <0.0005; **** for P value < 0.0001. All the P values > 0.05 have been considered not statistically significant. 57

Figure 40: Overall growth difference between the conditions after 5 days. Up to 5 μM it is possible to see an increasing difference between the 2 treatments. Nevertheless, at 5 μM the difference decreases again. Cells incubated with MSI/DMSO for 5 days. 58

Figure 41: Overview on the morphology of the cells with different treatments; a) MSI 1 μM treated cells; b) DMSO 1 μM treated cells; c) no treatment control 58

Figure 42: Human muscle cells three days after switching to differentiation medium; a) MSI 1 μM treated cells; b) DMSO 1 μM treated cells; c) control 59

Figure 43: SM, size marker; 1, C2C12 myoblasts; 2, C2C12 myotubes; 3, human myoblasts; 4, human myotubes; 5, L6 myotubes; 6, L6 myoblasts; 7, T37 myoblasts; 8, LRP4 antigen 1; 9, LRP4 antigen 2; a) western blot immunodetection of β-actin. All the samples tested showed the band for β-actin protein; b) western blot immunodetection of LRP4. Only L6 myoblasts showed an expression in addition to the positive controls. 60

APPENDIX FIGURES

Figure S1: Agrin stimulated myotubes. Nuclei stained with DAPI, in blue. AChR stained with α-bungarotoxin, in red; a) 1:1000 agrin stimulation; b) 1:500 agrin stimulation; c) 1:200 agrin stimulation; d) 1:100 agrin stimulation; e) 1:50 agrin stimulation; f) 1:20 agrin stimulation; g) 1:10 agrin stimulation; h) 1:5 agrin stimulation. 86

Figure S2: Myotubes on laminin coating stimulated with soluble agrin. Nuclei stained with DAPI, in blue. AChR stained with α-bungarotoxin, in red;; a) no agrin; b) 1:1000 agrin stimulation; c) 1:500 agrin stimulation; d) 1:200 agrin stimulation; 87

Figure S3: Agrin stimulated myotubes on laminin coated coverslips. AChR stained with α-bungarotoxin stained myotubes on laminin a) 1:50 agrin stimulation; b) 1:100 agrin stimulation. .. 87

Figure S4: Laminin stimulated myotubes on laminin coated coverslips. Nuclei stained with DAPI, in blue. AChR stained with α-bungarotoxin, in red;; a) laminin coated coverslips, 1:100 laminin; b) gelatine and agrin 1:50 coated coverslip, laminin 1:100 stimulation; c) gelatine and agrin 1:10 coated coverslip, laminin 1:100 stimulation.....88

Figure S5: MSI test glass coverslips, 24 well plate. Every day wells have been stained with DAPI, and nuclei counted with ImageJ. a) Graph with summarized results of counting; b) example a picture for counting nuclei of MSI treated cells, day 2. C) example of a picture for counting nuclei of DMSO treated cells, day 2.....88

Figure S6: Comparison of number of cells for the different titrations of MSI a) total number of cells for an MSI titration test; b) difference between cells treated with MSI and cells treated with DMSO per each titration.....89

Figure S7: Overall growth of cells over 5 days for each condition; a) 1μM concentration; b) 2 μM concentration; c) 3 μM concentration; d) 4 μM concentration; e) 5 μM concentration.....90

Figure S8: MSI treated cells. On the left column, a plate overview with 4x magnification, to have an overview on the culture. On the right column, a focus on the morphology of the cells; a) MSI 1 μM; b) MSI 2 μM; c) MSI 3 μM; d) MSI 4 μM; e) MSI 5 μM; 92

Figure S9: DMSO treated cells On the left column, a plate overview with 4x magnification, to have an overview on the culture. On the right column, a focus on the morphology of the cells; a) DMSO 1 μM; b) DMSO 2 μM; c) DMSO 3 μM; d) DMSO 4 μM; e) DMSO 5 μM; 94

Figure S10: Pictures highlighting the morphology and development of cells for each condition, 2 days after switch to differentiation medium. On the left column, MSI treated cells. On the right column, DMSO treated cells. a) 1 μM; b) 2 μM; c) 3 μM; d) 4 μM; e) 5 μM;.....96

LIST OF TABLES

Table 1. Clinical subgroups of myasthenia gravis. Extracted from[75]. 17

Table 2: Recipes of the different media used in cell culture 24

Table 3: Recipes of the different solutions used in CBA 27

Table 4: Recipes of the different buffers for TBA 28

Table 5: Recipes of the buffers used in immunoprecipitation assay 29

Table 6: SDS PAGE gels recipes 34

Table 7: Different agrin dilutions to stimulate AChR clustering on gelatine coated coverslips. 44

Table 8: different agrin dilutions on laminin coated coverslips 46

Table 9: Coating and stimulation molecules used to induce AChR clustering on human myotubes. The "Y" in the results section indicates results comparable with early clustering. The "X" indicates a that showed upregulation of AChR and possible microclusters. The "-" indicates no upregulation of AChR nor clustering effect. 51

APPENDIX

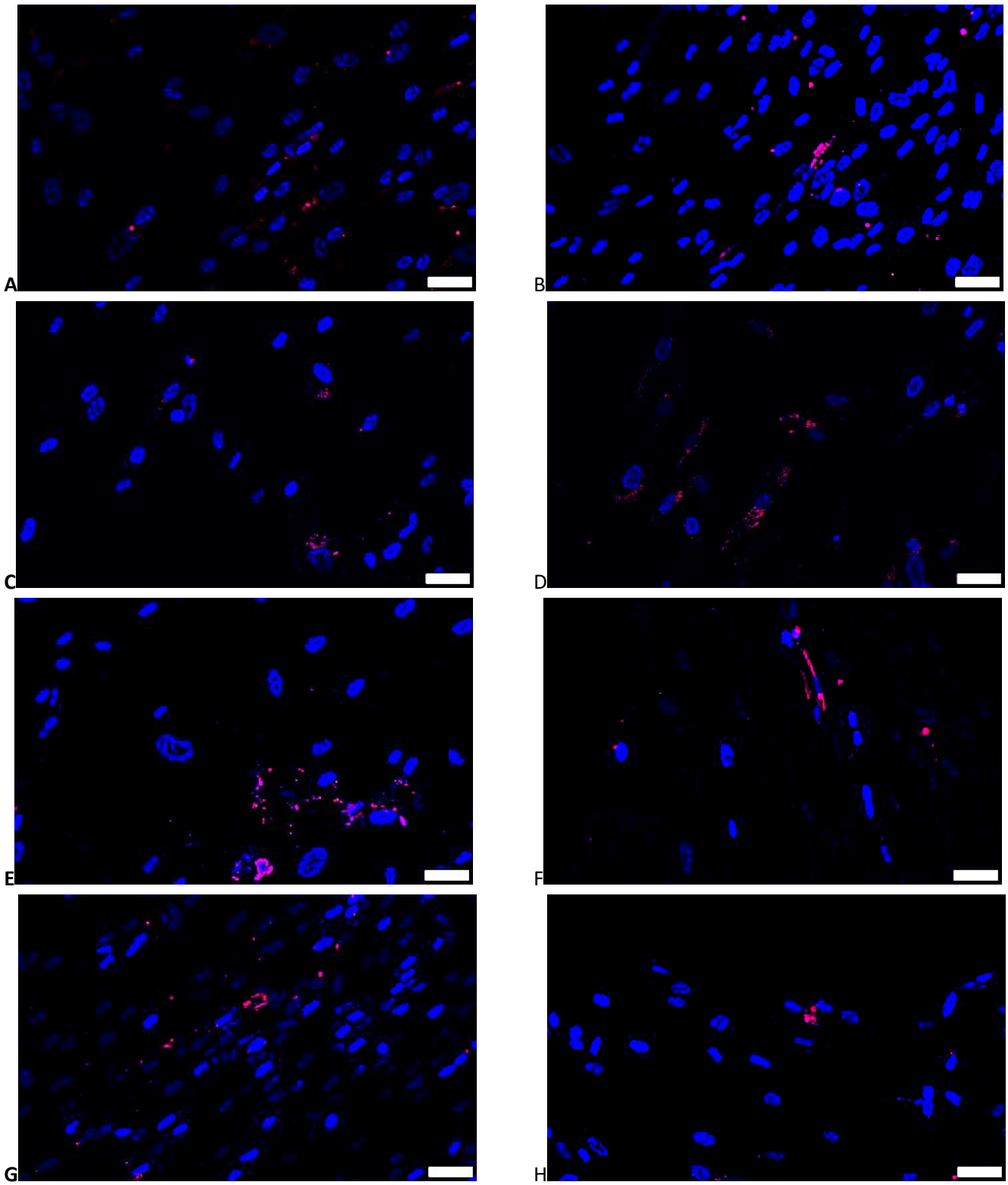

Figure S1: Agrin stimulated myotubes. Nuclei stained with DAPI, in blue. AChR stained with α-bungarotoxin, in red; a) 1:1000 agrin stimulation; b) 1:500 agrin stimulation; c) 1:200 agrin stimulation; d) 1:100 agrin stimulation; e) 1:50 agrin stimulation; f) 1:20 agrin stimulation; g) 1:10 agrin stimulation; h) 1:5 agrin stimulation.

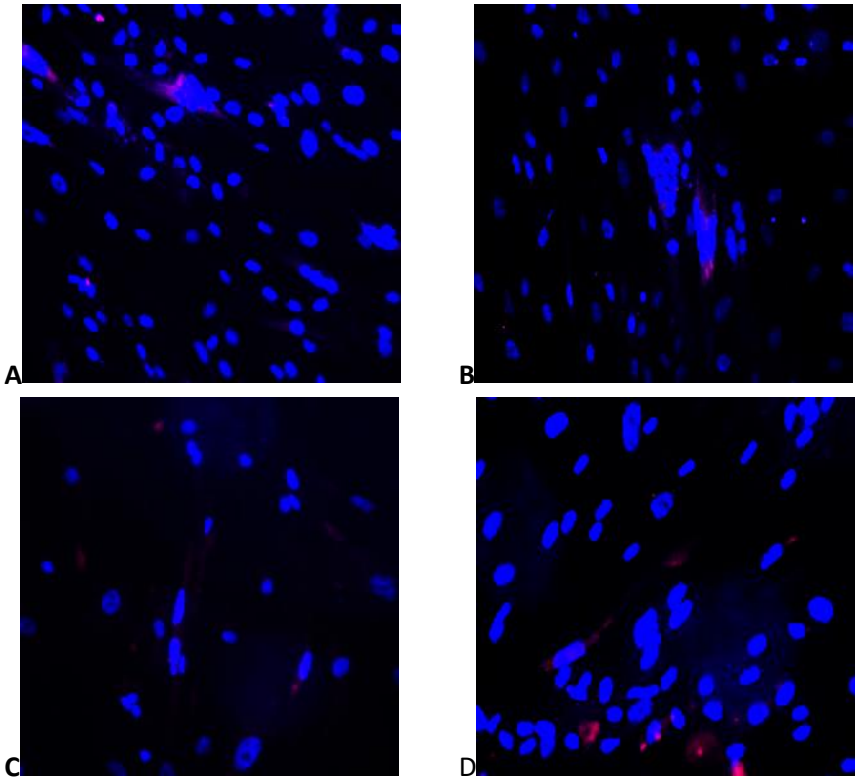

Figure S2: Myotubes on laminin coating stimulated with soluble agrin. Nuclei stained with DAPI, in blue. AChR stained with α-bungarotoxin, in red;; a) no agrin; b) 1:1000 agrin stimulation; c) 1:500 agrin stimulation; d) 1:200 agrin stimulation.

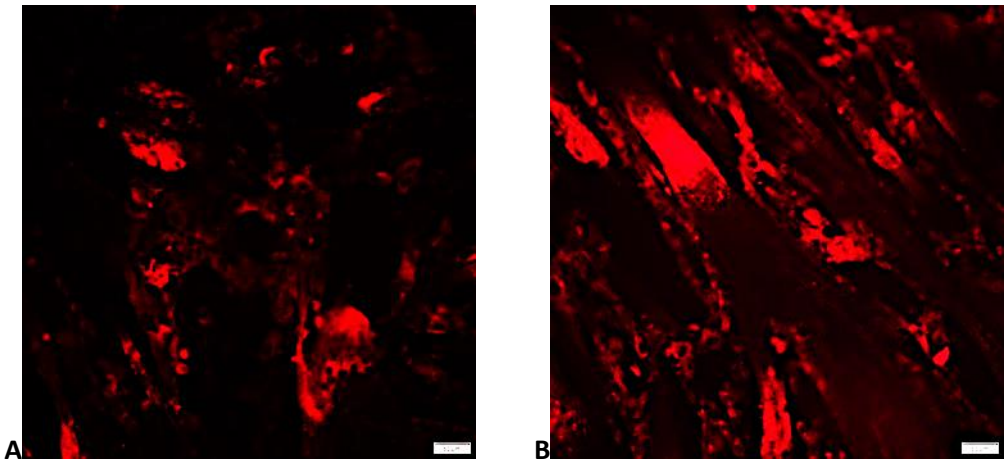

Figure S3: Agrin stimulated myotubes on laminin coated coverslips. AChR stained with α-bungarotoxin stained myotubes on laminin a) 1:50 agrin stimulation; b) 1:100 agrin stimulation.

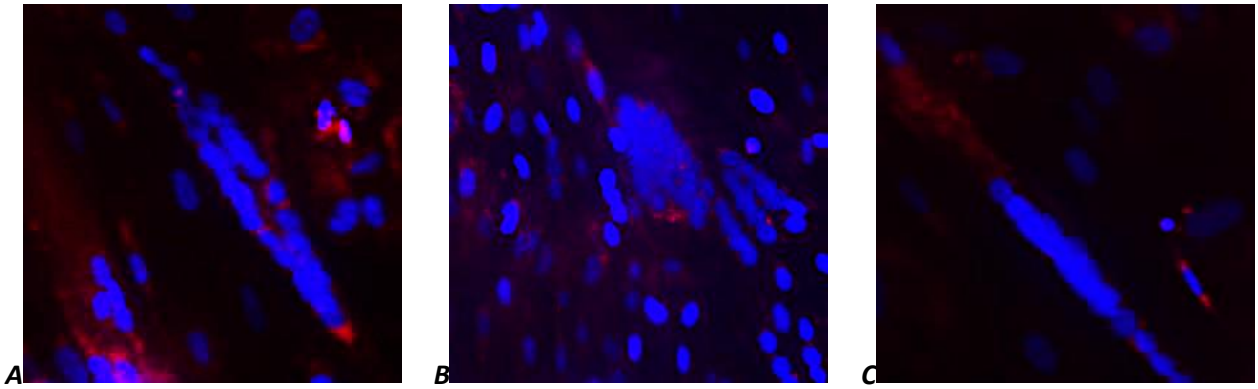

Figure S4: Laminin stimulated myotubes on laminin coated coverslips. Nuclei stained with DAPI, in blue. AChR stained with α-bungarotoxin, in red;; a) laminin coated coverslips, 1:100 laminin; b) gelatine and agrin 1:50 coated coverslip, laminin 1:100 stimulation; c) gelatine and agrin 1:10 coated coverslip, laminin 1:100 stimulation

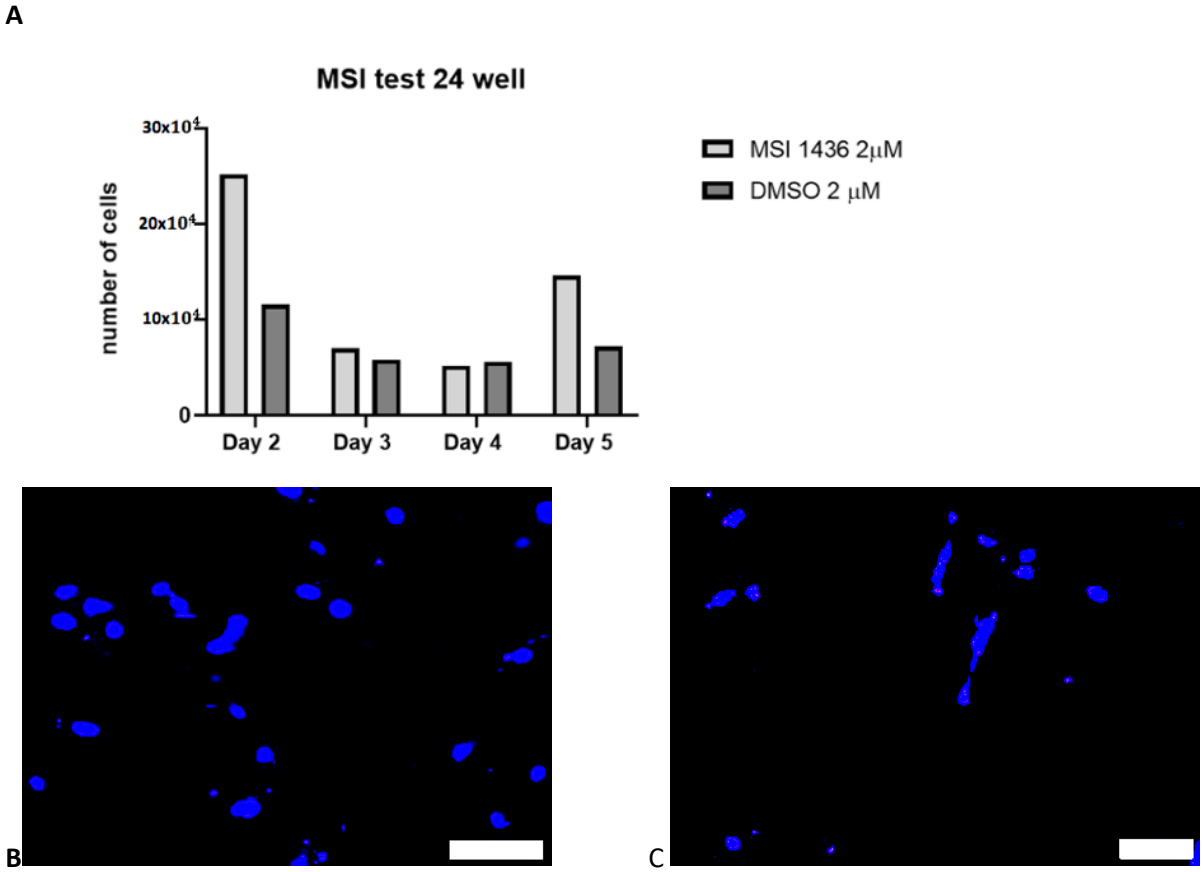

Figure S5: MSI test glass coverslips, 24 well plate. Every day wells have been stained with DAPI, and nuclei counted with ImageJ. a) Graph with summarized results of counting; b) example a picture for counting nuclei of MSI treated cells, day 2. C) example of a picture for counting nuclei of DMSO treated cells, day 2.

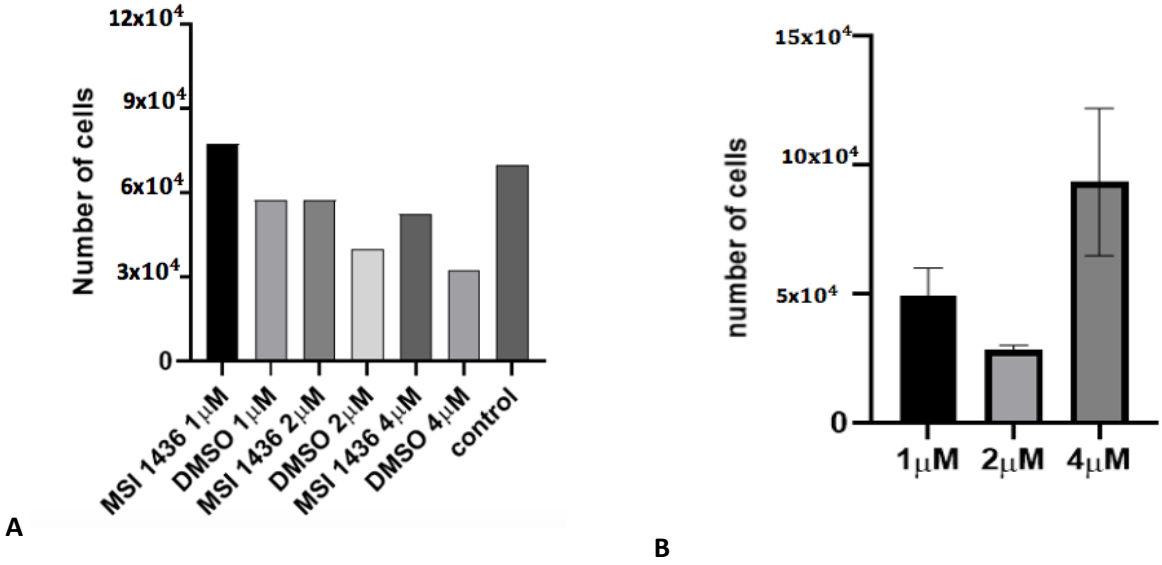

Figure S6: Comparison of number of cells for different concentrations of MSI a) total number of cells for an MSI titration test; b) difference between cells treated with MSI and cells treated with DMSO per each titration.

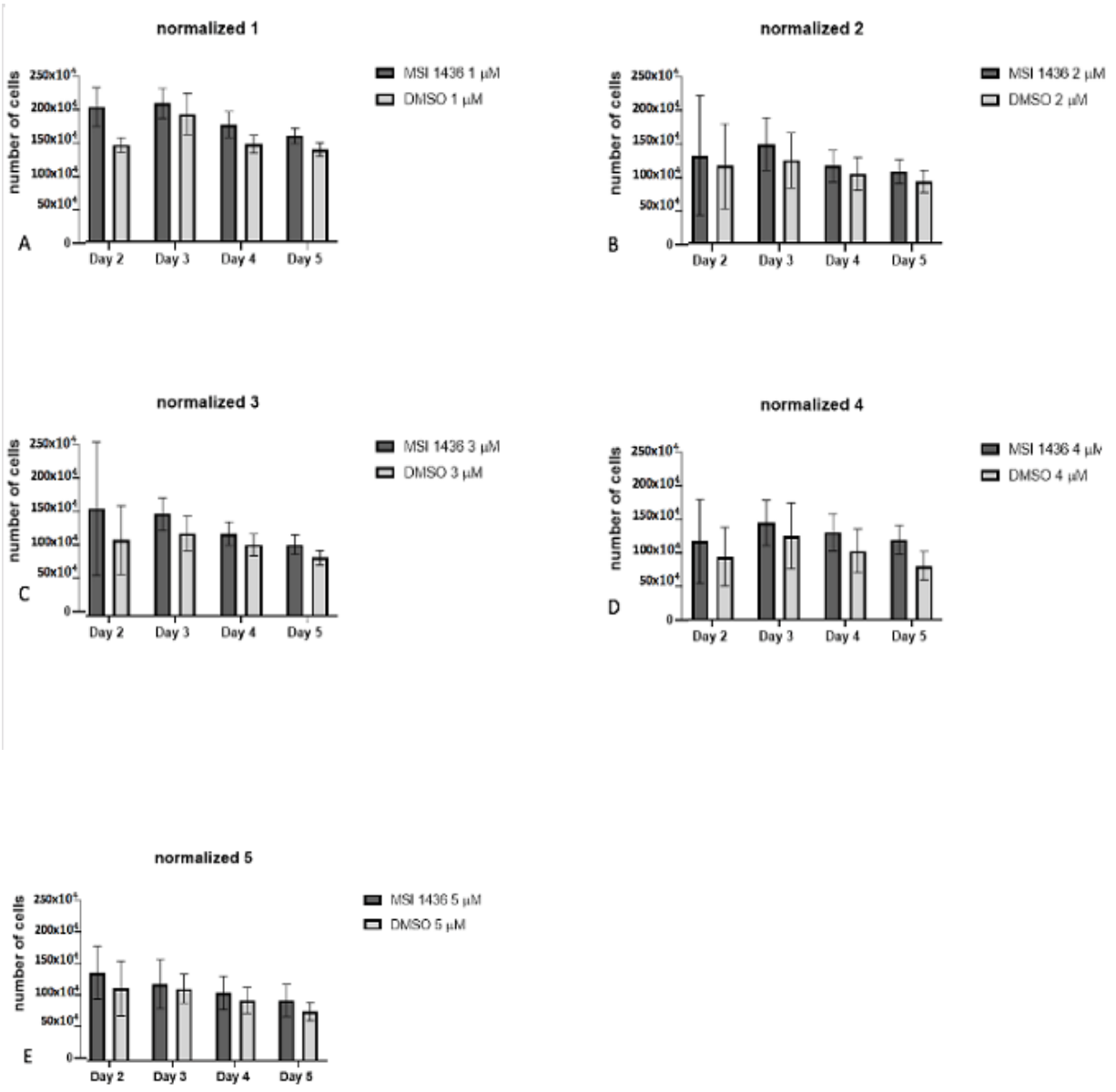

Figure S7: Overall growth of cells over 5 days for each condition; a) 1µM concentration; b) 2 µM concentration; c) 3 µM concentration; d) 4 µM concentration; e) 5 µM concentration.

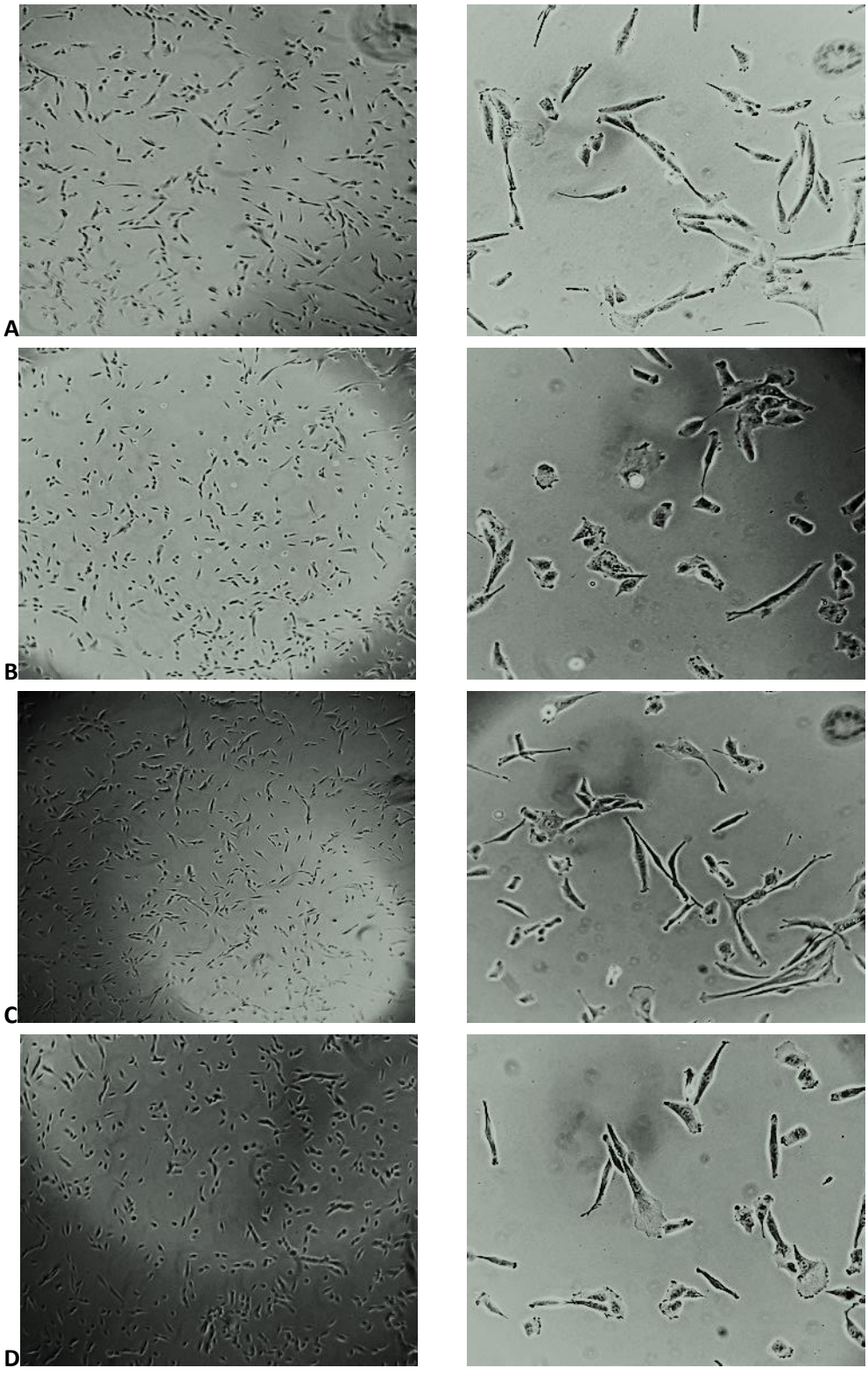
A
B
C
D

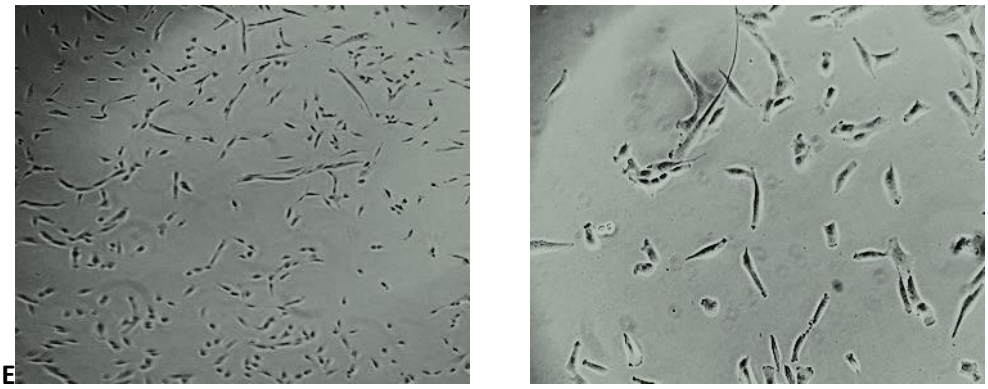

Figure S8: MSI treated cells. On the left column, a plate overview with 4x magnification, to have an overview on the culture. On the right column, a focus on the morphology of the cells; a) MSI 1 μM; b) MSI 2 μM; c) MSI 3 μM; d) MSI 4 μM; e) MSI 5 μM;

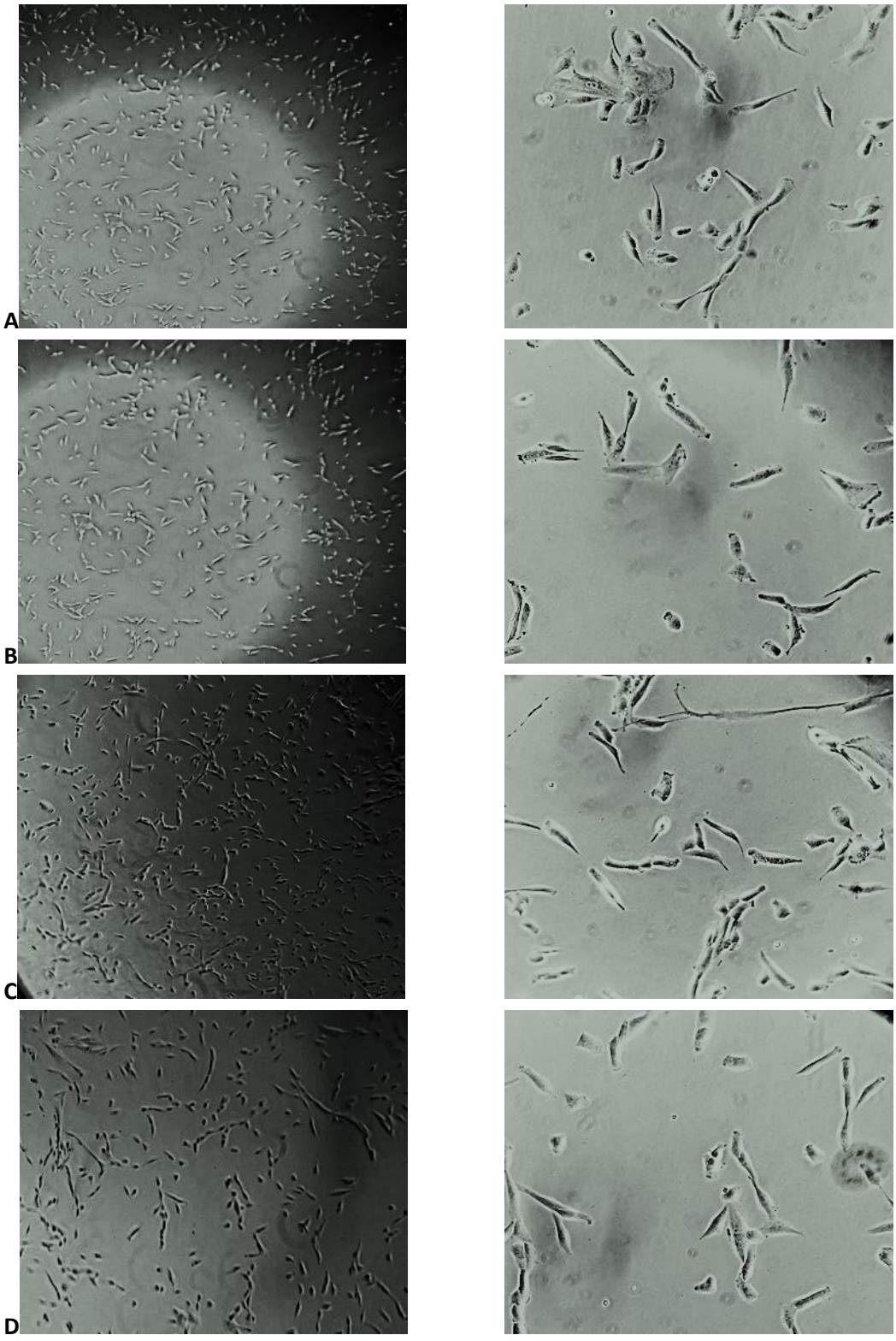
A
B
C
D

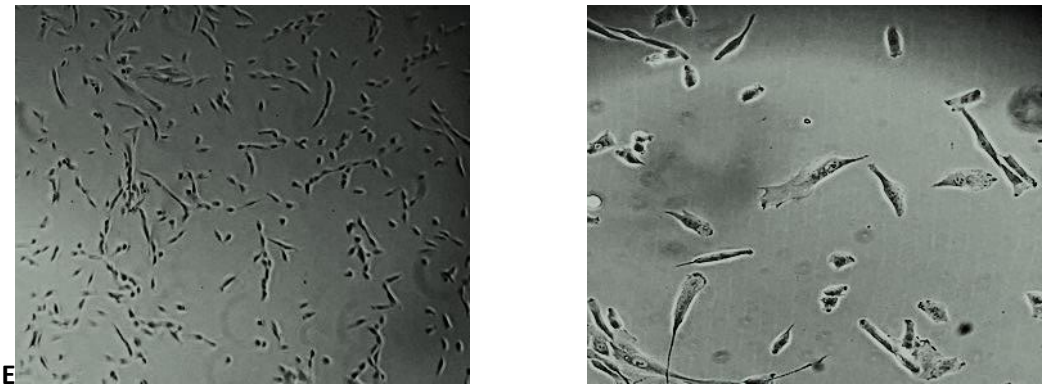

Figure S9: DMSO treated cells On the left column, a plate overview with 4x magnification, to have an overview on the culture. On the right column, a focus on the morphology of the cells; a) DMSO 1 μM; b) DMSO 2 μM; c) DMSO 3 μM; d) DMSO 4 μM; e) DMSO 5 μM;

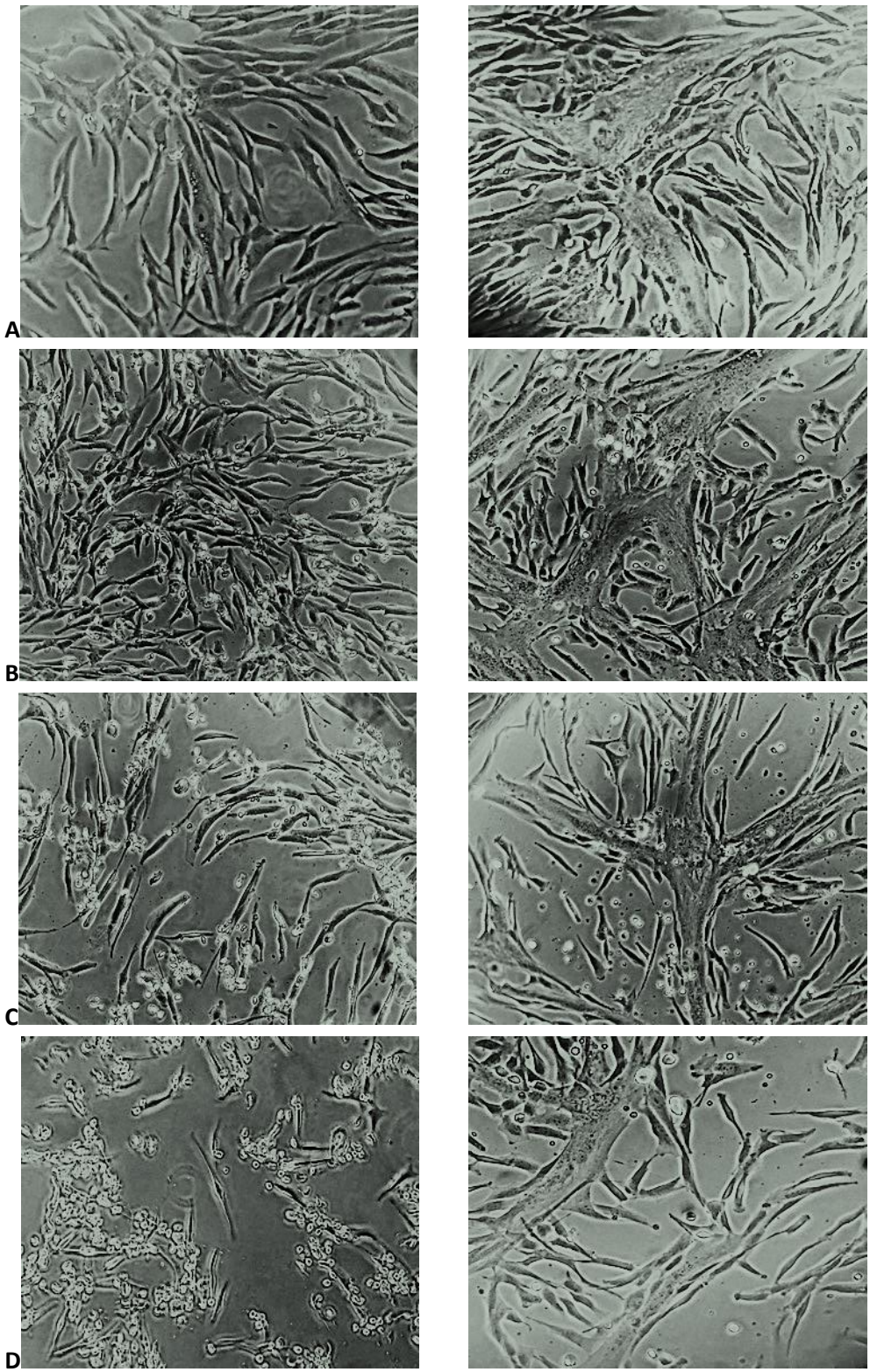
A
B
C
D

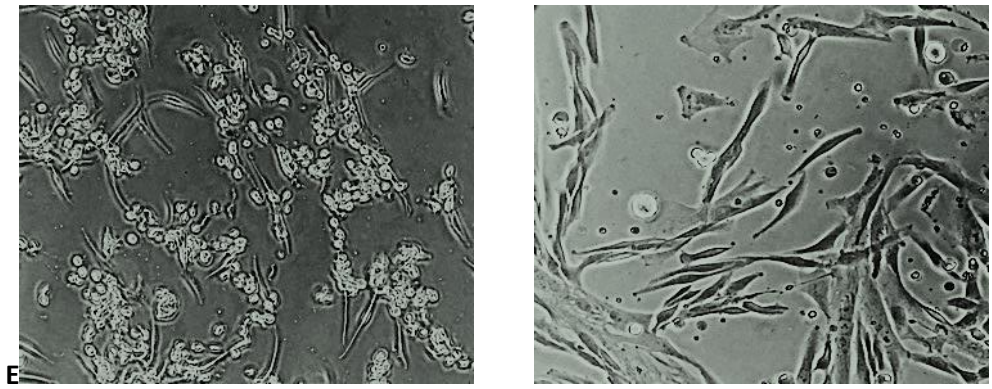

Figure S10: Pictures highlighting the morphology and development of cells for each condition, 2 days after switch to differentiation medium. On the left column, MSI treated cells. On the right column, DMSO treated cells; a) 1 µM; b) 2 µM; c) 3 µM; d) 4 µM; e) 5 µM;